



ILH
INSTITUT FÜR
LEICHTBAU MIT
HYBRIDSYSTEMEN



Coating Materials
& Polymers



UNIVERSITÄT PADERBORN
Die Universität der Informationsgesellschaft

Functional Adhesives and Functionally Graded Adhesives in Fiber Metal Laminates

THE INFLUENCE OF DIFFERENT ADHESIVE TYPES ON THE
PROPERTIES OF FIBER METAL LAMINATES

DISSERTATION FOR THE ATTAINMENT OF THE GRADE

DR. RER. NAT OF THE FACULTY OF NATURAL SCIENCES AT THE
UNIVERSITY OF PADERBORN

Jan Dietrich

M.Sc.

born December 25, 1986 in Paderborn

Supervisor: Prof. Dr. Wolfgang Bremser

Second supervisor: Prof. Dr. Thomas Tröster

Acknowledgements

I would like to express my dearest thanks to anyone who helped me completing this work.

Prof. Wolfgang Bremser for the opportunity of writing- and for supervising this thesis

Prof. Thomas Tröster for being my second supervisor

Alan Camberg for supporting me a lot with the simulation and engineering aspects

The whole Lhybs team, Thomas Heggemann, Lars Achterberg, Katja Engelkemeier and Matthias Wille

Nadine Buitkamp and Manuel Traut for their support with the SEM

Everyone from the CMP group and beyond who helped

My wife Tiantian, parents and family

Selbstständigkeitserklärung

Hiermit erkläre ich, dass ich die vorliegende Arbeit mit dem Titel „Functional Adhesives and Functionally Graded Adhesives in Fiber Metal Laminates“ selbstständig und ohne unerlaubte fremde Hilfe angefertigt, keine anderen als die angegebenen Quellen und Hilfsmittel verwendet und die den verwendeten Quellen und Hilfsmitteln wörtlich oder inhaltlich entnommenen Stellen als solche kenntlich gemacht habe.

Ort, Datum

Unterschrift

I. Kurzfassung

In der vorliegenden Arbeit wurde der Einfluss des Klebstofftyps auf die Gesamteigenschaften von Faser-Metall-Laminaten untersucht. Kernidee der Arbeit ist die Umsetzung eines funktionalen Eigenschaftsgradienten in der Klebschicht. Derartige Gradienten helfen intrinsische Spannungen der Klebschicht abzubauen, sowie Spannungskonzentrationen unter Belastung zu vermeiden. Dieses Konzept wurde aus der Natur abgeleitet, wo es in Grenzphasen von Materialien mit unterschiedlichen Eigenschaften ubiquitär vorkommt.

Drei Klebstofftypen wurden untersucht: Steife duroplastische Epoxidklebstoffe, wärmehärtende Elastomerklebstoffe und thermoplastische Klebstoffe auf Basis von Polyolefinen. Der Arbeitsansatz ermöglicht einen Überblick über die Effekte der Klebstoffe, während gleichzeitig innovative Ansätze der Klebstoffentwicklung- und Modifikation untersucht und entwickelt wurden. So umfasst die Arbeit die nachträgliche Modifikation von kommerziellen Klebstoffen, die vollständige Neuentwicklung eines wasserbasierten Klebstoffsystems mit Nanokompositverstärkung sowie den Test eines neuartigen elastischen strukturellen Klebstoffes, basierend auf EPDM-Kautschuk. Thermoplastische Klebstoffe zur strukturellen Verklebung stellen ebenfalls ein Feld mit hohem Nutzungspotenzial dar, das jedoch zum Zeitpunkt der Erstellung dieser Arbeit noch auf seinen Durchbruch in der Anwendung wartete.

Ein großer Teil dieser Arbeit lag in der Entwicklung eines Klebstofffilms, dessen wesentlicher Rohstoff wasserbasierte Polyurethandispersionen sind. Um die Eigenschaften des Klebefilms zu verbessern und die Steifigkeit zu kontrollieren, wurde ein Nanokomposit aus einem hochverzweigten Polyesterpolyol und dem Schichtsilikat Montmorillonit hergestellt. Das Schichtsilikat hat überraschenderweise eine Wechselwirkung mit dem hochverzweigten Polyol und beeinflusst dessen Dispergierbarkeit. Die Einführung des Nanokomposit in den Klebstoff führte zu wesentlichen Verbesserungen der mechanischen Eigenschaften.

II. Abstract

The effect of the choice of adhesives onto the properties of fiber-metal laminates (FMLs) was examined around the core idea of introducing a gradient of properties into the adhesive. Such a gradient can be helpful in reducing intrinsic stresses and stress concentrations under load. This concept was derived from nature, where it is ubiquitous at the interphases of dissimilar materials.

Three fields of adhesives were examined: Rigid thermosetting epoxies, elastomeric thermosetting adhesives and thermoplastic adhesives based on polyolefins. The work's approach gives an overview of effects of the different adhesive classes and looks into innovative adhesive developments. It explores new concepts of modifying properties of existing adhesive types, the formulation of a water based elastomeric adhesive that incorporates nano particles, the testing of a new type of EPDM-based thermosetting adhesive and the use of thermoplastic adhesives for structural car body applications.

The findings of the work are diverse, as the implementation of a material gradient in the adhesive is not superior *per se* to other tested modifications. An influence of an elasticity gradient was not evident in all tested systems, but very pronounced in others, especially those including elastomeric adhesives. The application of elastomeric adhesives bears a high potential for the introduction of special properties into the FML. In a combination of an elastomeric PU-based adhesive with a rigid epoxy-based adhesive, the order of the adhesives had a massive influence and the combination itself gave a significant advantage.

A large part of this work was the development of an adhesive film that uses waterborne polyurethane dispersions as the binder. To reinforce the adhesive and control its stiffness, a functional nanocomposite filler based on hyperbranched polyester polyols and montmorillonite clay was introduced. A surprising interaction of the clay with the polyol results in its influence onto the dispersibility of the hyperbranched polyol. The incorporation of the nanocomposite in the adhesive leads to a great enhancement of the mechanical properties of the adhesive.

Contents

I.	Kurzfassung	4
II.	Abstract	5
1	Introduction.....	8
2	Motivation	10
2.1	Controversy about the Importance of Light Weight Construction	10
3	State of the Art	12
3.1	Fiber-Metal-Laminates	12
3.2	Structural Adhesive Bonding	13
3.3	Adhesive Bonding of Hybrid Materials.....	15
3.4	Functionally Graded Materials	17
3.5	Functionally Graded Materials in Nature	18
3.6	Functionally Graded Adhesives	19
3.6.1	Functionally Graded Adhesives in Single-Lap Joint	20
3.6.2	Functionally Graded Adhesives in Planar Joints.....	22
4	Analytical and Theoretical Background.....	24
4.1	Mismatch of Materials and Contact Damages	24
4.2	Mechanical and Microscopic Analytics.....	25
4.3	Tensile Test	26
4.4	Lap-shear strength test.....	27
4.5	Dynamic Mechanical Analysis (DMA)	28
4.6	Quasi-Static Flexural Testing	29
4.7	Dynamic Three-Point Flexural Test / Charpy Impact Test.....	30
4.8	Scanning Electron Microscopy (SEM)	31
4.9	Energy-Dispersive X-Ray Spectroscopy (EDX).....	33
5	Experimental part.....	35
5.1	Simulation of the FRP/Metal Joint in FML.....	35
5.2	Modified Adhesives Approach.....	38
5.2.1	Evaluation of Fillers for Modification	38
1.1.1	EPDM-based approach	49
5.2.2	Polyurethane Based Approach.....	53
5.3	Combined Adhesive Approach	67

5.4	Thermoplastic Adhesives Approach	72
5.4.1	Complex Fiber Metal Laminate with Thermoplastic Adhesive	73
5.4.2	Bending Test Results	75
5.4.3	Impact Test Results	76
5.4.4	Fiber Metal Laminate Component with Thermoplastic Adhesive	78
6	Summary	85
7	Discussion and Conclusions.....	87
7.1	The functional gradient of modulus and functional adhesive in bonding FMLs	88
7.2	Perspectives for further work.....	89
8	References.....	91
8.1	List of Figures.....	91
8.2	List of Tables	94
8.3	Literature References	94
9	Appendix.....	98
9.1	List of commonly used abbreviations in this work	98
9.2	Publications and Patents	98
9.3	Technical Data sheets of used commercially available adhesives	99
9.3.1	DuploTEC® 690 SBF	99
9.3.2	3M™ Structural Adhesive Tape	101
9.3.3	BETAMATE™ 1620 MB.....	103

1 Introduction

Lightweight materials offer high potential in aerospace-, automotive-, ship building, architecture and many other areas. Fiber metal laminates have less density (leading to less weight) and better mechanical properties when compared to conventional materials or parts made purely from fiber reinforced plastics. Parts made from FML are also less expensive than those made entirely from CFRP.

This work investigates the adhesive bonds of this special class of hybrid material: “fiber metal laminates” (FMLs). FMLs are hybrids consisting of alternating staples of fiber reinforced plastics (FRP) and metal sheets. The thickness of the metal sheets is usually around 0.5 mm, the fiber composite sheets around 1 mm. The adhesive layers are usually in the thickness range from 100 μm to 150 μm . They are in many cases the weakest point and thus a predetermined breaking point of the laminate. As this work shows, the adhesive layers are also an area where the properties of the whole laminate can be influenced greatly.

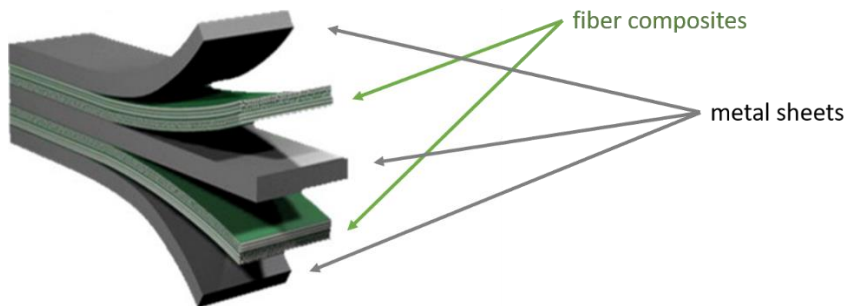


Figure 1: Structure of a fiber metal laminate (Adaptation from ^[1])

In practice the adhesive layers are often formed by the matrix material present in the FRP sheets. Introducing another distinct adhesive constitutes an additional production step and more costs. The adhesive layer is often also not considered prominently in simulations of fiber metal laminates. In this work, it is shown that the role of the adhesive layer is eminent in the system FML. It can be used as a set screw for properties and to introduce new functions into the FML. This is what is meant by the term “functional adhesive” in the title of this work.

Furthermore the idea to transfer a principle from nature, that has already successfully been applied to adhesive bonding of single-lap joints^[2] to FMLs was investigated in this work: Applying a gradient adhesive layer to mitigate the stress disparities in the adhesive layer and the laminate itself.

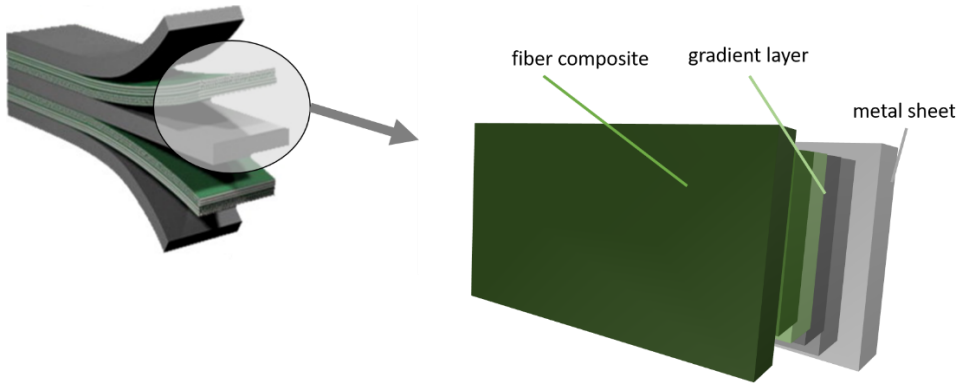


Figure 2: One of many adhesive layers inside a fiber metal laminate and the gradient layer approach (adaptation from^[1])

The idea of functionally graded adhesives was first applied in the 1960s^[3] even before the term functionally graded material (FGM) was coined. In the following decades there was not much research on the topic. It has, however, become an active field again recently. This is partly due to the upcoming of new technologies which enable to the production of graded materials, such as 3d printing. This has also inspired research in the field of adhesives. During the making of this work in 2017 the International Journal of Adhesion and Adhesives dedicated a special issue on the topic “Functionally Graded Adhesively Bonded Systems”^[4]. Fiber metal laminates are an active field of research and development themselves but functionally graded adhesives have not been covered in any research so far. Because of their many interphases, FMLs are especially interesting to adhesive research. Because of their high potential in lightweight construction they are a field that should not be neglected.

This work also explores the application of very different types of adhesive in Fiber Metal Laminates, such a novel EPDM- and polyurethane based adhesives. Also, methods for the combination of different adhesive types were developed and tested. A lot of effort was put in the application-oriented modification of a commercial epoxy-based adhesive.

A major driving force for the development in lightweight materials is the focus of regulators on the environmental impact of materials. Within this trend, the development of adhesives is no exception. Regulations of coatings, adhesives and sealants with regard to volatile organic compounds are a challenge that formulators face around the world. Based on polyurethane dispersions, an adhesive was formulated that can be applied in FML and beyond. Using a self-developed multifunctional filler material, mechanical properties were enhanced greatly- and the necessity of an additional thickener made obsolete.

2 Motivation

A hybrid material draws its advantages from the fact that it combines the useful properties of different materials. A fiber metal laminate, which is a special array of hybrid material, contains very different materials in terms of mechanical and interfacial properties.^[5]

When two dissimilar materials are joined, the result is a huge gap of material properties. This gap leads to a build-up of internal stresses and contact damages. During loading premature failure below the expected capacity of the joint typically occurs at such interfaces. Fiber Metal Laminates possess large interfaces between dissimilar materials. Therefore, this central problem of bonding hybrid materials is especially prominent in fiber metal laminates.

Biological organisms of a certain complexity contain hard and stiff parts embedded into soft, elastic tissue material. Nature has to deal with the same problem that material science faces in joints of dissimilar materials for automobile or aircraft applications. To solve or at least mitigate the consequences of sharp interfacial property changes, nature evolved graded interfaces. This way property dissimilarities are bridged smoothly.

In this work graded interfaces between different materials in fiber metal laminates are explored. The attempt is to be understood as a bionic approach, without being bound to this model. The difference of the field to nature must be considered, but still remains a major source of inspiration. In the “State of the Art” section, it will be detailed that this has been the case in similar approaches in the field of adhesives before.^[6]

As will be described in detail in the following, the concept of functionally graded materials and functionally graded adhesives is suitable to intermediate and reduce stresses between dissimilar materials.

Although one might assume the contrary, the influence of the adhesive onto fiber metal laminates is not self-evident, as FMLs can also be “glued” by part of the matrix material of the FRP. The introduction of an adhesive into the production process of FMLs is an additional time- and resource consuming step that requires rationalization in the eyes of (many) engineers. It is therefore also the aim of this work to elucidate the usefulness and potential of using an additional adhesive that is purposely introduced. The interphases of an FML are many and are a point of intersection for additional functions, features and for the tuning of properties.

2.1 Controversy about the Importance of Light Weight Construction

A large degree of this work’s motivation and rationalization is the further development of the technology of lightweight materials. The importance of lightweight construction for fuel consumption reduction in combustion engine powered cars has so far been the undisputed. With the increasing speed of the introduction of battery powered electric vehicles, even during the 3-year period of this work the question of the importance of lightweight construction in the automobile area came up.

A study on the topic of lightweight construction by McKinsey from the year 2012[2] projects the share of lightweight materials in cars to increase from 29% in 2010 to 67% in 2030.

Controversy was sparked by a study conducted at the University of Duisburg-Essen at the Center Automotive Research (CAR) in 2017.[3] The study tested two battery powered electric cars (BMW i3, Tesla Model S) under the same conditions, but with added loads of 100, 200 and 300 kg. With increasing weight, the cars had only a minimal increase in power consumption of maximally 0,6%. The measured increase was within the detectors' tolerance for inaccuracy. The reason for the low impact of the vehicle's weight, so the study's authors, lies in the recuperation of energy that is possible with electrically powered vehicles. The study's conclusion was that lightweight construction in battery powered electric cars is nearly meaningless and therefore has lost its justification. It received much attention in German press and among industry experts.

The study was followed by commentaries such as one by Ulrich Schiefer, a long-time developer at BMW, implying incompetence in the evaluation of the study's data [4]. According to Schiefer the BMW i3 is much more efficient than the tesla model3 (13 kWh per 100 km compared to 18 kWh) because of its body being based on carbon fiber reinforced plastics (CFRP). The i3 therefore needs almost a third less power for the same distance.[4]

Many Industry leaders [5] and members of the scientific community agree that lightweight construction is important to increase electrically powered car's efficiency and extending the range with a better cost-benefit calculation than simply adding battery capacity [5,6]. Additionally, to the effect that is generated by the lowering of the vehicle's weight it is often possible to simplify a component's production process, for example using a one-step process with new lightweight material compared to multiple step processes with conventional materials.

Carbon fiber reinforced plastics have 50% of the weight of conventional steel used in car construction but cost 570% its price [2]. Hybrid materials combine various cheaper lightweight materials such as aluminum and high strength steel with fiber reinforced plastics where they have the most impact. This way, with hybrid materials it is attempted to gain the highest possible weight reduction while maintaining a moderate price increase.

3 State of the Art

3.1 Fiber-Metal-Laminates

A fiber metal laminate (FML) is a hybrid material that is made up of alternating layers of metal and fiber reinforced plastics. Many definitions exist, but to the least an FML has to consist of one FRP and one metal layer. FMLs that are produced with the matrix material of the FRP as the bonding agent to the metal sheet(s) are called “intrinsic hybrid laminates”.^[7]

To overcome the problem of poor fatigue strength of aluminum alloys and poor impact- and residual strength of carbon fiber reinforced composites, starting in the 1950s the development of hybrid materials that combine both metal and fiber reinforced plastics began. It was found that in laminates of alternating layers of metal and composite material, the adhesive layers behave as crack dividers, if the crack start in one of the sheets of the laminate only.

In 1978 the Faculty of Aerospace Engineering at the Delft University of Technology introduced the first fiber metal laminate material called ARALL (Aramid Fiber Reinforced Aluminum Laminate). Later developments include the use of carbon fibers and high strength glass fiber instead of aramid fiber.^[5]

As already mentioned, the main advantage, which leads to the development of fiber metal laminates is their high fatigue resistance. This is due to the behavior of cracks and the restraint of crack opening. The fracture toughness of the combined materials (metal alloy and fiber reinforced plastics) is higher than the individual fracture toughness of the components alone.

Another advantage of FMLs is their excellent moisture resistance, due to the barrier effect of the metal. The moisture absorption of FMLs is lower compared to fiber reinforced plastics. The high melting point of the fibers inside the hybrid material leads to an overall high fire resistance of FMLs. The low density of FMLs is the reason why this material is used in light weight construction. Because a structure made up of FMLs usually requires less parts and reforming steps, it is possible to save costs in the manufacture and the operation of, e.g. a car or machine that comprises FML parts. The overall cost of FML-parts is still higher than parts that consist purely of metal^[5]

Table 1: Advantages and Disadvantages of FMLs[5]

Advantages	Disadvantages
High fatigue resistance	Process circle times compared to pure metal parts
High strength	Overall costs
High impact resistance	
Moisture resistance	
Fire resistance	
Low density	

The most prominent example of FML commercialization is the Airbus A380, whose fuselage is made in part of the material “GLARE” (Glass Laminate Aluminum Reinforced Epoxy) As the name suggests, GLARE is made of alternating sheets of thin aluminum alloy and glass fiber reinforced epoxy. Like ARALL it originates at the University of Delft. [8]

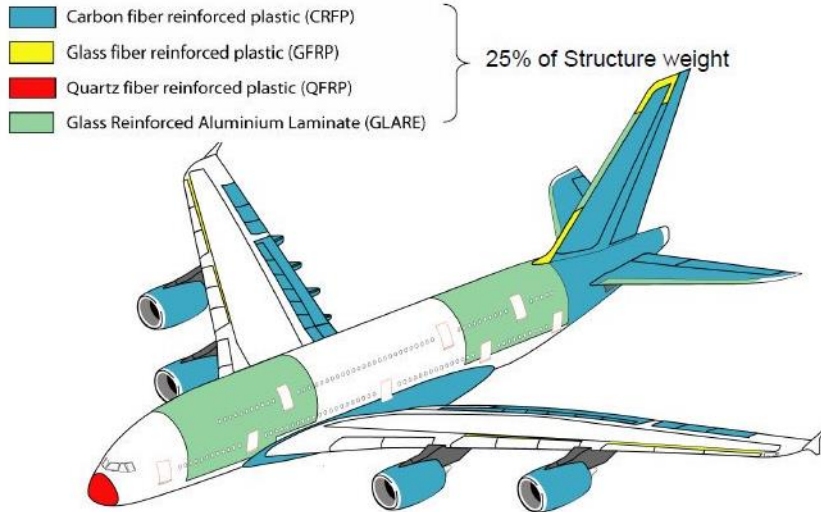


Figure 3: Composites in the airbus A380^[9]

Current developments in the FML field include automating the production to reduce costs and integrating electrical diagnostics to monitor structural health.^{[10] [11]}

Challenges include surface treatment, missing testing standards, thermal residual stresses and machining. A problem is the use of FMLs as a replacement for metal parts without change of the geometry of the part. This approach is called “black metal approach” and is still widely used despite of benefits that come with a change in geometry.^[7,11,12]

3.2 Structural Adhesive Bonding

Structural bonding is a key technology in lightweight construction, especially via hybrids: It allows the joining of highly dissimilar materials, the design of individually shaped joints and the distribution of loads over a large area. Mechanical fastening is expected to only provide half the tensile strength of its weakest adherent. A single lap joint can provide the same tensile strength as the weakest adherent. This is due to high stress concentrations in mechanical joints.^[13]

The disadvantages of structural adhesives (and adhesives in general) are: no disassembly without damage possible, high sensitivity to environment, very hard damage monitoring and abrupt failure. The uncertainty regarding its long-term stability is the biggest disadvantage of adhesives today.^[13]

It is not clearly defined what a structural adhesive is. The “Encyclopedia of materials: Science and Technology” defines it via its use:

“A structural adhesive can be defined as a material used to transfer loads between adherents in service environments that are typically load bearing [...]”^[14]

This definition differentiates the adhesive's use from other very common fields of adhesive application, such as attaching signs, ornamentation or parts that are not contributing to the stability and integrity of a structure. Intuitively an adhesive that is used in load bearing of a structure should be strong. When selecting the adhesive under this primary attribute the choice will probably be a rigid two-part epoxy or a cyano acrylate. Such adhesives however have very little strain capability (<0,3%) and might cause severe failures in the designated application. The ultimate bond strength can also be increased by changing the geometry of the bond, e.g. increasing the bond area. An adhesive with higher strain capability can then be chosen over a strong one.^[15] Except for strength and maximum strain, other important criteria for the selection of adhesives can be surface preparation effort, substrate compatibility, initial bonding strength, cure time, chemical and water resistance, sound characteristics and aesthetic properties.^[15,16]

There are hundreds, if not thousands of adhesive types that come in two components, one component, thermoset, thermoplastic, liquid, tape, UV-, heat-radiation and room temperature cured. The most abundant chemistries in use are^[15]:

- Epoxies
- Polyurethanes
- Acrylic
- Cyanoacrylate

A new trend that is currently underway are structural thermoplastic adhesives based on polyolefins and polyamides.

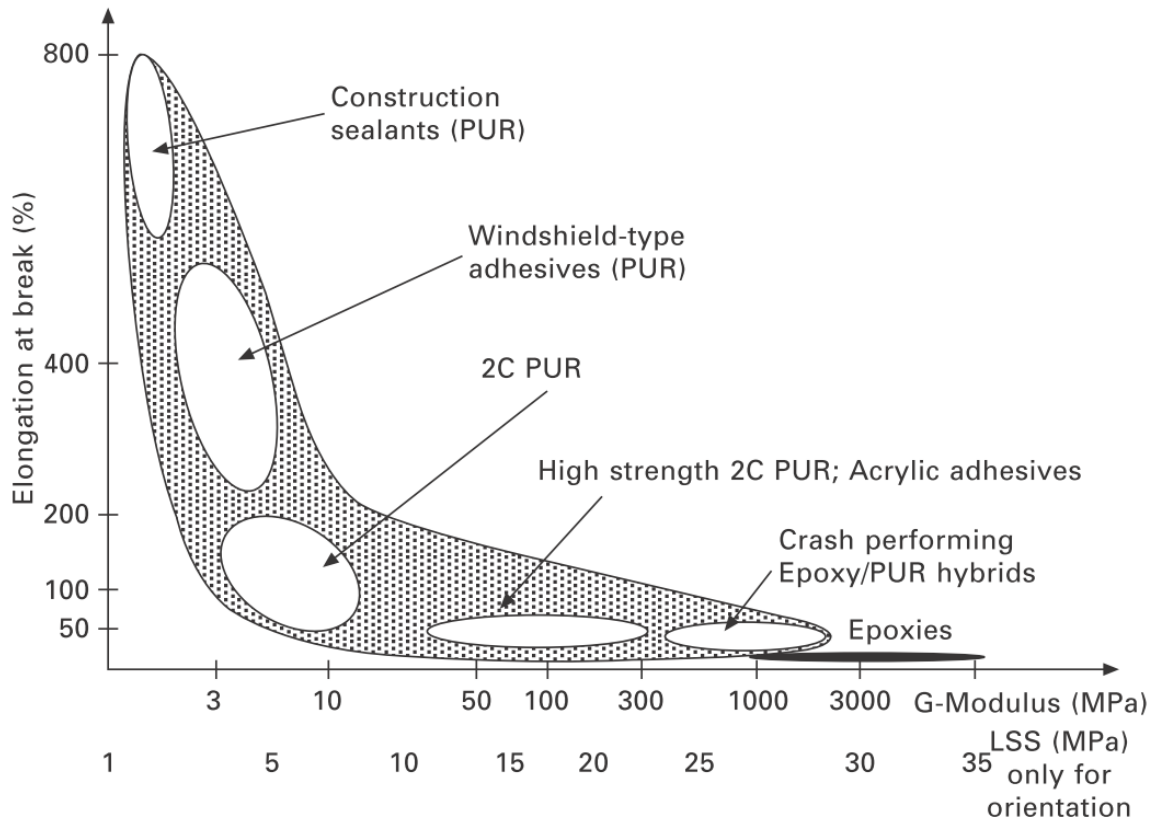


Figure 4: "Landscape of adhesives" from Bernd Burchardt, Sika Adhesives. LSS is the lap shear strength, the most common value to classify an adhesive's strength.^[16]

Figure 4 shows the attempt of an overview of available elastic properties of adhesives. Of the available adhesives polyurethanes show the largest spectrum of properties, ranging from rigid to elastic. The lap shear strength in most cases decreases with higher elasticity, although this is not a law of nature. Many factors increasing the tensile strength of an adhesive however decrease the elasticity, for example the amount of hard segments in a polyurethane.^[17]

3.3 Adhesive Bonding of Hybrid Materials

Hybrid materials in this context are joints of fiber reinforced plastics and metals. Many hybrids are produced as local reinforcements of components. Another common technique is to patch components using RFP. Common bond types are shown in Figure 5.

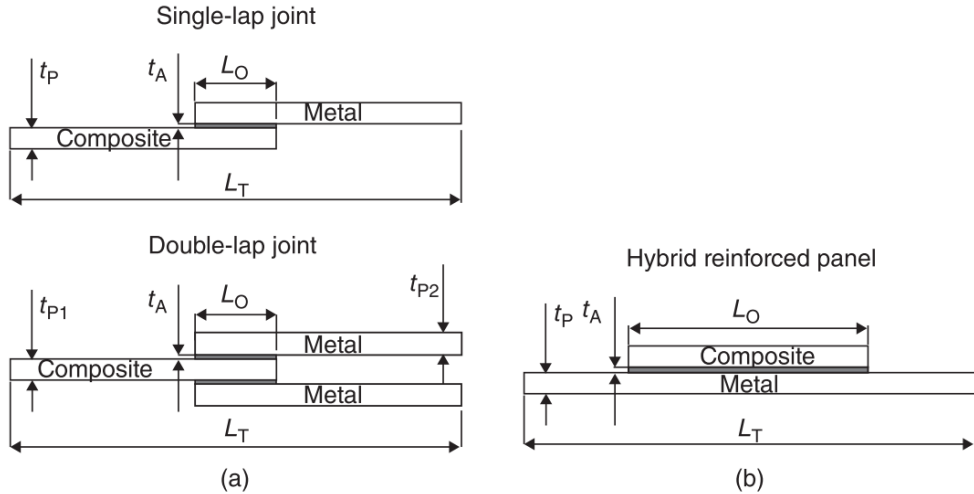


Figure 5: The most common bond types of hybrid materials^[13]

Adhesive joints of hybrid materials show unfavorable stress distributions and tensions because of the dissimilar properties of the adherents. The tensions arising from the mismatch of elastic properties is explained in more detail in section 4.1. Another reason for tensions in hybrid materials is the difference of the thermal expansion coefficient of FRPs. This is summarized as the $\Delta\alpha$ -problem (α is the coefficient of thermal expansion). This problem can occur whenever a hybrid bond is subject to temperature changes. If the bond is part of an aircraft component it might go through extreme temperature variations due to its changing altitude, heating due to friction of air or simply different climates of the aircraft's area of operation. Most adhesives and FRPs with thermosetting matrix are cured at elevated temperatures (typically at 150-180°C). Components used in automobile bodies will be exposed to the heat used to cure electrophoretic deposition (EPD) coatings. In practice the heat of EPD curing is used to post-cure the adhesive.

When an adhesive is subjected to thermal curing, the two adherents with different thermal expansion coefficients will expand or even compress if the coefficient is negative. Depending on the adhesive's own thermal coefficient and rigidity three scenarios are possible: The adhesive will slip between the two adherents, one of the adherents deforms or one of the adherents stretches. When the curing completes the adhesive is no longer fluid and the matrix of an FRP becomes rigid. The consequence again can be threefold: A failure of the bond occurs if the stress is larger than the adhesive can sustain. If one of the adherents is the weakest part, it will fail instead of the adhesive. Most commonly a permanent deformation of the structure is observed.^[13]

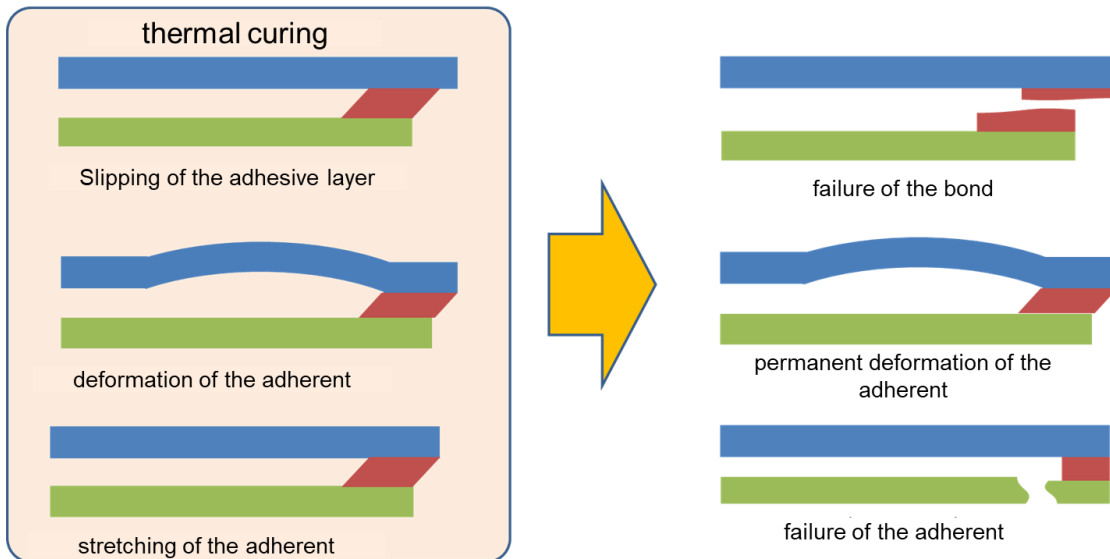


Figure 6: Emergence and problems of tensions between the adherent and adhesive due to different thermal expansion

Many attempts have been made to solve this problem, however, even if temperature differences in the production are eliminated, problems with tensions can still occur because of the environment the component is subjected to.

3.4 Functionally Graded Materials

Functionally graded materials (FGM) possess a gradual variation of composition and thereby properties in one direction of the material's volume. For example, the materials stiffness increases gradually along one axis within the material.

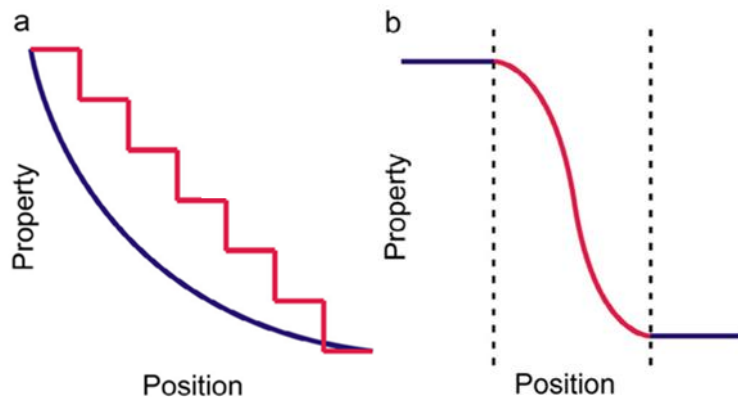


Figure 7: Concept of functionally graded materials: gradual or stepwise property distribution^[18]

The concept of functionally graded materials was proposed around the year of 1984 by the Japanese NKK Corporation. They were developed as thermal barrier coatings for aerospace applications. ^[19,20,20] Figure 8 shows an FGM that serves as a thermal barrier. It consists of ceramic on the surface and increasingly of metal towards the bulk. This way a sharp transition of the thermal expansion coefficient is avoided.^[21]

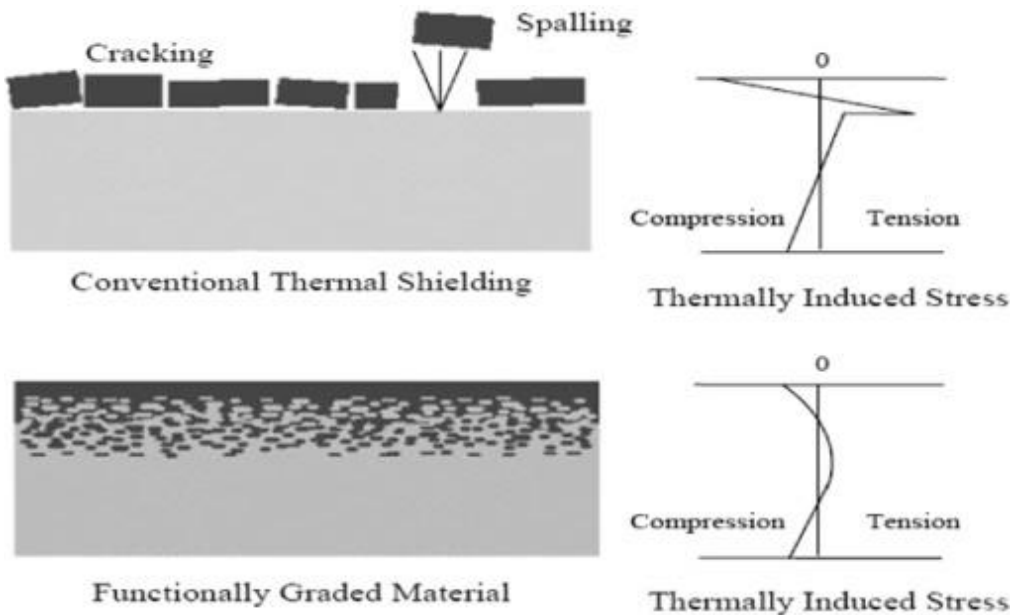


Figure 8: Conventional thermal shielding vs a functionally graded material (left); thermally induced stress in the material (right) ([21])

In a paper published in 2009 Kashtalyan et al. from the university of Aberdeen^[22] examined the effect of a functionally graded interlayer integrated into a coating between the top coat and the substrate. The aim was to find out if such an interlayer could help reduce tension between the substrate and the coating. The effect of a functionally graded interlayer on the bending response of coated rectangular plates subjected to mechanical loading was modeled mathematically. The Young's modulus of the interlayer was assumed to vary exponentially through the interlayer. The work concludes that a graded interlayer eliminates the gap in the in-plane normal shear stresses in the interface without increasing stress values in the topcoat. In single layer functionally graded coatings it was found that the stresses throughout the thickness of the coating were decreased while stress levels at the interphase increased. For stiffer coatings protecting much softer substrates intrinsic tensile strains that cause cracks and failure of the coating were eliminated.^[22]

3.5 Functionally Graded Materials in Nature

“When trying to imagine the early life forms that populated our planet, even without having a specific picture in mind, we probably think of strange creatures that have the consistency of slimy pudding or tofu”.^[6] When evolution lead to the occurrence of scaffolds, baskets, shells and bones, adaptation also occurred with regards to the main mechanical problem when soft matter is in contact with a stiff material: “contact deformation and damage”^[23]

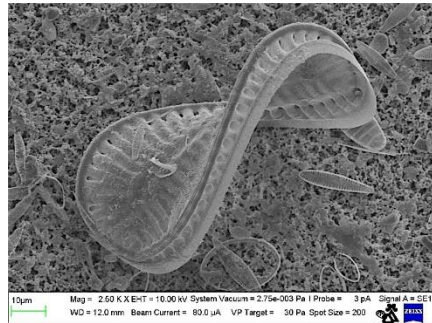


Figure 9: SEM Picture [source: Wikipedia commons] of a diatom. This primitive kind of algae developed a stiff silica-based scaffold. This type of organism is contributing around half the organic material in the ocean and is responsible for 20% of oxygen produced on the planet each year^[24]

The scientific examination of many interfacial boundaries and zones in biological organisms found that nature's answer to the problem of contact deformation is gradient interphases. They have been examined in detail in worms' jaws and in mussel byssi. The mussel byssus is a well-examined object in adhesive technology. At the end of the byssus is one of nature's top performing adhesives that helps mussels stick to various surfaces underwater with strength unmatched by man-made adhesives. But the byssus itself is also interesting, if it is regarded as a large macroscopic interphase or at least a mediator between the hard and stiff surface that the mussel is attached to and its soft tissue.

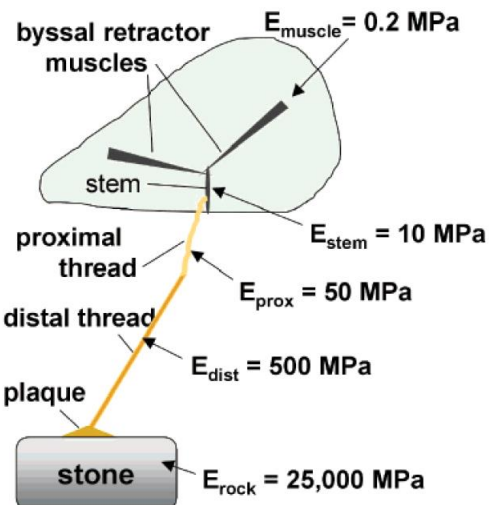


Figure 10: Functional gradient in a mussel byssus^[6]

The idea of applying gradients with nature as the model is not new. It was for example discussed in a detailed publication by Liu et al. in 2017. ^[18] The history of the idea of a gradient layered adhesive is discussed in the following section.

3.6 Functionally Graded Adhesives

Functionally graded adhesives were first developed even before the term FGM was coined in the early 80s for heat shield coatings. Like the heat shield application, functionally graded adhesives were also first tested in the context of space aviation. In 1961 the Republic Aviation Corporation of Farmingdale, USA applied a graded adhesive in bonded rocket motor cases.

With an increased interest in functionally graded materials in general in the 1990s, 2000s and until recently, research has also been conducted in the field of functionally graded adhesives.^[3]

3.6.1 Functionally Graded Adhesives in Single-Lap Joint

Adhesive bonding offers a number of advantages over other types of bonding such as welding, screwing and riveting. The load stress can be distributed over a large area, avoiding stress concentrations; corrosion can be avoided. When combining composites and metals it is the bonding type of choice, because other kinds of bonding such as welding do not work at all.

In some joint configurations, such as the single-lap joint, there are, nonetheless, unfavorable stress configurations present.^[25]

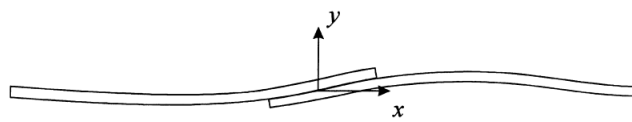


Figure 11: Deformation of a single-lap-joint under tensile loading^[25]

The single-lap joint has been studied extensively with early theoretical work done by Volkersen as early as 1938^[26]. Modern modeling by finite element analysis shows the stress distribution in the adhesive layer of the single lap joint (Figure 12).

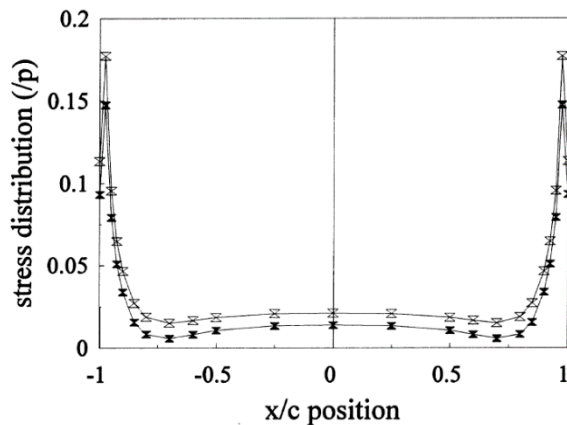


Figure 12: Longitudinal stress distribution along the centerline of the adhesive layer of a single lap joint (case of two composite materials)^[25]

The stress level increases significantly towards the edges of the adhesive layer due to the deformation of the joint (Figure 12), before dropping again at the very edge of the layer (“stress free” condition at the end of the joint^[27]). This non-uniform stress distribution leads to a lesser bond strength^[27]

Efforts were made to compensate the stresses in the regions at the edges of the single-lap joint by changing the geometry of the joint^[28]. Others focused on changing the adherent composition at the joint interface, such as by fiber placement.^[29]

Recent studies investigate the use of functionally graded adhesives (FGA) in single lap joints. The elastic modulus of the adhesive is altered to balance the non-uniform stress distribution of the joint. For example, Carbas et al.^[27] used carbon black nano-particles to vary the modulus of epoxy based adhesives. By adding an amount of up to 20% of particles the adhesive's modulus was adjusted between 1.4 GPa (20 Volume-% particles) and 1.7 GPa (0%-Volume particles). The addition of the carbon black also reduced the yield strength of the adhesive by up to ca. 15% for the highest filler grades.

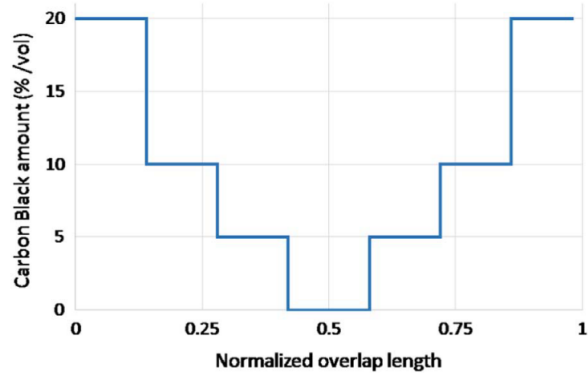


Figure 13: Adjustment of the adhesive modulus in the single-lap joint by Carbas et Al.^[27]

The modulus of the adhesive was adjusted in the joint according to the stress distribution. The adhesive layer has a lower modulus towards the joint's edges, where higher stress distributions are located according to theory and modelling. According to the published data this method leads to an increase of the joint's performance of 20%.^[30]

A similar, yet more sophisticated approach was developed by Chiminelli et al. at the Aragon Institute of Technology in Zaragoza, Spain. Instead of modifying an adhesive, a so-called adhesive mixing approach was used.^[31]

A major challenge of functionally graded adhesives is the efficient application. To deal with this problem, an adhesive mixing apparatus was constructed that allows a seamless application of a gradient adhesive single lap joint.

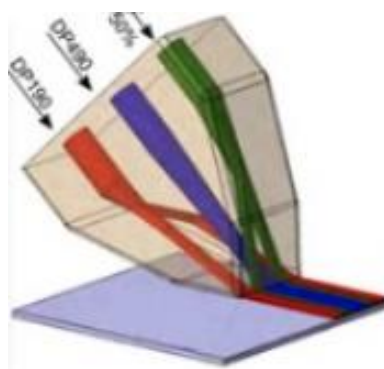


Figure 14: Application apparatus for a functionally graded adhesive by Chiminelli et al. (3M Scotch Weld DP490 tough-elastic epoxy (blue), 3M Scotch Weld DP190 (red), flexible epoxy adhesive and green 1:1 mixture of the two adhesives)^[31]

In the study the Spanish group reports a load improvement of 70% in a single-lap joint of a carbon fiber composite material to aluminum, compared to the optimal monolithic adhesive.^[27,31]

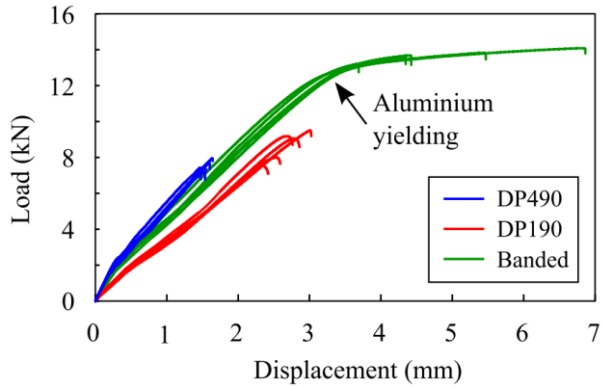


Figure 15: Load improvement by a functionally graded adhesive in a single-lap joint according to Chiminelli et al.^[31]

The aforementioned studies all focus on the optimization of single-lap joints. In Fiber Metal Laminates however, the joint between the layers of the laminate are planar. Another study by Apalak et al.^[32] investigated the effect of a functionally graded adhesive in a single-lap joint between a ceramic (Al_2O_3) layer and a pure metal (Ni) layer by finite element analysis. In this system the effects of the fringes of the overlap were again critical for the performance and failure of the system and the influence of the gradient was little.

In a fiber metal laminate, the bond is not characterized by fringe zones. The joints are planar and do not overlap on the edges. The stress distributions are dependent on the loading and field of installation of the fiber metal laminate. Section 4.7 describes the behavior of FMLs in three-point bending tests. The loads applied in these tests are much more suited to analyze the performance of FMLs and their adhesive layers. The principle of using a functional gradient to equal out stress concentrations in the adhesive layer and the methods are however similar. The stress concentrations and derived orientation of the gradient are different on the other hand.

3.6.2 Functionally Graded Adhesives in Planar Joints

A thorough research of the available literature did not outcrop any publications on the application of a functional gradient adhesive in fiber metal laminates. A study conducted by the United States Army Research Laboratory in 2009^[33] investigated the application of a functionally graded adhesive in the joint of a rubber (neoprene) and a metal. As stated in the published work the idea for this procedure was taken from the structure of squid beaks. Squid beaks are made from very rigid, stiff organic material that is surrounded by soft tissue. Nonetheless, they can transfer strong forces without the soft tissue being damaged. This is due to the fact that a functional gradient exists between the beak and the soft tissue material.

In the approach a nitrile rubber-based flexible adhesive (3M 847) was modified by addition of CaCO_3 , talcum and fumed silica. Layers of the adhesive containing 1, 5, 10 and 15% of the filler were then applied to the rubber substrate and bonded to the metal. After curing the joint was tested by clamping a holder to the rubber substrate and subsequently loading it with weights of 5, 10 and 12,5 pounds. The respective heavier load was applied when the joint could withstand loading for 3 minutes. Further testing was done with an Instron material testing device.

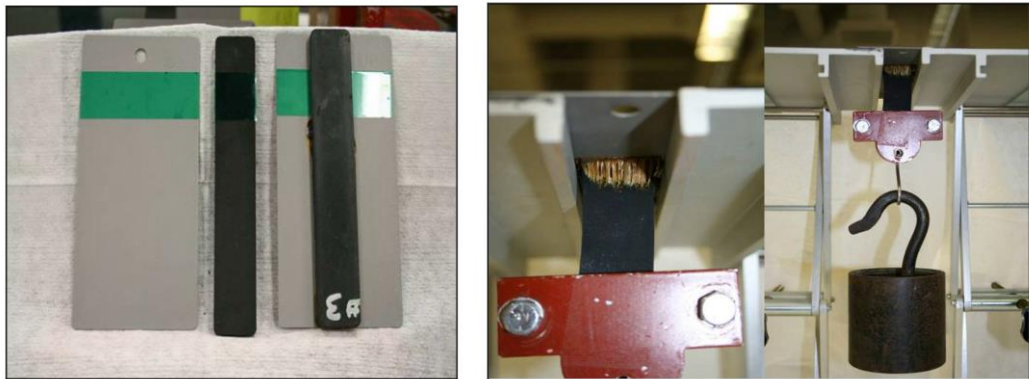


Figure 16: Substrates and substrate testing of rubber and metal joints as described by Stabler et al.^[33]

In the tests, interfaces with three layers of 0, 1 and 5% of either filler material yielded the strongest bond.^[33]

4 Analytical and Theoretical Background

4.1 Mismatch of Materials and Contact Damages

A structure consisting of two different materials suffer from contact deformation when under load. The degree of contact deformation depends on the difference in the materials' stiffness. This difference is called the mismatch. In simple systems, the contact deformation can be calculated if geometry and elastic properties of the materials are known. Such a simple system is a butt joint of two Materials A and B.^[6]

Closely tied to the stiffness of the materials is the Poisson ratio ν . When a material sample with a given length l is stretched by longitudinal forces F the Poisson ratio indicates if and how much the volume of the sample changes. The Poisson ratio is defined as follows:

$$\nu = -\frac{\varepsilon_{yy}}{\varepsilon_{xx}} \quad (1)$$

With ε_{xx} the axial strain and ε_{yy} the transverse strain. If the tension is constant over the cross section of the sample the Poisson ratio becomes:

$$\nu = -\frac{\Delta d/d}{\Delta l/l} \quad (2)$$

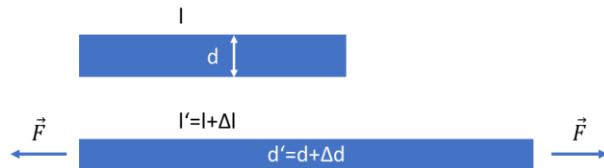


Figure 17: A sample is stretched by longitudinal forces F

A Poisson value of $\nu = 0,5$ means the volume is constant, $\nu < 0,5$ means the volume increases (e.g. metals) and a Poisson ratio of $\nu < 0$ means the sample's thickness d increases.^[34]

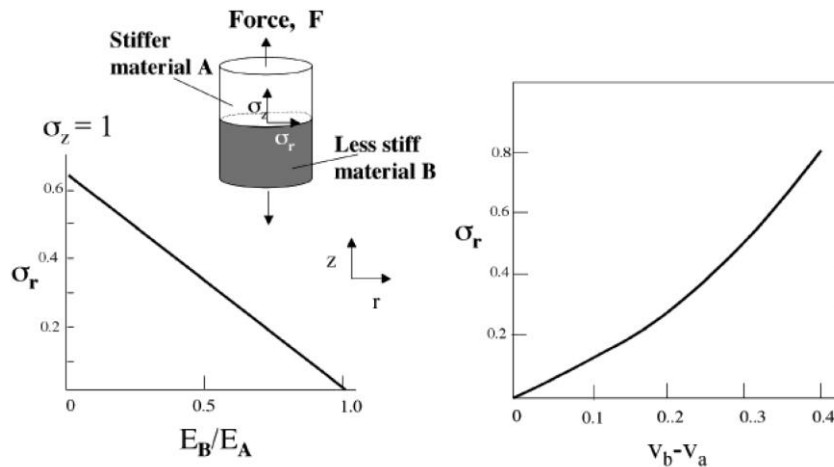


Figure 18: The graphs show the radial stress in relation to the stiffness of one material (B) in a butt joint consisting of two materials with different stiffness E . In the first graph the Poisson ratio ν is fixed at 0,4; in the second graph the difference between the Poisson ratios varies at a fixed stiffness ratio of 1^[6]

In the case of a butt-joint (Figure 18), loading with a force F leads to overall homogenous stress σ_z . If the stiffness of A and B is not the same, the deformations ϵ_A and ϵ_B will also differ. In the contact zone the difference between the deformations leads to interfacial stresses: σ_θ (circumferential stress) and σ_r (radial stress). They act normal to the applied stress σ_z and can be calculated according to formula (3):

$$\sigma_\theta = \sigma_r = [v_B - v_A E_B / E_A] [\sigma_z / (1 - v_B)] \quad (3)$$

The determining variables for interfacial contact damages are the stiffness values of each material E_A and E_B and the Poisson ratios v_A and v_B .

The radial stress σ_r reflects the mismatch and plays a crucial role for the structural failure in the contact zone of two materials.

4.2 Mechanical and Microscopic Analytics

The performance of an adhesive joint in FMLs depend on a complicated interplay of many interdependent factors. These factors are mainly the different load situations such as tensile and peel stresses that are superimposed. The situation becomes even more complicated when a multi-layer laminate or even a whole component is being investigated. A material and component also have a history, because of the manufacturing, reforming and curing that takes place. During the production processes, stresses are introduced by thermal curing and reformation. On the other hand, the adhesive can influence the manufacturing. For example, the viscosity of the FRP material is reduced extremely when heated which also leads to the fibers being set in motion. Especially during reformation uneven stresses have to be applied that can lead to an unwanted displacement of fibers. The adhesive can act as a barrier for this fiber floating or reduce stress levels locally if applied correctly.

The following microscopical methods served the purpose of surveying the modifications made on the adhesives, such as the distribution of additives in the adhesive joint and the interaction of combined adhesives joints. They were also used to find out about the influence of the adhesive onto the neighbouring materials.

Scanning Electron Microscopy (SEM) was used to visualize the distribution of adhesive modifiers inside the joint. In combination with **Energy-Dispersive X-ray spectroscopy (EDX)** it was possible to gather information on both, the combined adhesives and the adhesive modification approach, by mapping chemical distributions.

Mechanical analytical methods were used to examine the impact of the modifications on the adhesive, on simple binary laminates and on more complex multi-layer laminates.

The foremost aim of this work is to examine the effect of gradient distributions of the modulus in the adhesive joint on the mechanical performance during load of fiber-metal-laminates. To find and verify the effect of inorganic fillers on adhesives' modulus, **tensile stress tests** were performed.

For the elastic adhesives used in this work the **dynamic mechanical analysis** proved to be a proper tool.

The **lap-shear test** was used to investigate the effect of the adhesive modifications on their performance in bonding.

To simulate typical load and failure incidents of the metal-fiber-laminates, **virtually static- and dynamic three-point flexural tests** were performed. The outcome of these tests was used to gain evidence for the influence of the adhesive modification on the performance of the fiber-metal laminates.

4.3 Tensile Test

The tensile test is a basic test to determine the material properties “tensile strength”, “breaking strength” and “maximum elongation” directly. Young’s modulus, Poisson ratio and yield strength can be obtained from the analysis of the results of the measurement. ^[35] ^[36] The test specimens and test procedures are standardized. The most common standard is ATSM D638 “Standard Test Method for Tensile Properties of Plastics”. Following this standard, the modified adhesives in this work were tested.

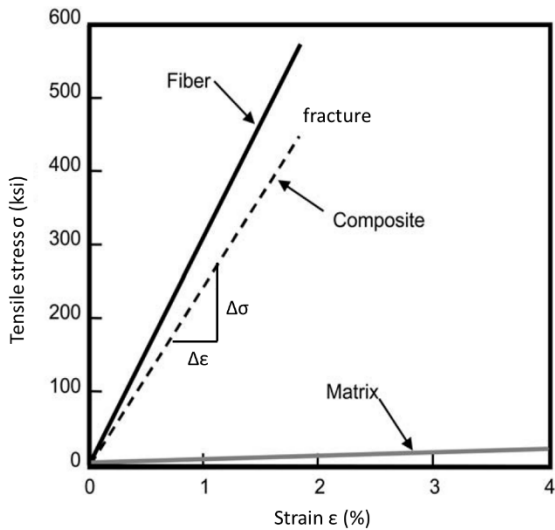


Figure 19: Stress-strain curves of fiber, matrix and composite (the si unit of stress is N/mm^2 ; adaptation from ^[37])

Tensile testing is usually carried out on a universal testing machine (Figure 20). The test specimen is placed between two crossheads, one of which can move and thereby apply a tensile force. The applied force and distance are measured electronically. The force is increased until the test specimen breaks. A machine designed for high forces and small elongations should not be used for a material whose expected properties are not in the machine’s effective range. Otherwise the measurement is unprecise or in extreme drowned in the measurement’s noise. The recorded data are usually displayed in a stress-strain diagram.^[35]



Figure 20: MTS Universal Testing Machine (MTS)

4.4 Lap-shear strength test

The lap-shear strength is the standard value that is commonly used to compare the adhesive strength of adhesives. This is due to its simplicity and the fact that single-lap-joints are the most common type of bonding. Even though an adhesive might not be intended to be used in a single-lap-joint, it is therefore helpful to find out general characteristics and produce a test value that is comparable.

The thickness of the substrate is an important factor in this test that influences substrate yielding. Very high strength structural adhesives are therefore tested with special arrangements, which are based on thick blocks rather than thin sheets, as in the lap shear test.

The lap shear test is performed in accordance with the US standard ASTM D1002 "Standard Test Method for Apparent Shear Strength of Single-Lap-Joint Adhesively Bonded Metal Species by Tension Loading (Metal-to-Metal)". Other substrates can be tested according to the same or similar procedures. An important factor influencing the result is the surface preparation of the substrate. In fact, the ASTM D1002 is used to compare surface preparation techniques.

The test specimens are prepared as depicted in Figure 21. They are then placed in a material testing machine and pulled at a rate of 80-100 kg/cm² of the shear area per minute. The loading is continued until failure occurs.

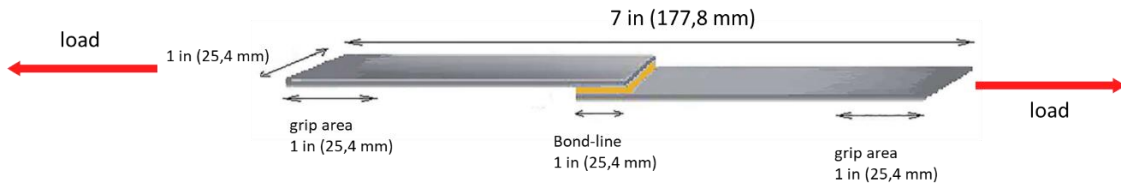


Figure 21: Test specimen of the lap shear test according to ASTM D1002. Dimensions given in inch as in the standard and in SI. [Adaptation from^[38]]

The failure can be adhesive, cohesive or substrate and is sometimes expressed in grades, such as substrate near cohesive failure to describe the quality of the failure. The normally preferred failure mode is cohesive.^[39]

4.5 Dynamic Mechanical Analysis (DMA)

Dynamic Mechanical Analysis uses small deformations of a material to study its response. The deformations are applied in a cyclic manner. Stress, frequency of the deformation and temperature can be varied during the analysis. It is frequently used to study the behavior and properties of polymeric materials such as rubber, plastics, coating free films and adhesives. DMA allows to get information about important material properties such as range of possible working temperatures, glass transition temperature, viscoelastic behavior, stiffness and toughness.^[40]

A DMA works by generating a sinusoidal movement by means of a force motor and transmitting it onto a sample via the so-called drive shaft. The “Linear Variable Differential Transformer” (LVDT), a sensor to measure distance, controls the movement of the drive shaft. The user can predetermine the stress or strain the sample is subjected to. A thermo sensor close to the sample fixture controls the temperature. Figure 22 shows the schematic of the Perkins Elmer DMA 8000.

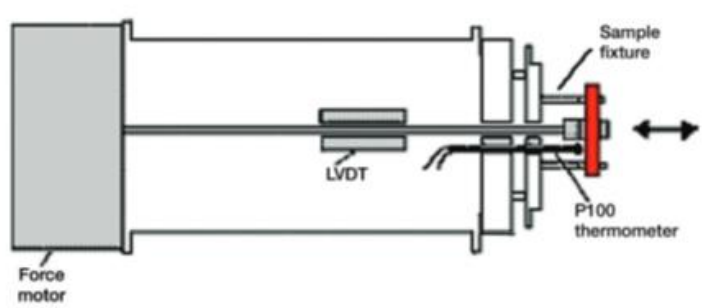


Figure 22: Schematic of the Perkins Elmer DMA 8000^[40] LVDT stands for “Linear Variable Differential Transformer”, a sensor that measures the movement of the driveshaft.

The received values are stiffness and damping, expressed as modulus and $\tan \delta$. Because the applied force is sinusoidal the DMA gives an in-phase component of the modulus called the storage modulus E' and an out of phase component called the loss modulus E'' . The storage modulus gives information about the material's elastic properties. The ratio of loss and storage modulus gives $\tan \delta$:

$$\frac{E''}{E'} = \tan \delta \quad (4)$$

The damping is a measure of the energy dissipation of the material.

The DMA is a very powerful tool that allows an experienced user to find out many things about a material, even more so if he is adept in mathematics also. For everyday use it is the method of choice for determining a value of the stiffness of thin films, such as adhesive films.

4.6 Quasi-Static Flexural Testing

The three-point flexural test is used to examine the flexural stress-strain response of a material. It provides information about the elasticity of the material in bending. The attribute “quasi-static” is related to the rate of the loading, which is slow compared to a dynamic flexural test. The test is used to characterize the material’s behavior under load and the failure behavior.

The quasi-static three-point flexural test was done based on DIN EN ISO 7438 (2016-07-00)^[41] since there is no standard for fiber-metal laminates. The test method is very simple and straight forward. Because FMLs are anisotropic, it is important to regard the fiber directions of the sample, especially if the FML contains a unidirectional tape. Figure 23 shows the arrangement of the test.

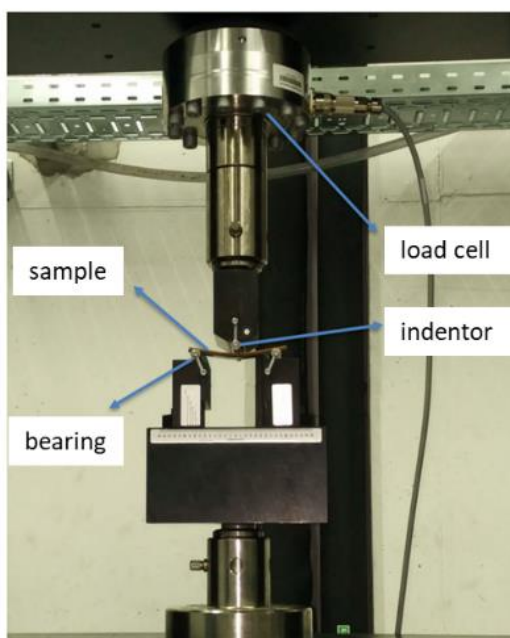


Figure 23: Arrangement of a 3-point flexural test
[courtesy of Deviprasad Chalicheemalapalli Jayasankar, LiA University of Paderborn]

The bending test is often used to analyze fiber reinforced plastics, because they are more often exposed to bending loads rather than axial loads. In bending the sample beam is subject to both compression and tension, so both types of stresses can cause failure. In an elastic beam the maximum tensile stress and compressive pressure are equal in magnitude.^[42]

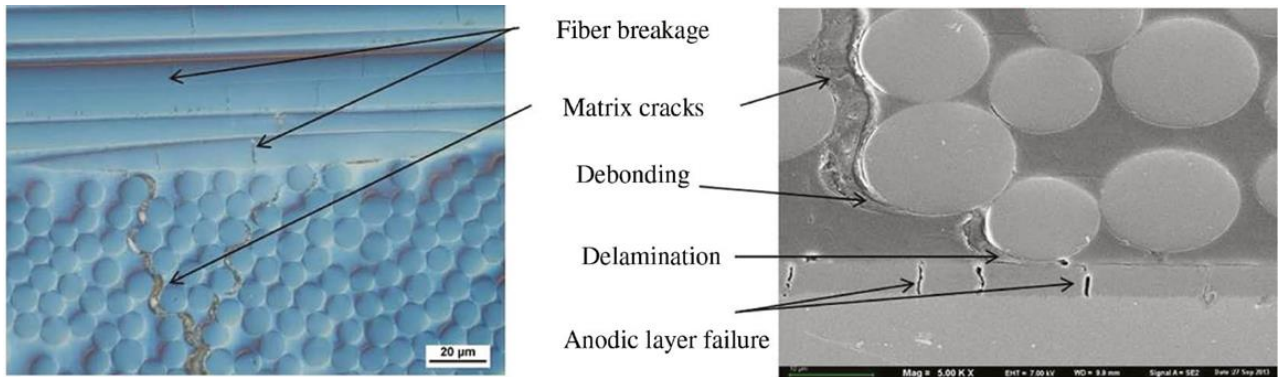


Figure 24: Microscopic failure that leads to the failure of FMLs in 3-point bending tests^[42]

The metal in FMLs normally deforms plastically, so the tension is transmitted to the fiber parts of the FML, which is comparably brittle. Figure 24 lists various microscopic failures that occur in the FRP. The majority of these failures leads to the formation of cracks. These cracks are deflected and caged by the metal parts of the FML and to a degree absorbed by the adhesive. The management of these cracks in the FRP are therefore an important field where FMLs and FRP material can be improved.

4.7 Dynamic Three-Point Flexural Test / Charpy Impact Test

The Charpy impact test is a standard test method to determine a material's notch toughness. In the test arrangement the sample is mounted in a holder. The holder is in the path of a pendulum that has a specially shaped hammer at its end (Figure 25).



Figure 25: CEAST pendulum impact tester for Charpy tests

In some cases, the sample is notched before the impact to assure its complete failure. This is not done with fiber metal laminates, however. The hammer is released from its position thus hitting the sample. The energy absorbed by the material can be calculated from the hammer's mass m , the height of its release position (h_1) and the maximum height the hammer reaches after the impact (h_2).^[43]

$$W = m \cdot g \cdot (h_1 - h_2) \quad (5)$$

In state-of-the-art test equipment this analysis is done automatically. Such apparatuses usually give the peak force and energy as well as total energy absorbed and a relation of the force and the deformation.

4.8 Scanning Electron Microscopy (SEM)

The fillers used to modify the adhesives to get the desired properties are in the micro- and nanometer dimension. The thickness of the adhesive interlayers created and the interphases of different adhesives that occur are as well in the micrometer scale. For the objective of this work it is essential to observe the local distribution of micrometer- and sub micrometer sized phenomena and objects.

To analyze the constituency of the material in the necessary depth and resolution, the scanning electron microscope is the first choice.

The scanning electron microscope was invented by Manfred von Ardenne in 1937 and commercialized for the first time by Cambridge Scientific Instruments in 1965. As the name suggests the principle that differentiates the SEM from its preceding electron microscopes is that fact that the image is produced by scanning the substrate instead of taking a picture of the whole at once.

The scanning process reduces a problem that plagues both light- and electron microscopes, the spherical aberration: electrons that enter the lens with a large angle towards the optical axis are scattered stronger than electrons entering the lens centrally. This increases the resolution of the pictures taken. The second error in both light- and electron microscopy is the so-called chromatic aberration. This error arises because refraction of lenses is dependent on the wavelength of the entering waves. With light microscopes this problem is solved by introducing diverging lenses. In electron microscopes this problem was solved only in the 1990s with overlaid magnetic fields produced by multipole elements.^[44] ^[45]

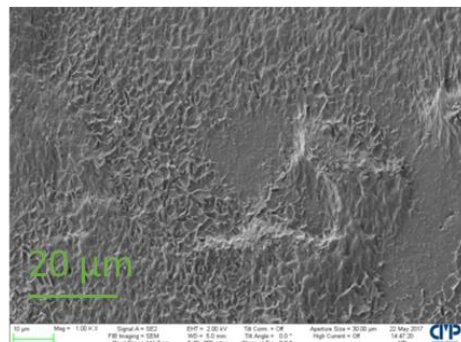
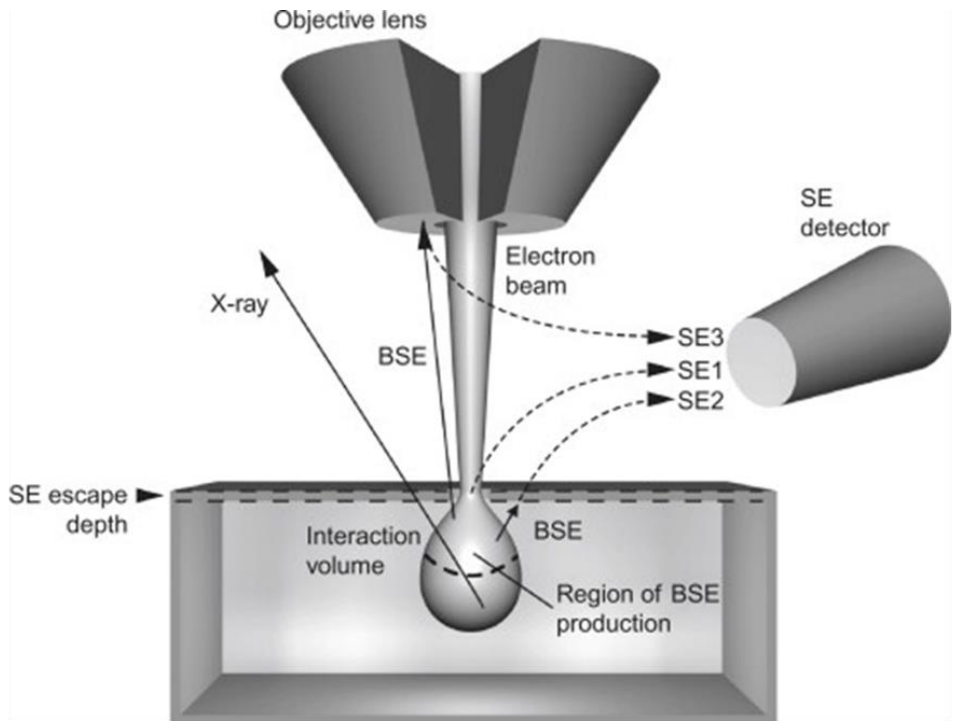
Electrons interact with the substrate in various ways that can be used to extract information. The electron beam that is sent towards the sample is called primary electron beam. The first source of information is so called secondary electrons that are released by collision from the sample. These electrons have a low energy and originate from the sample surface and a few nanometers of the surface-near phase of the sample. They give information about the topography of the sample. The picture's contrast is due to the angle of a sample's surfaces and to a high degree on the sample's material composition. Conducting material that is not grounded is charged over time and appears brighter, isolating material appears darker. Materials with a higher density of heavy elements appear brighter.

Another type of electrons is the backscattered electrons (BSE) that originate from the primary electron beam and are scattered back elastically from the sample. BSEs penetrate the sample's

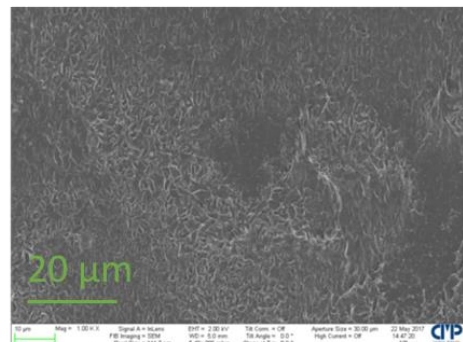
volume to some micrometers (1-2 μm , depending on the primary electron beam's voltage). Lighter elements scatter the primary electrons to a lesser degree than heavier ones and therefore appear darker in the detected picture. Because of these two facts BSEs are more useful to get information about the sample's material composition than secondary electrons.^[46]

Variants of the scanning electron microscopy are:

- “Environmental Scanning Electron Microscopy” (ESEM)
The electron beam is only produced in high vacuum which allows the sample to remain in light vacuum and without a sputter coating.
- “Scanning Transmission Electron Microscopy” (STEM)
A variant of transmission electron microscopy (transmitting single high energy electrons through thin samples) combining the raster scanning technique to produce images.
- “Scanning electron microscope with polarization analysis “(SEMPA)
A special detection method allows to measure the secondary electron's spin. This method allows the display of magnetic domains in magnetic materials.



SE2-detector



In-lens detector

Figure 26: The figure shows the same sample (a polyurethane based adhesive with mineral fillers) region mapped by the SE2-detector and the In-lens detector. The upper section of the figure shows the placements of the lenses inside the SEM and the regions the different types of detected electrons originate from. ^[47]

4.9 Energy-Dispersive X-Ray Spectroscopy (EDX)

If an electron is removed from an inner shell of an atom, an electron of higher energy immediately replaces it. In the process the electron assuming the lower energy state releases the energetic difference. This energy is transmitted via a photon in the x-ray spectrum and is characteristic of the atom, or element that it is released from. The intensity ($\frac{dP}{dX}$) of the emitted energy is proportional to the element's abundance.

Since the characteristic x-ray radiation can be stimulated by the collision with a focused electron beam, EDX is naturally combined with SEM in most cases. There are however stand-alone versions and even hand-held devices that allow, for example, quick identification of

metals. These systems are normally described with the acronyms XRF but rely on the same mechanisms of analysis. The excitation of the electrons is achieved via x-ray in these cases. To increase the spatial resolution, EDX can be combined with TEM. Thinner substrates and higher accelerating voltage cause less scattering of the electrons and thus a make for higher spatial resolutions.^[46,48]



Figure 27: Handheld XRF and stand-alone XRD-device [Dongguan Hongtuo (left) and Wikipedia commons (right)]

5 Experimental part

The experimental work consists of three different approaches to realize a functional gradient of stiffness in the adhesive bond between metal and FRP sheets of the fiber-metal laminate. The effect of different types of adhesives without a gradient was also examined along, as different types were used to realize the gradient.

In the first attempt a commercial epoxy adhesive as a representative of the most commonly used structural adhesive type was modified. The gradient was implemented by stacking layers of modified adhesive. The stiffness was modified by adding inorganic particles to the adhesive.

The second part deals with the combination of different adhesive types such as epoxies, polyurethanes and EPDM-based elastomeric adhesives. The latter classes of adhesives are an innovation in the field of structural adhesive bonding and especially in the field of fiber-metal laminates. A polyurethane adhesive was completely developed in this work and tested together with similar commercially available adhesives by Lohmann GmbH & Co. KG, Neuwied. The EPDM adhesives were provided by Gummiwerk Kraiburg GmbH & Co. KG, Waldkraiburg.

In the third part thermoplastic adhesives based on polypropylene and polyethylene with different stiffness were combined stack wise. Because the laboratory at the university lacks the ability to extrude such adhesives, they were made with the help of a commercial adhesive manufacturer: Nolax AG, Switzerland. The thermoplastic adhesives were tested in combination with FRP-material based on a thermoplastic matrix, so called organic sheets. This combination is especially interesting for the reforming and because organic sheets allow very short process times in the production of parts.

Before starting the experimental work, simulations of the FRP/metal joint in a fiber metal laminate with and without a gradient were carried out. The simulations were done at the chair for "Leichtbau im Automobil" by and with the help of M.Sc. Alan Camberg.

5.1 Simulation of the FRP/Metal Joint in FML

As pointed out in section 4.6 bending is the most common load scenario for fiber metal laminates and bending tests the common method of evaluation.

Because the stress state in 3-point bending is more complicated, 4-point bending is used in many numerical approaches. In the experimental 3-point bending was used, because it is more common in literature.

The joint of FRP and metal in fiber metal laminates is characterized by the adherent's dissimilarity. Figure 28 depicts the modulus inside the fiber metal laminate in the interphase of the joint materials. The values are typical for the materials and, vary slightly according to the materials used. In reality the interphase of the FRP and the adhesive interlayer (or interlayer produced by intrinsic bonding) is not as definite. During curing the matrix materials flow and a transport of fiber happens to some degree.

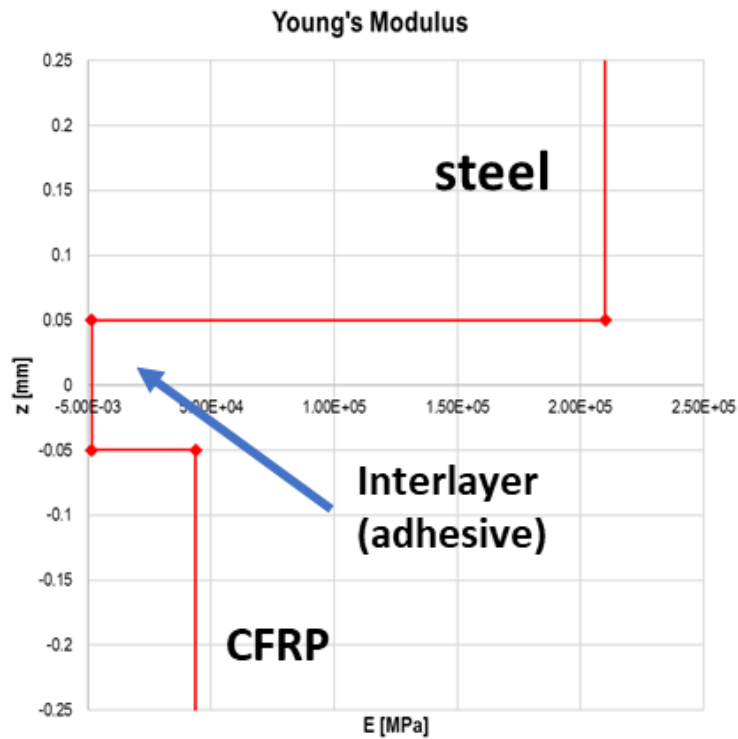


Figure 28: Modulus in a fiber meal laminate in the interphase of the adherents and interlayer

One of the consequences of the materials' dissimilarity is depicted in the following figure:

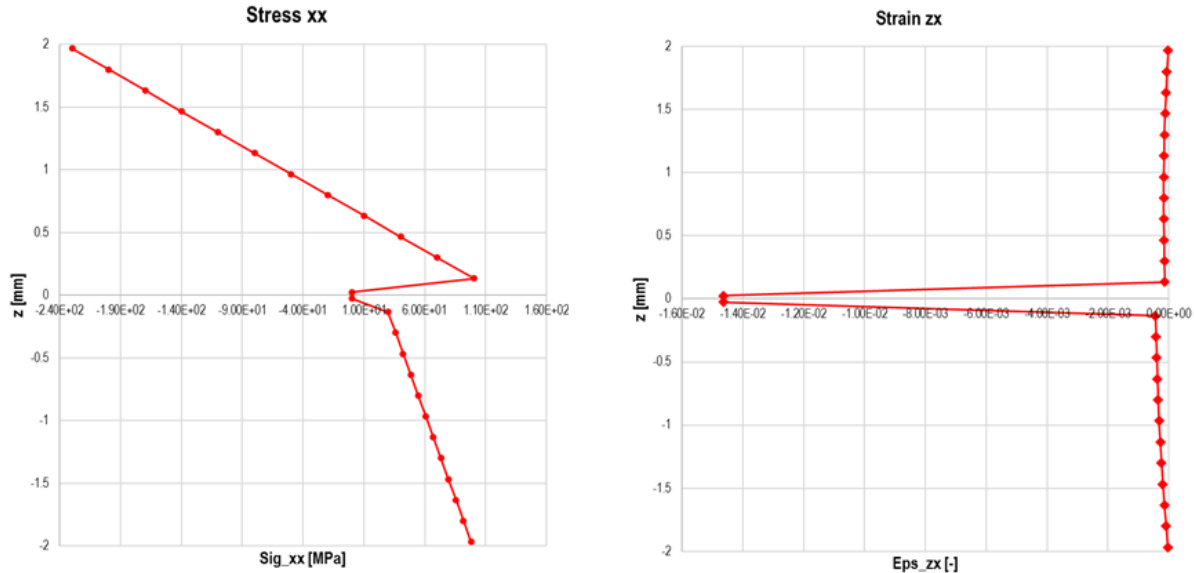


Figure 29: $\frac{1}{4}$ -model of a 4-point bending of a fiber metal laminate with two layers (one FRP, one steel as in Figure 28). The gap of modulus in the interlayer leads to a stress- and strain distribution that acts as a notched bar impact.

In a bending experiment, the gap in the materials' modulus leads to a peak in the strain distribution. It is very adverse for the materials' performance as it acts as a notched impact in

the system under load. Failure of the material below its basic strength is often the consequence.

To get a two-dimensional distribution of the stress and strain in the FML during bending a finite element analysis was done:

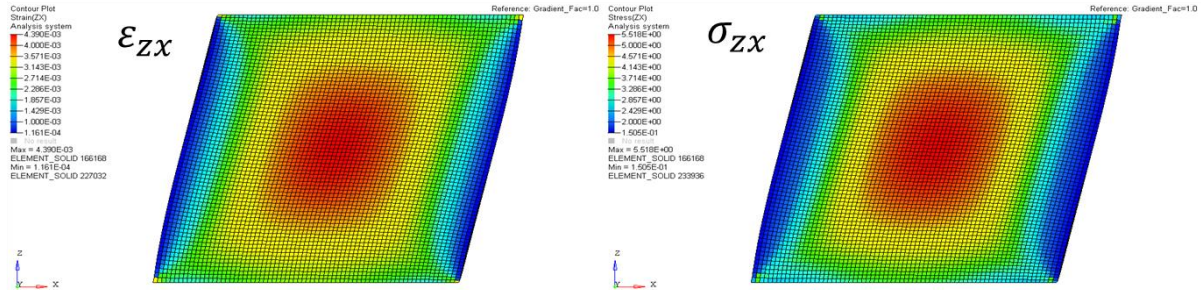


Figure 30: FEA-Analysis of a fiber metal laminate's interphase between the steel (top) and FRP (bottom) parts

Figure 30 shows the stress and strain concentration in the middle of the interlayer between the metal and the FRP part of the FML. This was compared to a graded interphase with a gradient factor of 1.6 in the joint. The factor was chosen from a literature research on epoxy modifications with recycled milled carbon fibers.^[49] This approach was later tested and used in the realization of a gradient adhesive layer (cf. section 5.2).

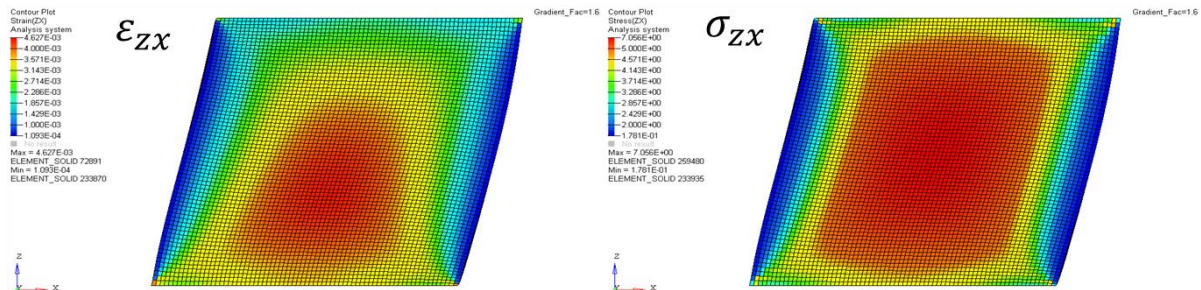


Figure 31: Stress distribution in the FLM's joint with a gradient interlayer. The gradient factor is 1.6 and trends linearly between the joints. As in the preceding figures the steel is in the bottom and the FRP in the top.

Figure 31 shows the stress distribution in the FML-joint with a gradient interlayer. The overall stress is higher compared to the ungraded approach. This is not problematic if it is below the basic strength of the material. The gradient is suitable to distribute the stresses inside the joint more equally, avoiding adverse stress concentrations.

5.2 Modified Adhesives Approach

5.2.1 Evaluation of Fillers for Modification

To insert a gradient of modulus into the bond in this approach an adhesive was modified by fillers. A typical structural adhesive was chosen. Then various ways of modifying it were tested and some fillers screened to find the best method.

Betamate 1630 is a full solid epoxy based one-component adhesive that is used primarily to bond automobile body parts. It represents a typical structural adhesive. Properties are listed in the table below.

Table 2: Table 2: BETAMATE 1630 properties list according to the technical data sheet[50]

Basis	Epoxy resin
Color	red
Solid Content	>99%
Viscosity	30 Pas
Standard Curing Condition	180°C, 30 min
Tensile Strength (DIN EN ISO 527-1)	29 MPa
Elongation at break (DIN EN ISO 527-1)	Ca. 11%
E-Modulus (DIN EN ISO 527-1)	1500 MPa
Lap Shear Strength (DIN EN 1465) on cold rolled steel (CRS 1403) 25 mm x 10 mm bonding dimension Adhesive layer thickness 0,2 mm	29 MPa

Betamate 1630 is a viscous, extremely tacky fluid. Because it contains an active curing agent it needs to be stored in a freezer compartment. The material used was packed in cartridges containing 360 g.

Because the adhesive is viscous and tacky it was tested to thin the adhesive using solvents. The adhesive is soluble in acetone and loses its tackiness when diluted by a solvent. However, because any residual solvent might mitigate the adhesive strength it was decided to modify the adhesive without the use of solvents. This was achieved by means of a dissolver unit. The adhesive was poured into a mug and stirred at 2000 rpm. The modifiers were then added, and the adhesive stirred for 15 minutes until a homogenous blending was achieved.

The fillers used as modifiers were:

- Titanium Dioxide (KRONOS 2043 titanium dioxide)
KRONOS 2043 is a pigment designed for systems filled above the critical particle volume.
- Brass chippings
Brass chippings were taken from the shop where they accumulate during machining.

They have an average size of 200 µm and an oblong shape. The brass chippings were tested to represent other kinds of metal chippings (e.g. steel)

- Sigrafil milled carbon fiber C M80-3.0/200-UN

Sigrafil milled carbon fibers are made in the same process as long carbon fibers (Oxidation, Carbonization, Sizing) but subsequently milled. Milled carbon fibers can also be produced as a recycled/ downcycled product of CFRP composites. Properties are listed in the table below.

Table 3: Material data of SIGRAFIL C M80-3.0/200-UN[51]

Mean fiber length	80 µm
Filament diameter	7 µm
Tensile strength	4 GPa
Tensile modulus	240 GPa
Elongation at break	1,7 %

- HBPE-modified Sigrafil milled carbon fiber C M80-3.0/200-UN

HBPE stands for hyperbranched polyester, a highly branched molecule with a vast number of functional groups. To investigate its effect on fiber-matrix interaction and mechanical properties of the blend, Sigrafil milled carbon fibers were surface-modified with hyperbranched polyester molecules of pseudo generation 4 (64 primary OH-groups).

It is known from literature that hyperbranched polymers can increase adhesion. The high amount of hydroxyl functional groups is likely to build H-bridges. Incorporating hyperbranched polyester polyols into epoxy resins also increased toughness while maintaining the modulus.^[50]

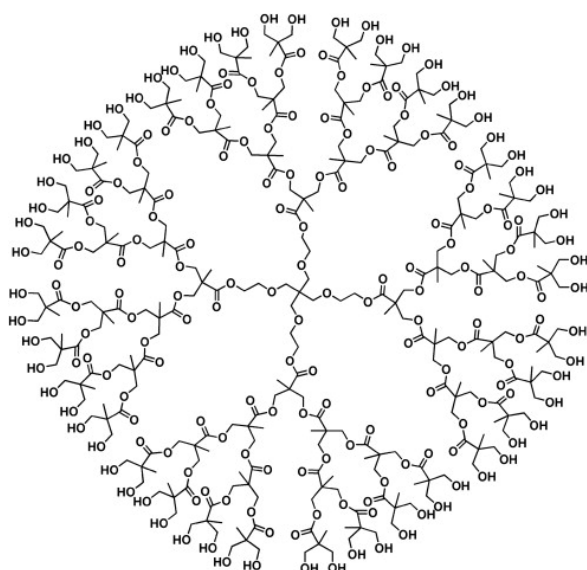


Figure 32: Hyperbranched Polyester polyol, 64 primary OH groups^[51]

The grafting was analogous to the procedure described by Sui et al.^[52] Instead of a polyglycerol, a hyperbranched polyester polyol was used. The procedure consisted of an oxidization of the carbon fiber surface with a mixture of sulfuric acid and nitric acid and subsequently chlorination with sulfuryl chloride. Finally, the hyperbranched polyol was grafted.

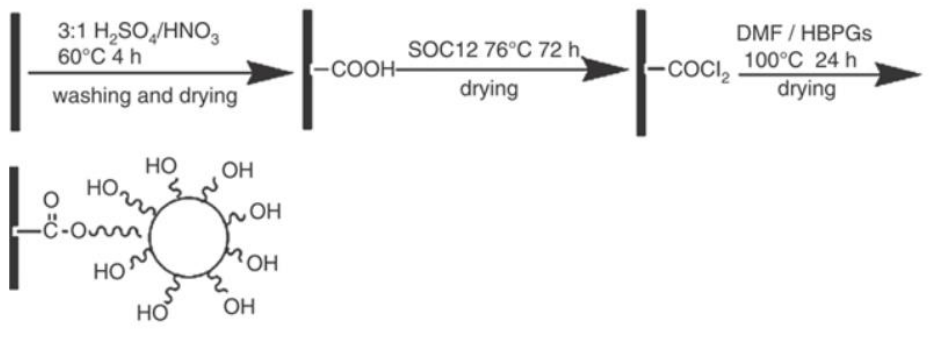


Figure 33: Sui et al: Grafting of hyperbranched glycerols onto carbon fiber surfaces^[52]

The milled carbon fibers were analyzed by SEM and EDX after the washing and drying- and after the polymer grafting step and compared with untreated milled fibers.

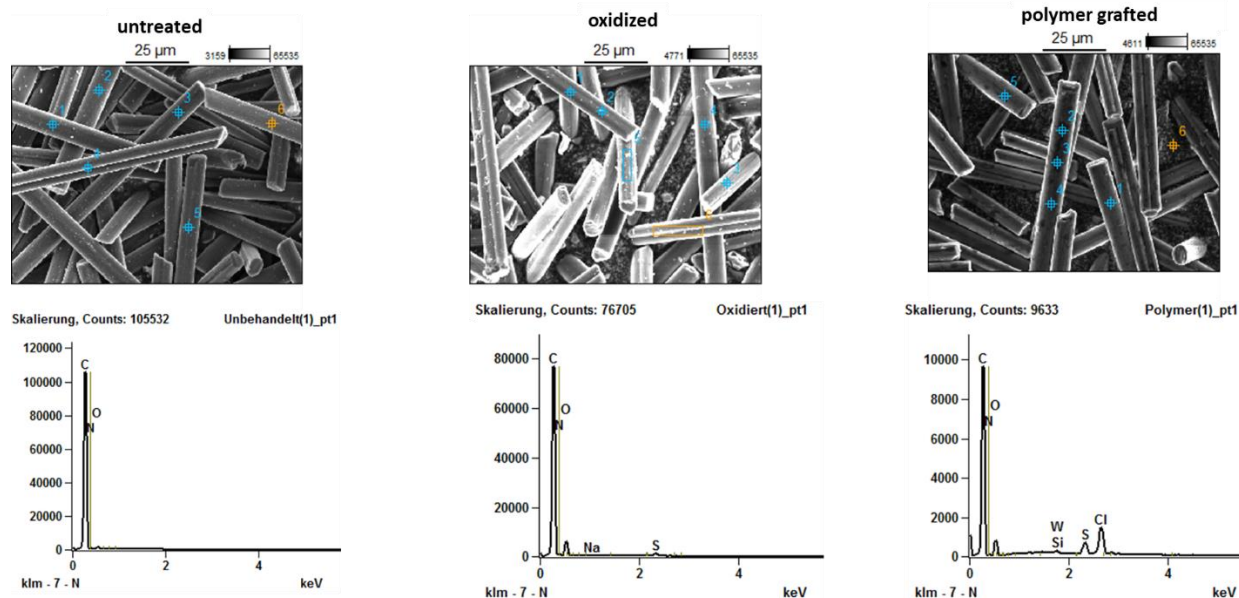


Figure 34: SEM pictures and EDX of Sigrafil 200-UN milled carbon fiber. The different count rates of oxygen and carbon as well as residual chlorine together with slightly changed morphology indicate a chemical grafting of the polymer

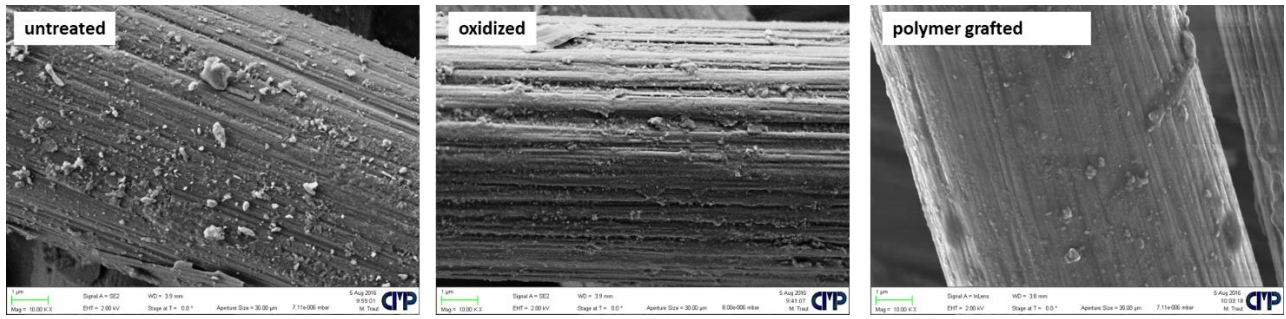


Figure 35: Morphology of the milled carbon fiber in different stages of the treatment. After the oxidation step the number of fiber debris particles on the surface has diminished. The contours of the fiber after the grafting procedure are less sharp. The prominent furrows seem to have been partially filled.

The analysis of the treated milled carbon fibers shows a changed morphology and surface chemistry after the grafting procedure. Because the grafted polymers do not contain different elements than the fibers themselves it is hard to directly prove the grafting from the data. The residual chlorine and different count rates however indicate that a chemical change happened on the surface. The changed morphology also supports this conclusion.

To produce specimens with constant dimensions, plates of the adhesive with a constant thickness were produced. A mold was made by covering two metal plates with a Teflon film. To adjust the thickness metal bars were used at the edges of the plates as spacers. After curing the adhesive in the mold into plates, the specimens were milled out. Ten specimens were produced each, the ones showing flaws like pores and cracks were sorted out. Table 4: Test specimens of modified BETAMATE 1630Table 4 shows pictures of the test specimens.

Table 4: Test specimens of modified BETAMATE 1630

Additive	Amount (% by weight)	Optical appearance
none		
Sigrafil milled carbon fiber (C M80-3.0/200-UN)	1	
	5	
	10	
HBPE-modified Sigrafil milled carbon fiber (C M80-3.0/200-UN)	5	

Titanium dioxide (KRONOS 2043 titanium dioxide)	5		
	10		
brass chips	10		

Some properties were observed from the specimens during their production: Many specimens containing brass metal chips had to be discarded, because of pores in the adhesive. The titanium dioxide made the adhesive somewhat dry and harder to work with.

To evaluate the effectiveness of the different fillers, quasi-static pulling experiments were used. The following graphs show the results. The milled carbon fiber modified by hyperbranched polyester polyol molecules was regarded separately:

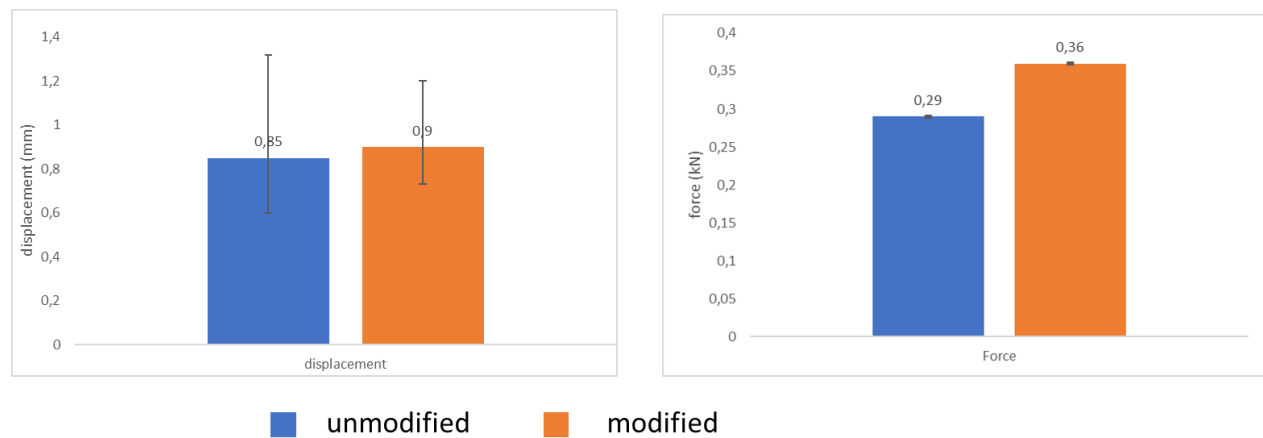


Figure 36: Comparison of the results of tensile experiments of modified and unmodified Sigrafil milled carbon fiber. 5 samples each were tested. The filler amount for the comparison was 5%.

The resulting averages for the modified milled carbon fiber material is 24% above the reference in force at breakage and 5% in displacement. Because of the high effort of producing the modified milled carbon fiber this approach was deferred for the following experiments, which are meant as a proof-of-principle.

In the following graphs the results of the tensile tests of all the other modification attempts are displayed:

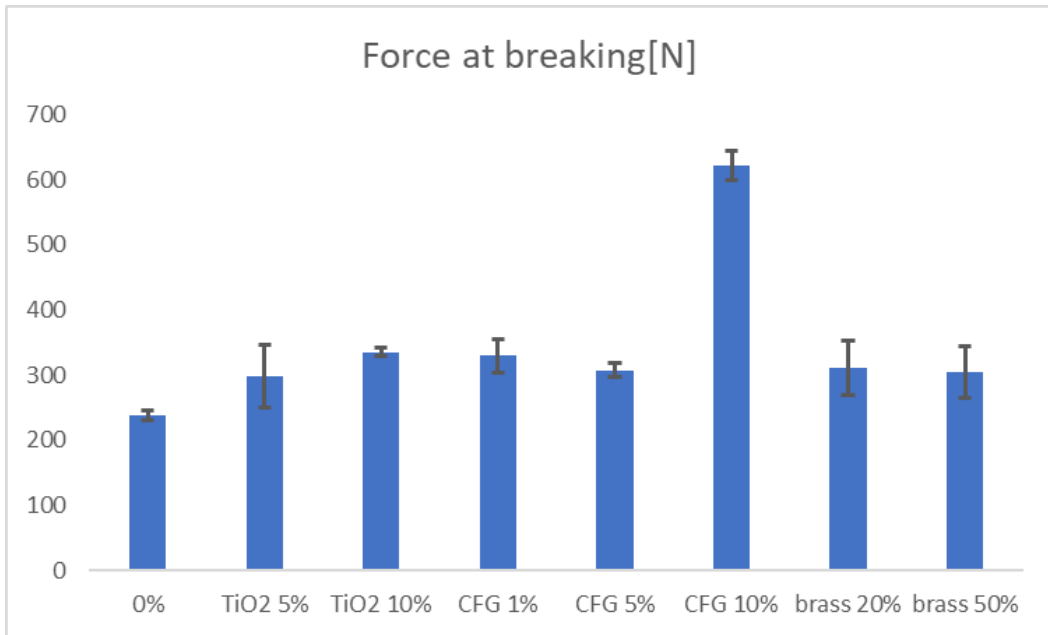


Figure 37: Comparison of the force at breaking of the modified adhesive specimens

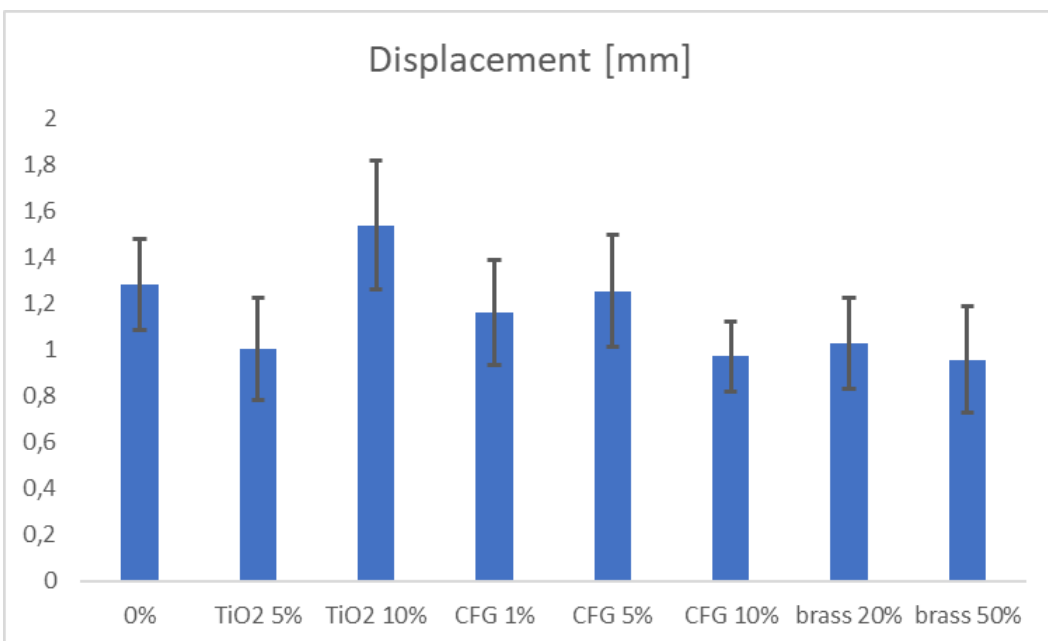


Figure 38: Comparison of the displacement (proportional to the elongation) of the modified adhesive specimens

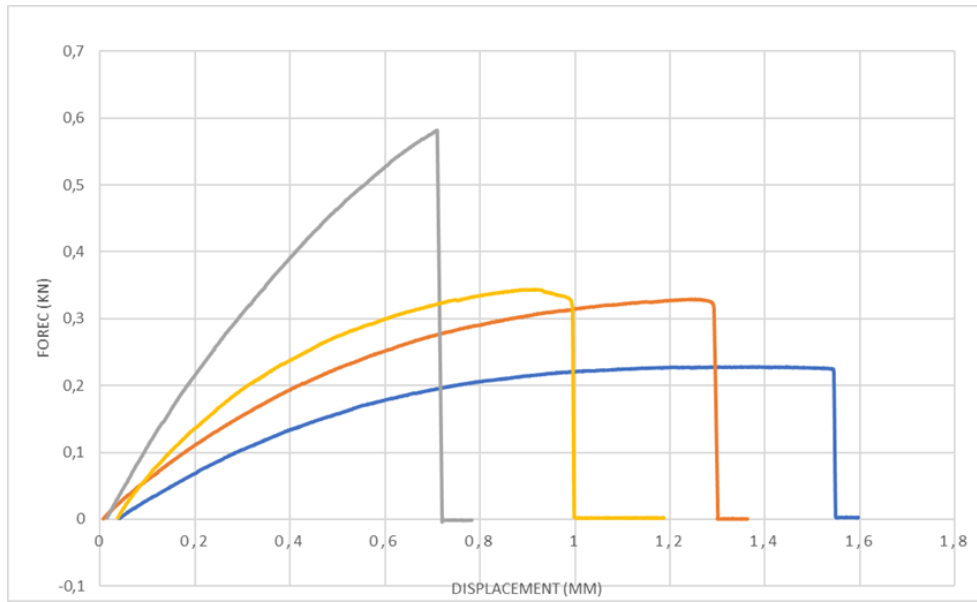


Figure 39: Graphs of the tensile testing of Sigrafil milled carbon fiber-modified BETAMATE 1630

Figure 39 shows the resulting graphs of several tensile experiments with different amounts of Sigrafil milled carbon fiber.

To investigate the influence of the modification on the elastic modulus of the adhesive, the slope in the linear section of the pulling diagram was used. The following graphs show the slope as a function of the filler (modifier) concentration.

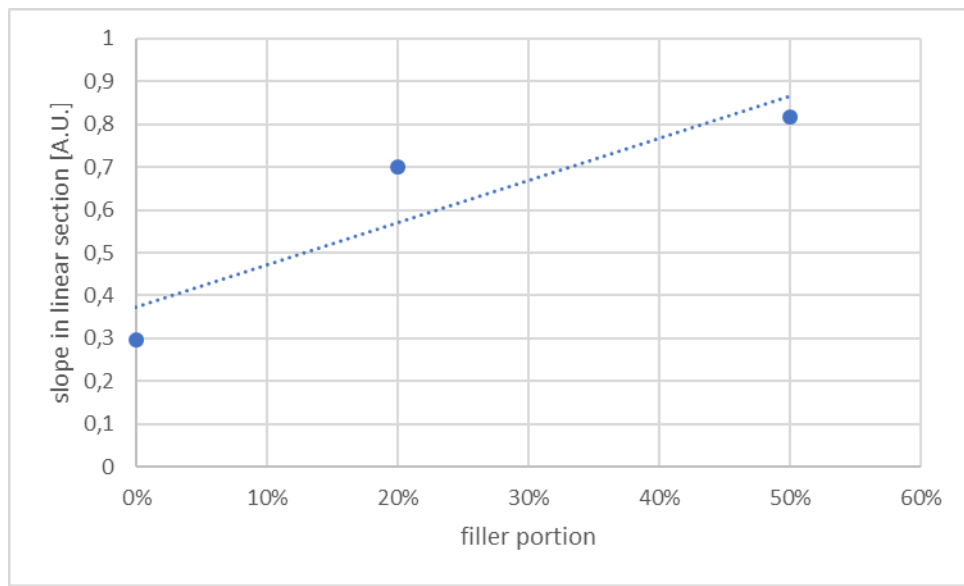


Figure 40: Slope in the linear section as a function of the brass-chip concentration

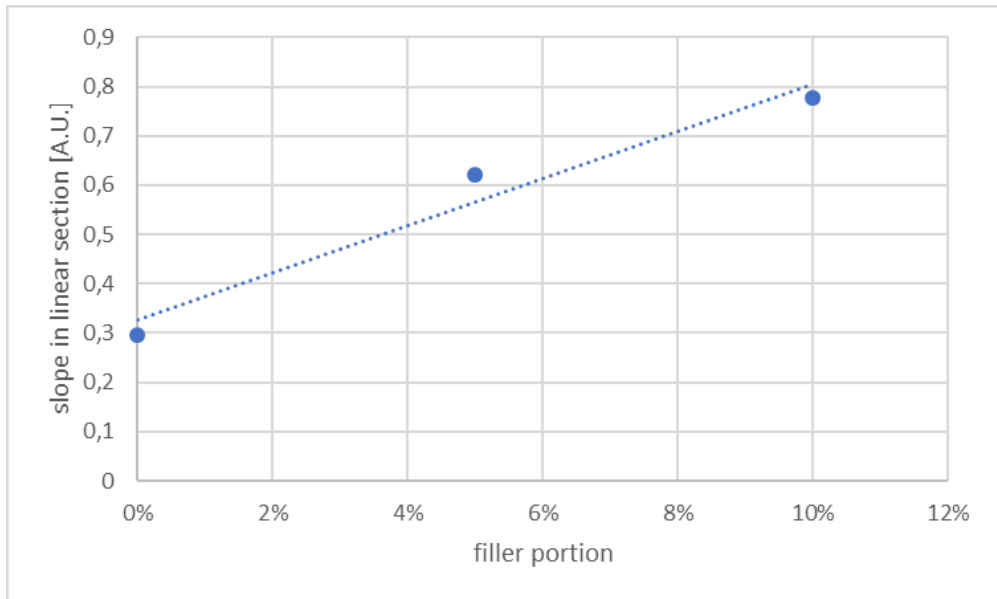


Figure 41: Slope in the linear section as function of the concentration of titanium dioxide

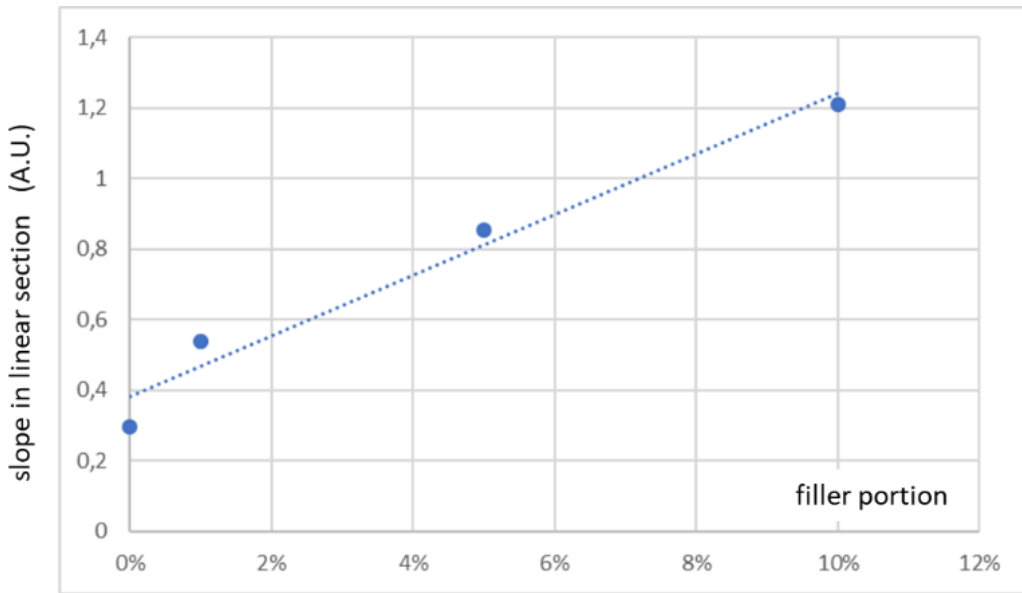


Figure 42: Slope of the linear section as a function of the concentration of milled carbon fiber

Because of the better workability and better performance, it was decided to use the milled carbon fiber to create the gradient system in the following experiments. Another advantage of the milled carbon fiber is its availability as a downcycled product of cured FRP material.

To test the effect of the adhesive modification on a fiber metal laminate, a test series was made. The test series consisted of one dual layer and three reference laminates. The modified adhesive was spread on the substrates and furnished with glass balls of a maximum size of 150 µm. The glass balls ensure that the layer thickness is constant. All excess adhesive material

was pushed out of the bond line during pressing of the laminates in a hydraulic hot press. Both the CFRP and steel substrates were coated with adhesive.

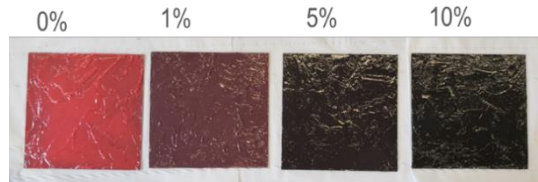


Figure 43: 15 x 15 mm steel sheets covered with adhesive of different modifier ratio

In the case of the graded bond, the adhesive of the steel plate was coated with adhesive containing 10% milled carbon fiber, while the CFRP plate was covered with non-modified adhesive.



Figure 44: Sketch of the production of 2-layer bond lines with liquid adhesives

After curing sample specimens were cut out of the plates by water cutting. From each plate 8 specimens were cut, 4 for static bending and 4 for dynamic bending tests.



Figure 45: Hybrid plates after water cutting. The bigger specimens are for static 3-point bending, the thinner specimens for dynamic bending (impact) testing.

To investigate the general quality of the bond and whether the gradient layer was still intact after curing the plates in the hydraulic hot press, a SEM-study was conducted. Figure 46 shows SEM-pictures of the bond with the milled carbon fiber fragments visible in the adhesive. The picture on the right of Figure 46 shows adhesive material that was pushed out of the bondline in order to establish a constant bond thickness. Although the material was subject to the pressure of the hydraulic press as well as flow when leaving the gap between the substrates, the layer structure was still intact.

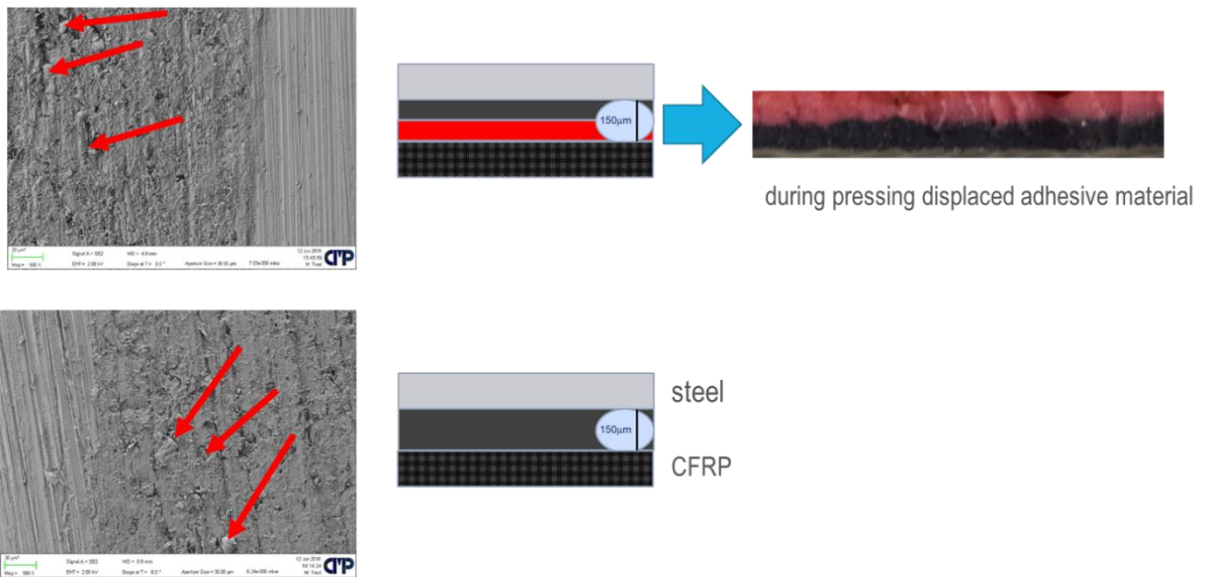


Figure 46: REM images and sketch of the bond line. Red arrows mark the added milled fibers in the adhesive. The picture at the top right shows material that was displaced during the curing process in the press. As can be seen the layers remain intact even after flowing out of the bond line.

To visualize the distribution of the milled carbon fiber within the adhesive layer, an EDX-scan was performed on the sample. The milled carbon fiber is composed almost exclusively of carbon and is therefore highlighted in the EDX image. Figure 47 shows the EDX-mapping of a part of the adhesive layer. The distribution of carbon indicates an intact layered structure.

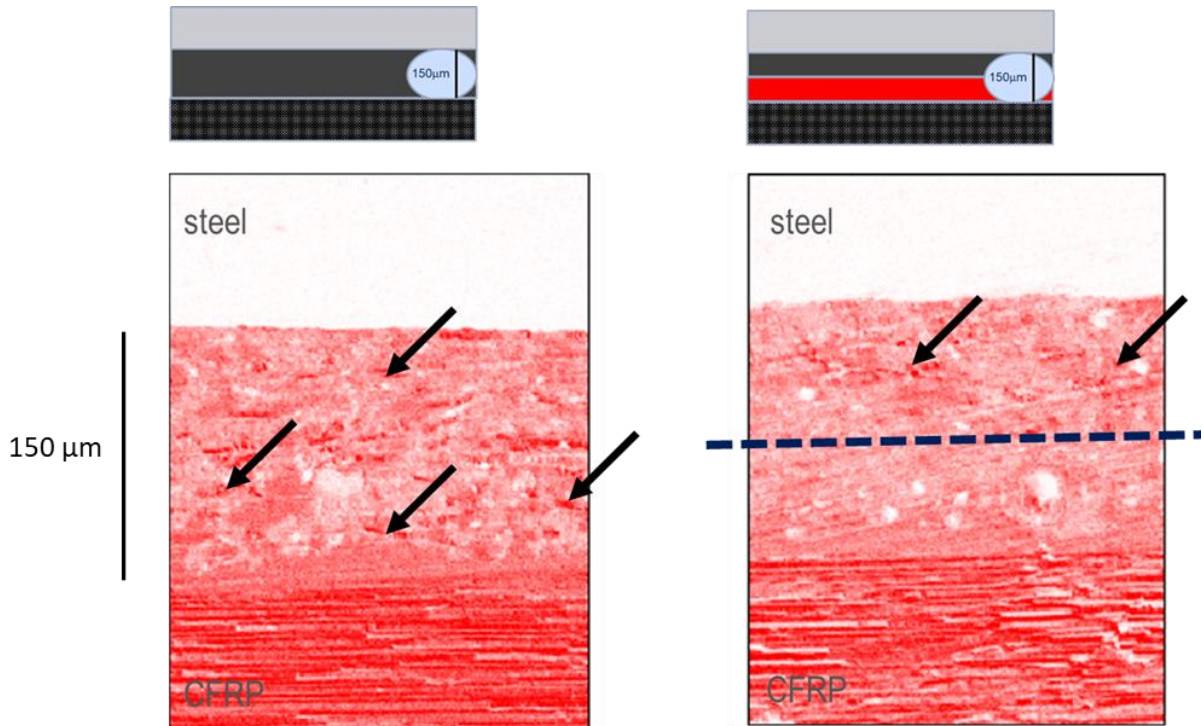


Figure 47: EDX-mapping images of the bond with a 10% filler ratio on the left and a graded bond (10% at the steel interface, 0% at the CFRP interface) on the right. A deeper red signifies a higher carbon concentration. The arrows mark some of the milled carbon fiber fragments within the adhesive layer.

As can be seen from the material that flew out of the press at the side of the sample plates (Figure 46) the modified and unmodified adhesives do not mix but form two distinct layers. The EDX mapping in Figure 47 confirms this.

The cut-out samples from the plates were tested in 3-point bending experiments:

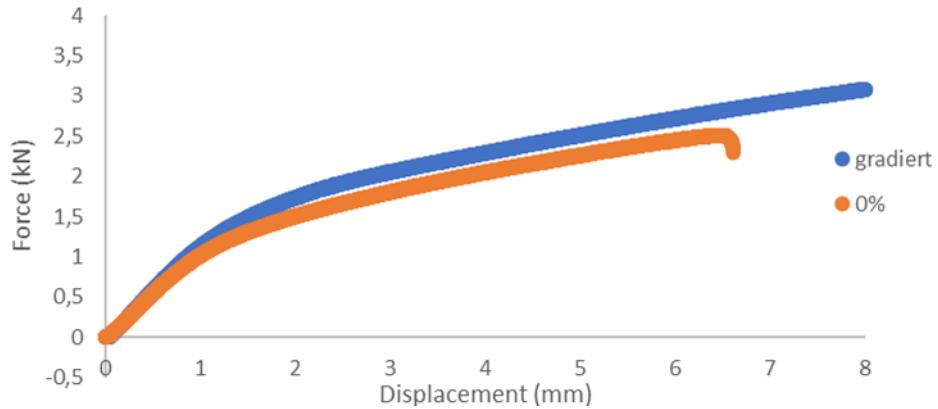


Figure 48: Comparison of 3-point bending results of the graded and ungraded adhesive samples

Looking only at the comparison of the gradient adhesive and the unmodified adhesive, the gradient adhesive shows a better performance. This is however put into perspective when looking at the references with modification, but without gradient layers.

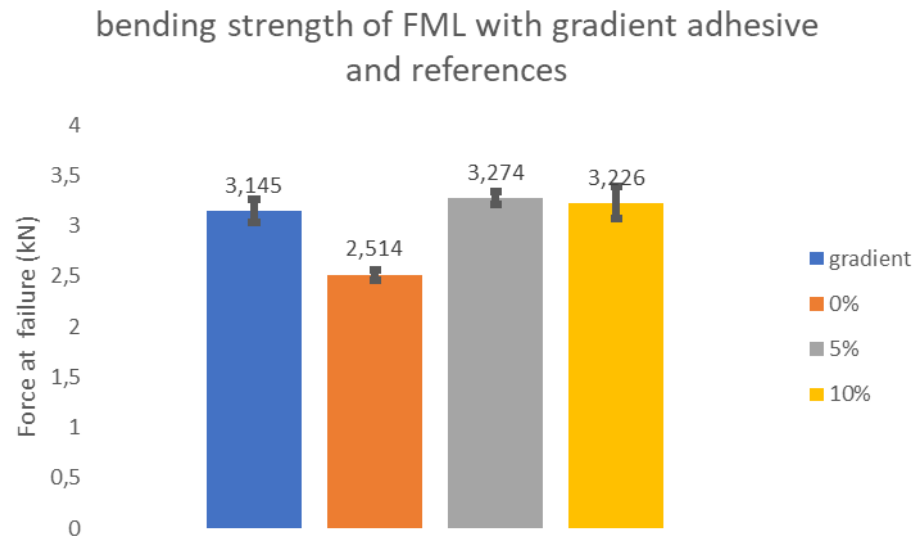


Figure 49: Comparison of the results of the bending test of the unmodified- and gradient adhesive with the reference FMLs (bending strength)

elongation at yield of FMLs with gradient adhesive and references

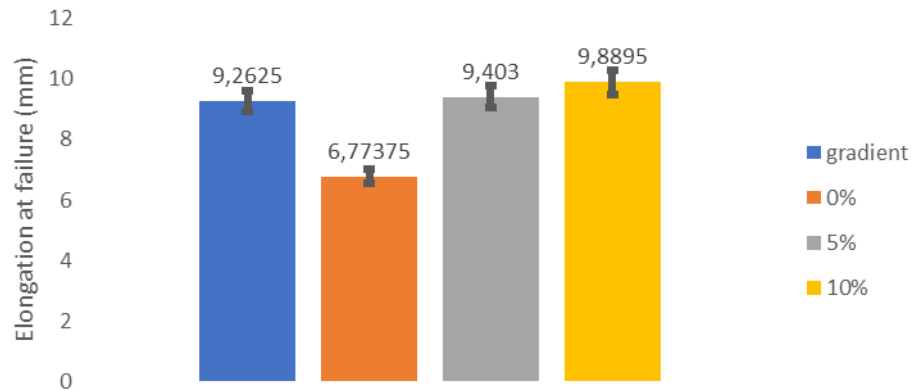


Figure 50: Comparison of the results of the bending test of the unmodified- and gradient adhesive with the reference FMLs (elongation at break)

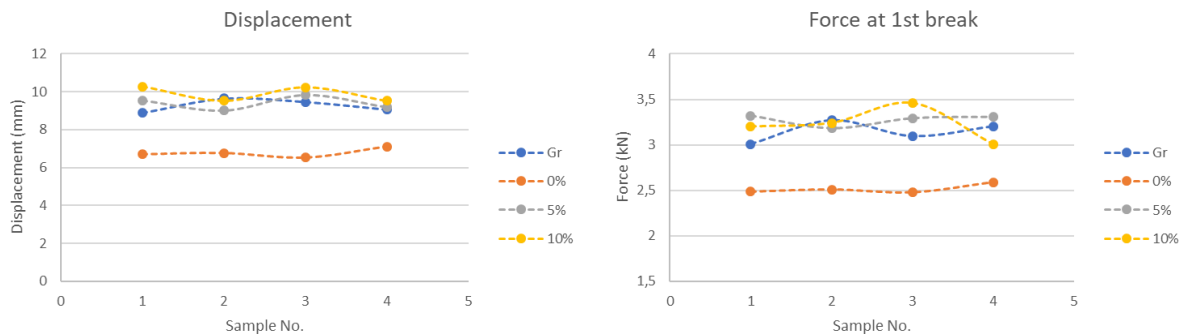


Figure 51: Line-up of the results of the bending test results

As the comparison shows, the modification lead to better performance in the experiments, independent of the gradient layer structure.

1.1.1 EPDM-based approach

In this approach two EPDM-rubber based (ethylene propylene diene methylene rubber) adhesives were tested and their effects on FMLs investigated. The EPDM rubber adhesive is a novel product by Gummiwerk Kraiburg that is sold under the brand “Kraibon”.

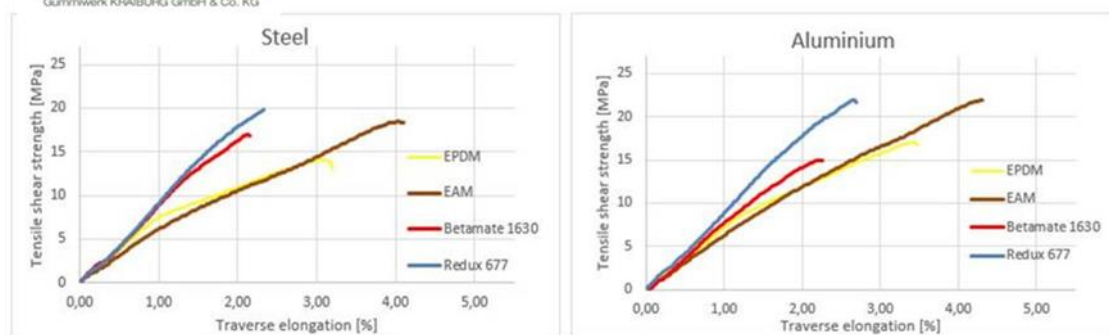


Figure 52: Comparison of structural epoxies to rubber bases adhesives, according to KRAIBURG data sheets

Kraibon is a thermosetting adhesive based on EPDM rubber. It comes as an un-vulcanized rubber imbued with a curing agent. Its distinctive feature is its adhesive strength that is comparable to structural adhesives based on epoxies. Like other thermosetting adhesive films, the shelf life of Kraibon at room temperature is limited. Figure 52 shows the tensile shear strength of two KRAIBON products based on EAM rubber (Ethylene-acrylic rubber) and EPDM compared to Redux 677 and Betamate 1630 (two common high strength epoxy adhesives used in structural bonding) bonded to aluminum and steel.

In this study KRAIBON was used to bond CFRP with an epoxy-based matrix to steel. Therefore, a lap-shear test was performed to test the adhesive strength in this constellation.

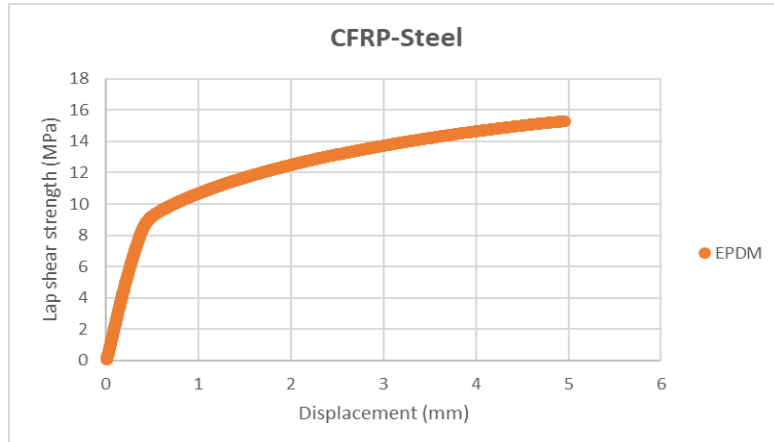


Figure 53: Lap shear test with EPDM-based adhesive KRAIBON, in the case of HAA9275/45 (0,4 mm) on prepreg (sigrapreg) and steel

Kraibon was at the time of the studies available in two grades, the properties of which are listed in the table below.

Table 5: Properties of Kraibon HVV9632/59

E-Modulus	143 MPa
Tensile strength	15,4 MPa
Elongation at break	88%
Film thickness	0,5 mm

Table 6: Properties of Kraibon HAA9275/45

E-Modulus	275 MPa
Tensile strength	14,9 MPa
Elongation at break	55%
Film thickness	0,4 mm

The film thickness is above the desirable thickness for FMLs. It is possible to extrude the EPDM to a lower thickness, unfortunately during the study the listed grades were the only ones available. The EPDM and the curing agent are both soluble in chloroform. Several tests were made to dissolve and doctor blade the EPDM at a lower thickness. However, lap-shear tests did not confirm an acceptable performance of these films. It was therefore decided to perform the tests with thicker substrates to compensate the effects.

To avoid any fringe effects the laminates were pressed as 15 x 15 mm plates from which specimens were cut out by watercutting.

Figure 54 shows a picture taken with a confocal microscope of the bond gap. The two grades of Kraibon, though hard to distinguish at first sight, display a slightly different structure. (EPDM 2 has elliptical shapes that are a little brighter than the background). The adhesives are very stable dimensionally, especially in comparison to some epoxy-based adhesives.

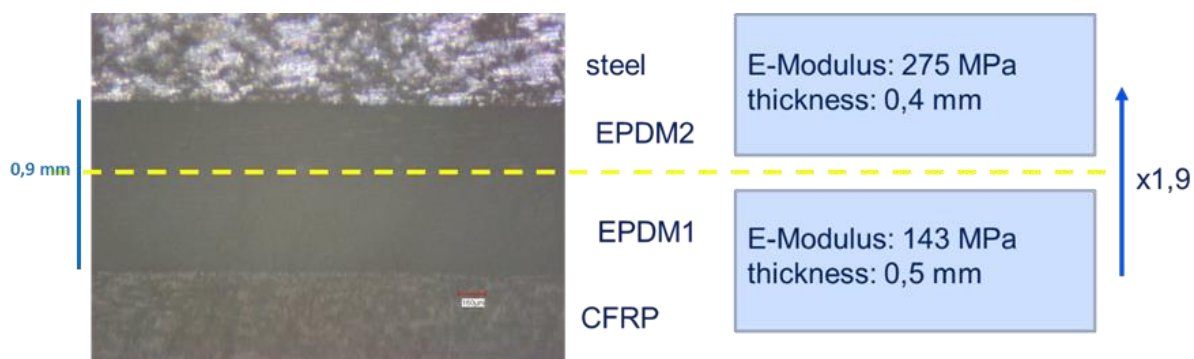


Figure 54: Confocal microscope picture of a laminate bonded by a stack of two EPDM-grades. The difference of the elastic moduli can be described by a gradient factor of 1.9

Table 7: Results of the 3-point bending (flexural) test of Kraibon-bonded laminates

sample number	Maximum Force [N]	Gradient	reverse Gradient	Sample number	Elongation [mm]	Gradient	Reverse Gradient
	1	2193,589	2720,561		1	5,534	10,048
	2	3071,208	2243,943		2	5,5337	7,621
	3	2908,703	2943,275		3	8,812078	10,782
	4	2370,058	2689,789		4	7,119	9,302
	5	3037,562	2692,705		5	10,781	9,08
	6	2744,821	n/a		6	9,4309	n/a
mean		2720,99	2658,05	mean		7,868446	9,3666

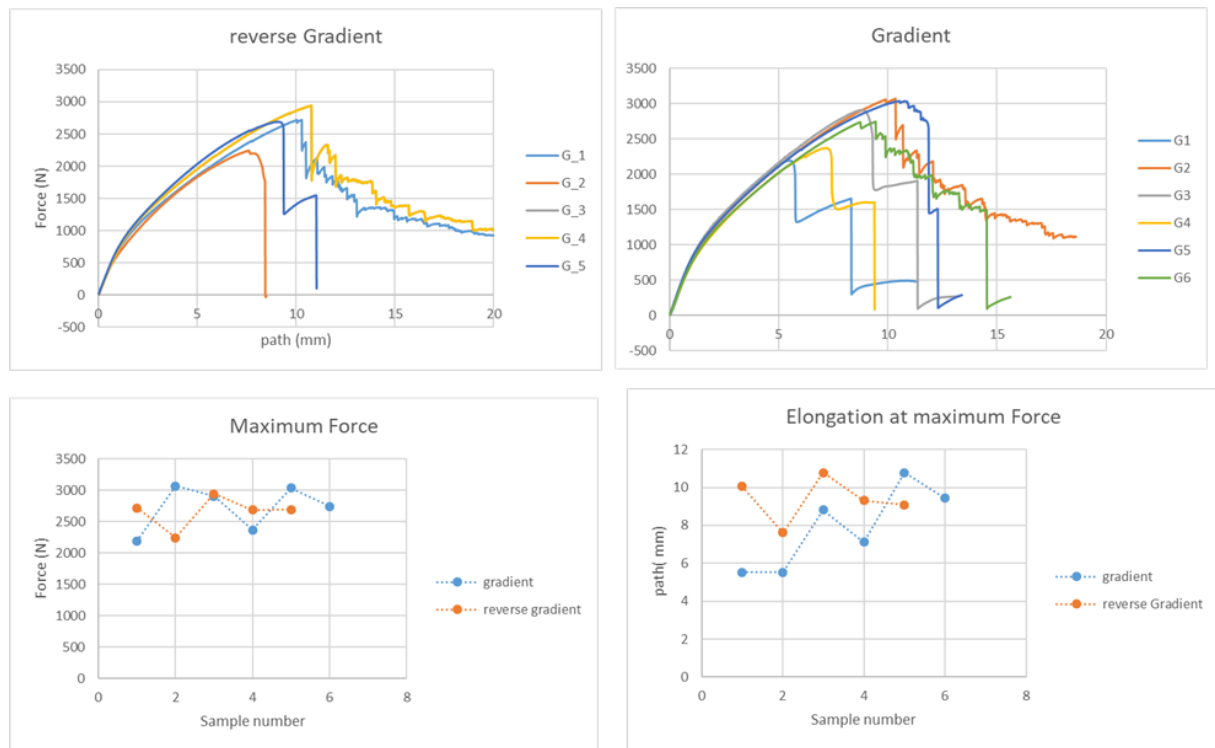


Figure 55: Graphic representations of the 3-point bending tests of Kraibon-bonded laminates

From the results, no significant difference can be observed that are due to the sequence of the gradient. The graphs of the bending experiments show two distinct failure modes: Breaking of whole unidirectional layers of the CFRP part (big steps) and breaking of fiber bundles (small zig-zag steps). A mixed form also exists. All types occur in both sample types. The breaking of fiber bundles seems to be favorable.

5.2.2 Polyurethane Based Approach

6.1.2.1 Formulation of a Waterborne PU-Adhesive and Production of Adhesive Tapes

In this section the effect of using an elastomeric polyurethane adhesive is investigated. The polyurethane-based adhesives tested are all made from waterborne dispersions. They contain isocyanate dimers that react similar to blocked isocyanates. The advantage of this technology is the absence of volatile reaction products during curing. Such volatile products can cause bubbles inside the adhesive, as there is no way of leaving the bonding area.

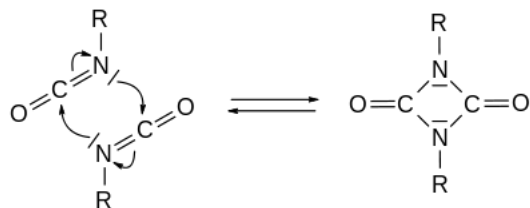


Figure 56: Chemical equilibrium of isocyanates and uretdione. At high temperatures the equilibrium is on the side of the more stable isocyanates. The reaction speed can be increased by catalysis^[53].

It is a concern in the field of adhesives as well as in the field of coatings to find capable technologies that decrease the use of organic solvents. Waterborne polyurethane adhesives have been used to bond textiles, shoe soles and automotive interior.^[54] In this part of the work it was the aim to investigate the usefulness and capability of adhesives based on waterborne dispersions as structural adhesives. An adhesive tape based on a waterborne dispersion and a nano-composite functional filler material was formulated to investigate their usefulness.

An adhesive film can be obtained by applying an adhesive dispersion onto release paper and subsequently drying it.^[55] As the binder, an anionic dispersion was used. Such dispersions are commercially available by Covestro, Alberding-Boley and others. As the curing agent, a commercially available TDI dimer dispersion (sold under the trade name Dispercoll XP 2514 BL) was used.

The release paper is a siliconized paper that leads to a poor wetting of the dispersion. To obtain a homogenous film, the viscosity of the dispersion needs to be elevated to a degree that hinders dewetting. For preliminary tests the adhesive was applied to galvanized metal sheets. The metal sheets were alkaline cleaned with the product "Gardoclean" (Chemetall).

Xanthane, Bentonite and various thickener additive brands by Borchers and Byk were used to increase the viscosity. It was found that high viscosity of the material alone did not necessarily lead to dewetting being stopped. Some thickeners were less effective although their effect on the viscosity of the dispersion was stronger. Many thickeners work by building up a network of secondary interactions such as H-Bonds as well as card-house structures. This is of interest as the hyperbranched molecules as well as layered silicates used to reinforce the adhesive at a later point have some similar attributes. This will be discussed later in this section.

Table 8 lists raw materials used and tested in the formulation of the adhesive.

Table 8: Raw materials tested in the development of the water-based adhesive tape

Name	Function
Dispercoll U53	binder
Dispercoll U54	binder
Alberdingk U 400 N	binder
Dispercoll XP 2514 BD	latent reactive curing agent
Borchi Gel PW 25	thickener
Borchi Gel 0620	thickener
Borchi Gel 1420	thickener
Xanthan	thickener
polyethylene glycol ($M_w = 500$)	adhesion promoter
polyethylene glycol methyl ether ($M_w = 500$)	Modifier, adhesion promoter
PVA (polyvinyl alcohol)	modifier, adhesion promoter
EVA (ethylene-vinyl acetate rubber)	elastomer



Figure 57: The picture shows different attempts at blading a film onto siliconized paper. The film in the upper left shows little dewetting, while the films on the upper and lower right show almost no wetting of the surface.

To cure the adhesive, it was placed in a hydraulic hot press. The sample preparation and testing were done in accordance with ASTM D1002 (lap shear test). Once the performance of the adhesive reached an acceptable level, it was tested in joints of prepgs (Sigrafil) and galvanized steel.



Figure 58: The hydraulic hot press used to prepare the samples. The press has a maximum pressure of 31 MPa and maximum temperature of 600°C.

Figure 59 gives an overview of the different factors that influence the adhesive performance and that were varied (partly) during the formulation. To eliminate factors and reduce complexity, the surface preparation of the metal sheets was kept the same during all tests.

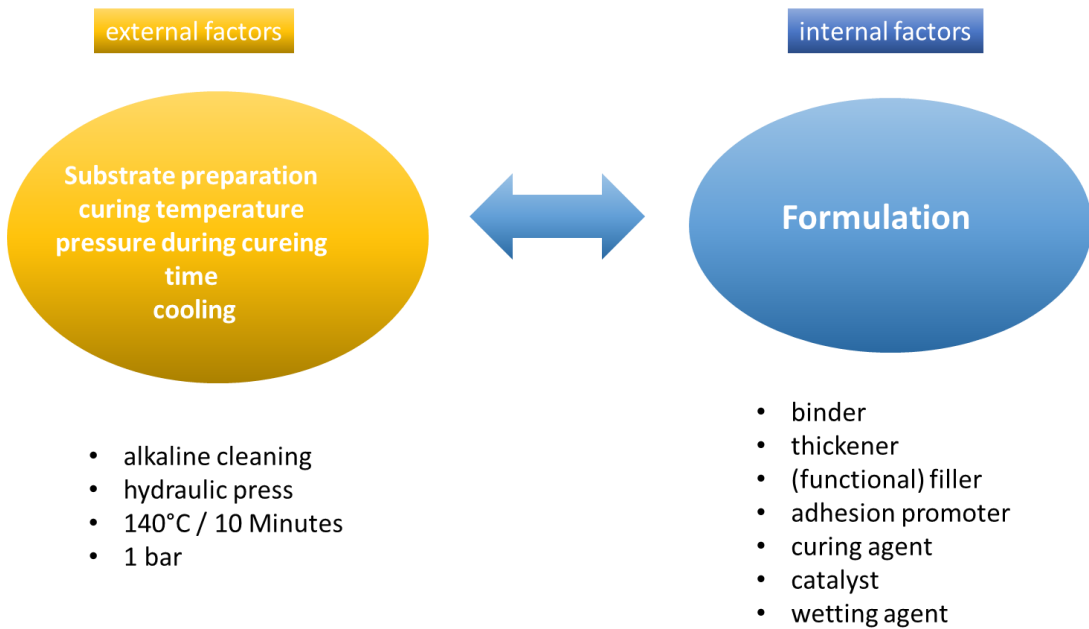


Figure 59: Factors influencing the performance of the adhesive investigated during the formulation process

In the process of development of the adhesive many raw materials were tested and naturally most of them did not give the wanted results. In the following section some of the more interesting failures and effects are shown before switching to the part that gave positive results.

The first attempts were tested on 10 x 150 mm steel cuts and cured under various conditions to get an idea of the best parameters. Figure 60 shows some of the earliest attempts that were hand-tested to save the effort of a time-consuming lap-shear test.



Figure 60: First attempts of joining steel cuts after hand-testing

In one attempt milled carbon fibers (same as used in the epoxy modification, Sigrafil C M80-3.0/200-UN) were used to modify the polyurethane dispersion. After raising the viscosity, the fibers could be dispersed in the binder. Figure 61 shows a photograph of the adhesive film with and without the milled carbon fiber.



Figure 61: Two adhesive tapes, one without fillers, the black film contains milled carbon fiber

The films were cut into dimensions according to ASTM D1002. They were then used to produce steel samples and tested.

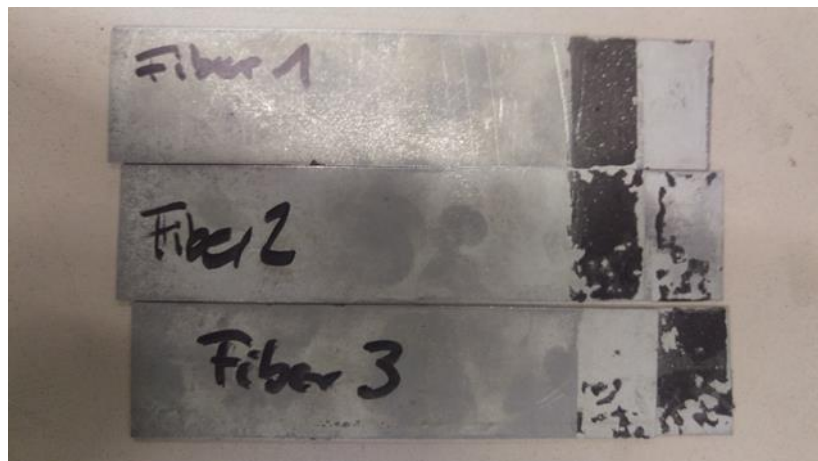


Figure 62: The picture shows lap-shear samples of adhesives modified by Sigrafil® milled carbon fiber. The three samples are from the same series. The samples are stapled to enable direct comparison of the lap areas.

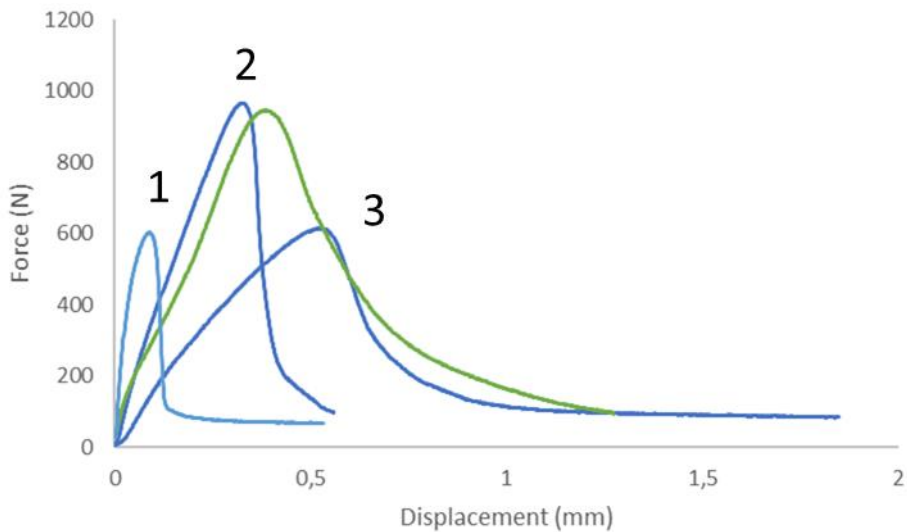


Figure 63: Results of the lap-shear test of milled carbon fiber filled adhesive in comparison to a reference adhesive without filling. The reference without milled carbon fiber is shown in green.

Figure 63 shows the results of the adhesives tested. They show a high degree scattering that might be due to inhomogeneities of the films and of the pressure during their production. All samples share a sharper, less plastic failure. Except for sample 3 the shear modulus is higher than in the neat sample.

To enhance the mechanical properties of the adhesive tape it was attempted to disperse hyperbranched polyester and polyesteramide polyol polymers in the dispersion. The hyperbranched molecules used are not soluble in water due to strong internal H-bonds. When heated to 60°C the H-bonds are broken and the molecules show some solubility.

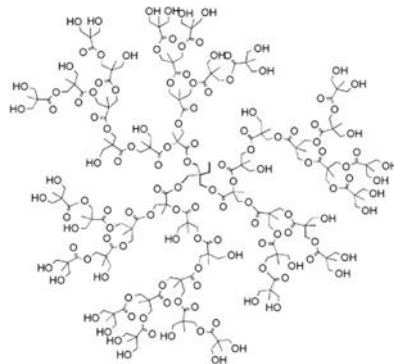


Figure 64: Complete structure of the hyperbranched polymer used in the first tests. It is a hyperbranched polyester polyol of the 4th pseudo-generation

When cooled down the molecules precipitate. It was found that a mixture of Cloisite Na⁺ (Montmorillonite clay with Na-counter ions) and one type of the hyperbranched polyester polymers can be dispersed in water. The mixture of clay and hyperbranched polymer was prepared according to the following specification that was developed based on literature^[56,57,57].

The hyperbranched polymer was heated to 150°C. Then water heated to 100°C was added and the mixture vigorously stirred. When a homogenous dispersion had formed 10% by weight of a Montmorillonite clay slurry was added and the mixture continued to stir. The slurry itself

was prepared by adding 20% by weight of clay to deionized water which was then placed in an ultrasonic bath until a gel-like slurry had formed. The clay/hyperbranched polymer dispersion was vigorously stirred and then heated until the water had evaporated enough to form another slurry. This was removed from the glass beaker and rolled onto siliconized paper. After drying at 70°C in the oven for 3 hours the material was dry and had a glass-like amorphous appearance. Finally, the material was milled to a fine white powder.

Figure 65 and Figure 66 show SEM-micrographs of a fast-ion-beam (FIB) cut that was made through a piece of the hyperbranched/clay mixture.

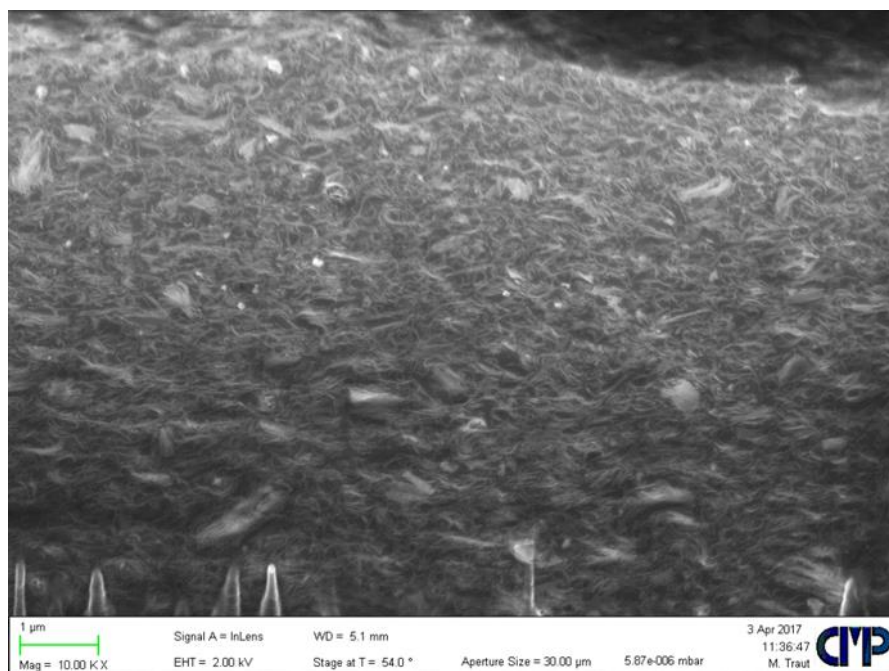


Figure 65: SEM-micrograph of a cut through a particle of the hyperbranched (polyester pseudo gen. 4)/clay mixture. The clay is mostly exfoliated. The larger white objects indicate stacks of silica clay that is only partly intercalated or present as intact stacks.

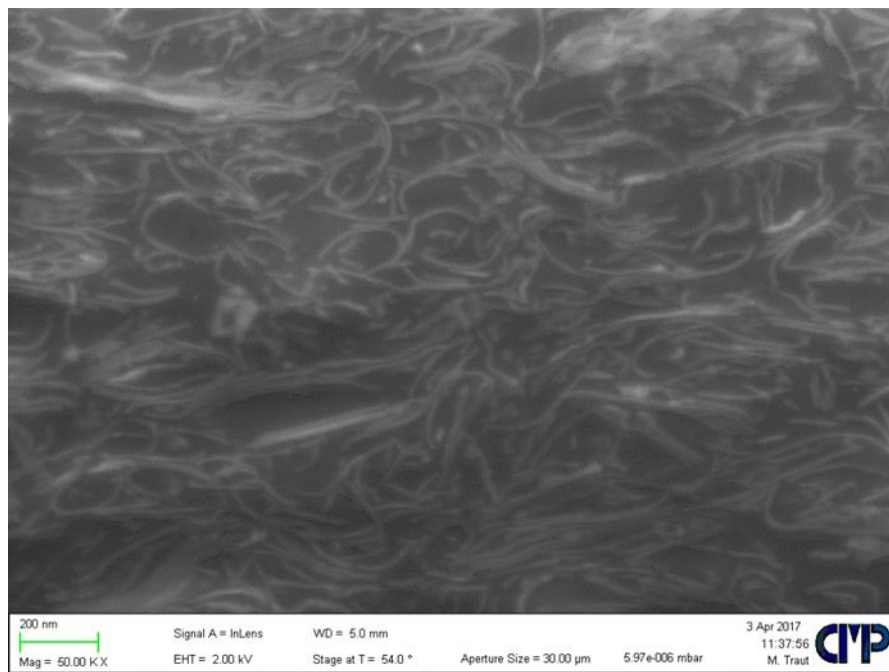


Figure 66: A section of the SEM-micrograph of Figure 65 at a higher magnification

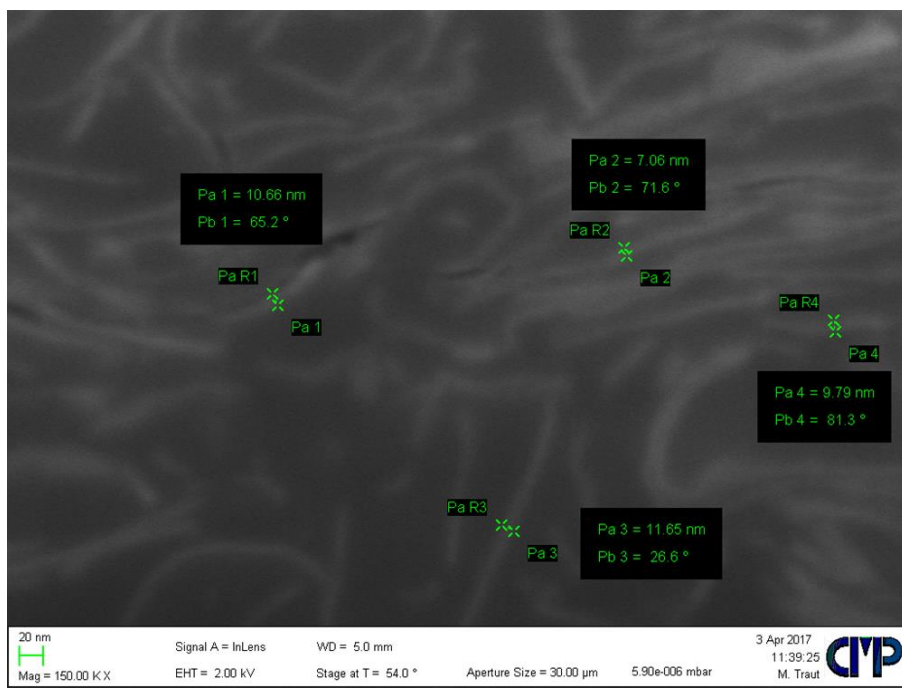


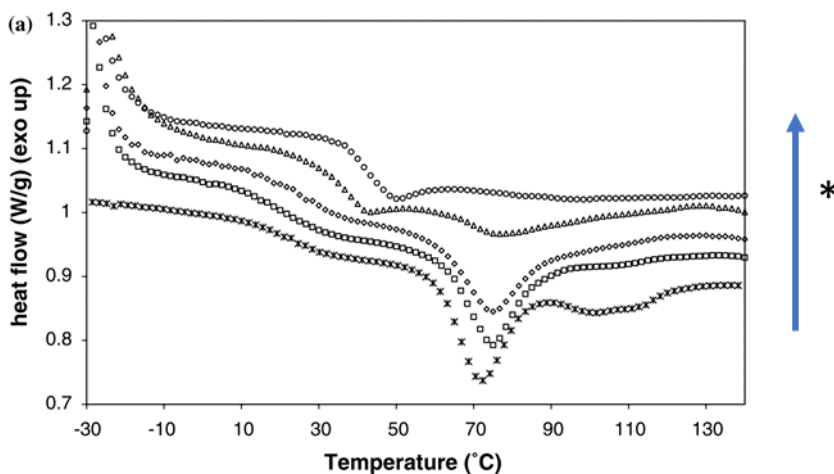
Figure 67: Survey of the layer thickness of the intercalated clay in the hyperbranched/clay mixture. The thickness indicates exfoliation.

With a percentage of 10% by mass clay, the hyperbranched/clay mixture is overfilled by the standards of other clay composites that are described in literature. The described mass percentages are mostly in the range between 0,5 to 5%.^[58]

It was found that the hyperbranched/clay mixture of a hyperbranched polyester showed a different dispersibility in water than the hyperbranched polymer alone, which, when dissolved in water, shows agglomeration and sagging.

Compared to linear polymers of the same compositions, hyperbranched polymers usually show a higher solubility^[59]. The poor solubility of the hyperbranched polyesters in water is probably due to the high intramolecular H-bonding. As mentioned earlier, when heated to 60°C the hyperbranched polyesters readily dissolve in water. This behavior is similar to some polyvinyl alcohols (PVA/PVOH). After heating in water, they undergo breakage of hydrogen bonds and form new hydrogen bonds with the water; forming viscous fluids in the process. The hyperbranched polyesters however precipitate when cooled down, returning to their initial state. During the production of the clay/hyperbranched composite, in the dispersion step of montmorillonite clay, water and the hyperbranched polyester are also heated above the point where hydrogen bonds are broken (60°). The water is subsequently removed but the clay with its large surface remains dispersed inside the polymer.

If the montmorillonite clay disturbs the hyperbranched polymers' intramolecular H-bonds, a DSC measurement should show an effect similar to a study that was performed by Thomasson et al.^[60] In their measurements they partially modified the functional groups of a hyperbranched polyester similar to the material used in this work with para-tolylisocyanate. This resulted in removing hydroxy groups. Figure 68 shows the effect of the removed OH-Groups and consequential decrease of intramolecular forces in the molecules.



*OH-groups in the polymer decrease

Figure 68: DSC curves for pristine and variously modified pseudo generation 4 (HB40) samples, from bottom up decreased number of OH: pristine HB40; HBpT14, HBpT18; HBpT119; HBpT140 (adaptation from^[60])

The peak at 70°C (the melting point of hyperbranched polyesters) is diminished as the number of hydrogen bonding partners decrease with the converted hydroxy groups.

A DSC analysis of the pure hyperbranched polymer (hyperbranched polyester pseudo gen. 4) and the clay-mixture showed the decrease of a large peak at the region where hydrogen bonds are expected.

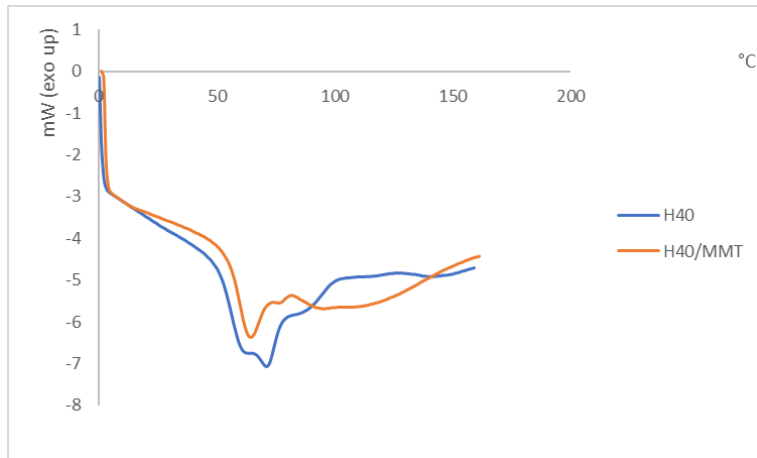


Figure 69: DSC curves of pure hyperbranched polyester pseudo generation 4 and the hyperbranched/clay mixture. The peak at 70°C is diminished.

The graph shows a double peak in the region near the melting point (70°C). The clay/polymer composite shows an overall diminished energy absorption. The largest peak of the pure polymer is gone and the second peak at lower temperature slightly smaller. The effect of the clay could be explained by a disturbance of the H-bonding of the hyperbranched polyester.

Large monovalent ions act as so called chaotropes, disturbing H-bonds and weakening the hydrophobic effect. The interaction of these ions in solution with surrounding water molecules is lower than the interaction between two water molecules. Kosmotropes on the other hand show stronger interaction with surrounding water molecules. The interaction between salts and other internal H-bond forming is well known from biological molecules such as proteins, which can be denaturized by addition of salts.^[61]

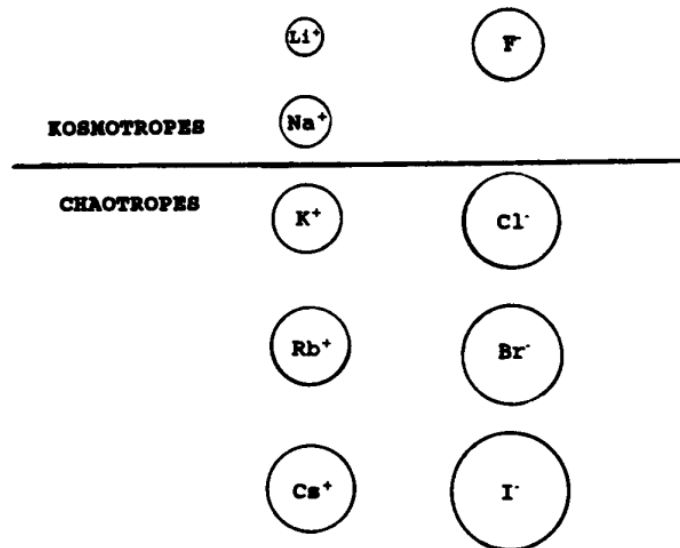


Figure 70: Classification of ions as kosmotropes (from Greek κόσμος = (world)order) and chaotropes (from Greek χάος = void, emptiness, disorder) as published by Collins et al in 1997^[61]

By using Shannon-Prewitt Values of effective ion radii^[62], the surface charge density of ions is estimated in table 9. The value for montmorillonite was regressed using atom force microscopy and the DLVO theory by Yu et al. This value is a mean value and depends on the particle size.^[63] Compared to other ions that are characterized as chaotropic agents such as iodine, the charge density of montmorillonite particles is expectedly low. It should be noted that a montmorillonite particle is neither an ion nor monovalent.

Table 9: Calculated charge densities of anions and regressed charge density of montmorillonite particles (based on effective ion radii found in^[62])

Anion	Surface charge density [mC/m ²]
F ⁻	971,2
Cl ⁻	456,6
Br ⁻	384,4
I ⁻	300,0
MMT ^{x-}	6,3 ^[63]

Nonetheless the DLC clearly shows an interaction between the montmorillonite and hyperbranched polymer that decreases its enthalpy of melting in the region where H-bonds are expected to be the primary cause of molecular cohesion. **It is therefore postulated that the montmorillonite disrupts the intramolecular H-bonds of the hyperbranched polymers in a similar fashion as chaotropic agents disrupt intramolecular H-Bonds in biological molecules.**^[61,64]

Two other polymer/clay nanocomposites were made in the same procedure as described:

Table 10: Structures and solubility of hyperbranched polymers tested as clay-polymer composites [61,66][66,67]

Hyperbranched Polyesterpolyole, pseudo generation 2	Hyperbranched Polyesterpolyole, pseudo generation 4	Hyperbranched Polyester amide, pseudo generation 1
Soluble in DMF, NMP, DMSO	Soluble in DMF, NMP, DMSO	Soluble in n-butyl alcohol, cyclohexanone, DMF, NMP, DMSO
Composite dispersion is stable in water	Composite dispersion is stable in water	Composite dispersion is not stable in water

Table 10 lists the hyperbranched polymers that were tested with unmodified montmorillonite clay (Cloisite Na). The lower pseudo-generation hyperbranched polyester showed no difference to the higher generation one. The hyperbranched aromatic polyester amide can be dissolved in solvent of lower polarity than the hyperbranched polyesters. However, its clay-composites showed no tendency to dissolve at all. Therefore, for the modification of the adhesive the hyperbranched polyester were used.

It is known from literature that waterborne dispersions can be reinforced by addition of clay. Rahman et al. used clay to produce polyurethane adhesives. Compared to the material without clay, the composite showed increased strength and strain in tensile tests. T-peel strength and modulus can be increased dependent on the amount of clay added and the surface characteristics of the clay. Lit et al. used montmorillonite clay to modify waterborne polyurethane dispersions and found a dramatic increase of tensile properties. [65]

To test its effect the clay/hyperbranched composite was added to the following formulation:

Table 11: Optimized Adhesive Formulation

Ingredient	Weight percent (wt/%)
Dispercoll U 53	71,38
Dispercoll XP 2514	14,3
Poly (ethylene glycol) methyl ether mPEG average Mn = 500 g/mol	14,3
Borchi Gel PW 25	0,02

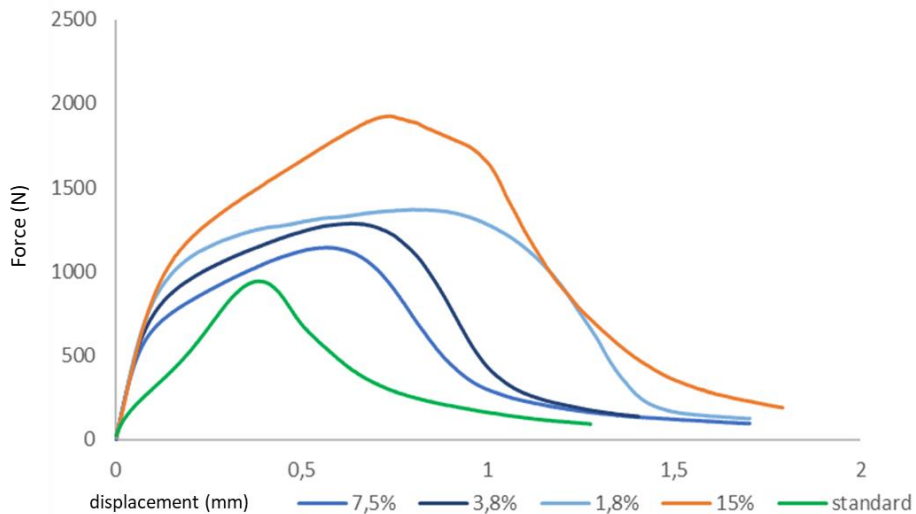


Figure 71: Lap shear strength of adhesive films with varied HBP/MMT-portions

Figure 71 shows the results of a test series of the Dispercoll U53-based formulation with modified weight percentage of the HBP/MMT-modifier. Compared to the standard formulation adhesion and lap shear strength are increased. A big influence onto the toughness of the bond is visible. The performance of the adhesive film with the largest amount of the modifier added is contradicting the trend of the other adhesive films (better mechanical properties at lower amount added).

During the tests of the formulation shown in Table 11 it was found that the MMT/HBP-composite had a strong effect on the dispersion's viscosity. More tests were conducted with a similar Dispersion, Dispercoll U 54. The effect of the composite on the viscosity was enough to leave out the thickener additive altogether. It was also tried to leave out the PEG also, that was included because it had shown increased adhesion to the metal substrate in the first place.

The resulting formulation only included the Dispersion as the base, the hardener and the composite:

Table 12: Simplified adhesive formulation

Dispercoll U 54	72 %
Dispercoll XP 2514	14 %
HBP/MMT-composite	14 %

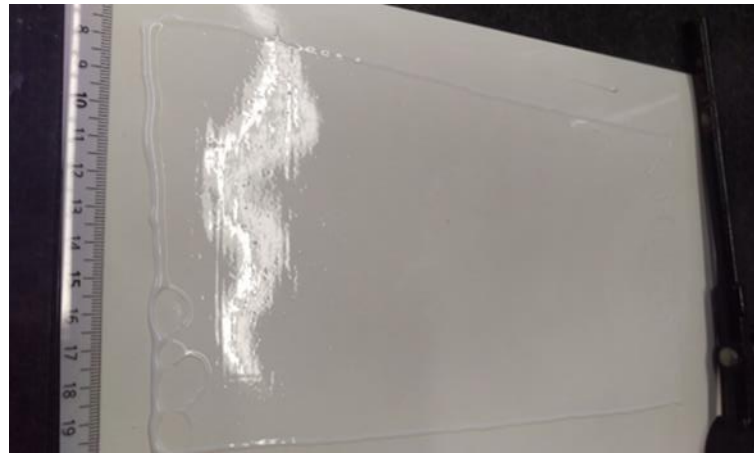


Figure 72: A photograph of the simplified formulation doctor bladed onto a siliconized paper

As can be seen in the photograph, films could be made from the simplified formulation without an additional thickener.

Films with varied concentration of the composite were made and tested in a DMA-experiment. The storage modulus was measured in a frequency shift. The aim was to find out about the effect of the composite on the cured adhesive's stiffness. As a reference a film without the composite was used which included thickener in order for a free film to be formed.

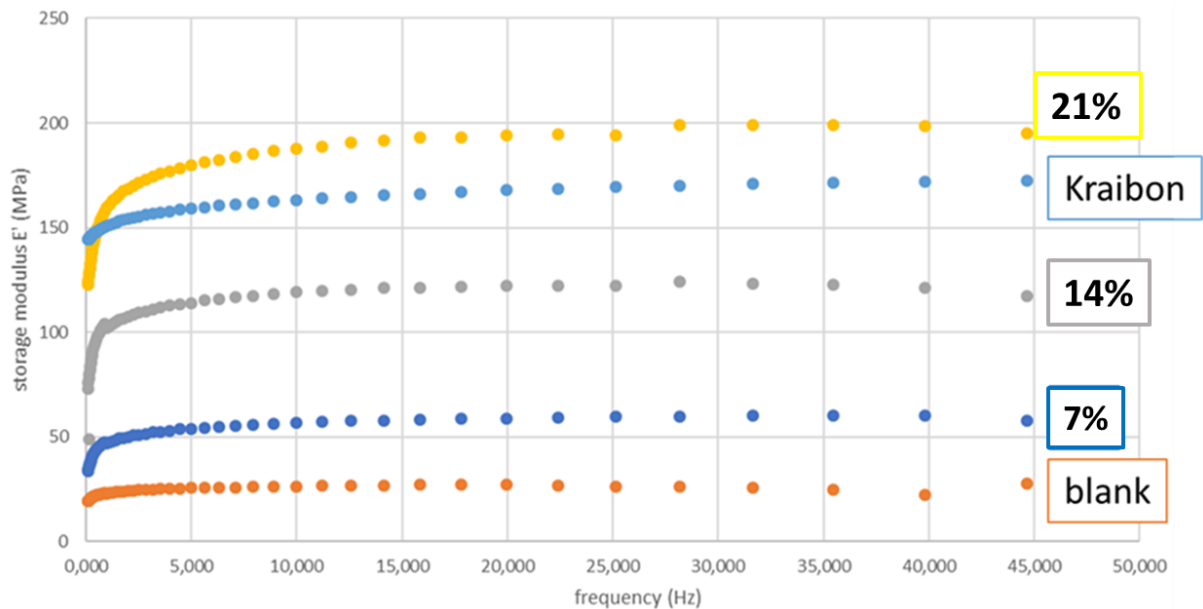


Figure 73: Results of the DMA frequency sweep of 5 different films based on polyurethane dispersions. For comparative reasons a film of the EPDM-based adhesive Kraibon was included in the tests

Figure 73 shows the results of the frequency sweeps. As a further reference, the elastomeric adhesive Kraibon was also included. Figure 74 shows the storage modulus plotted against the composite content:

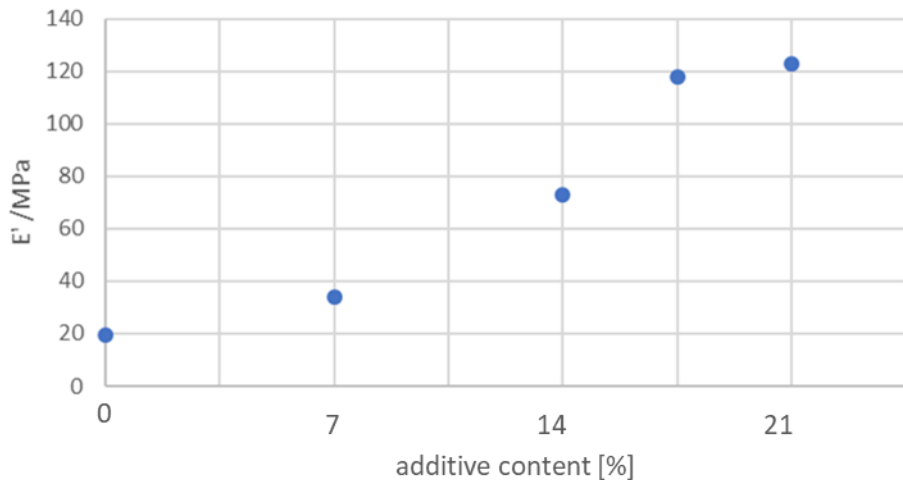


Figure 74: Plot of storage modulus against the additive (composite) content

In the area between 0 and 21% the relation between the modulus and the filler content is apparently linear. The comparison with the material It is shown that the very flexible material can be made much stiffer, the modulus increased by a factor of 6 by the addition of the composite.

To evaluate the adhesive applicability in fiber metal laminates further lap-shear tests were performed. The substrate was the standard alkali-cleaned steel and prepgs made by Sigrafil. As a reference the prepgs were also bonded intrinsically, using the matrix epoxy resin. The second reference was the polyurethane adhesive Duplo tec 690 SBF by Lohmann. For the tests a composite content of 14% was chosen, because this made a film with a similar modulus as the Duplo tec 690 SBF. Figure 75 shows the results of the lap-shear tests:

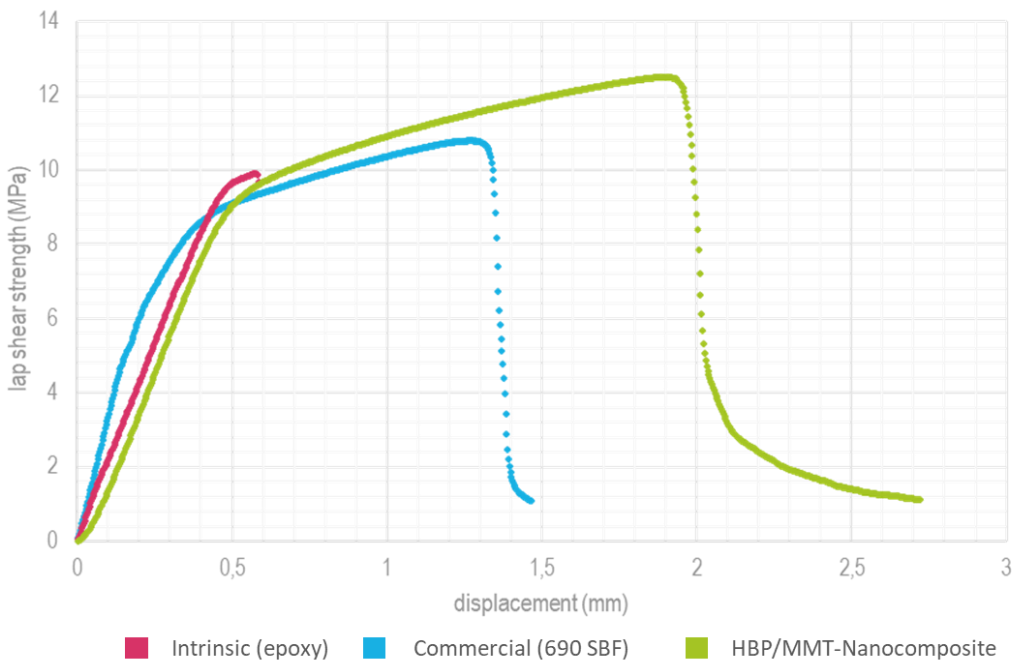


Figure 75: Lap-shear test of PU-adhesives and intrinsically bonded prepreg (Sigrafil)

The graphs in Figure 75 show the results of lap shear-tests. The failure mode was a brittle break-off with the intrinsically bonded prepregs. The debonding happened in all cases on the metal substrate (adhesive failure).

The adhesive strength of the HBP/MMT-nanocomposite samples was 18% above the commercial samples and 30% above the intrinsically bonded samples.

In the next step, simple fiber metal laminates were produced with the same prepregs and metal. Because the production of the composite was not at a scale enough for experiments comparable to previous section, smaller laminates were produced. The production was successful, however 3-point bending experiments on the DMA did not give satisfying results and could not be reproduced.

Because of the better availability of the commercial polyurethane adhesive Duplotex 690 SBF, it was used in the following section “Combined Adhesive Approach”. The 690 SBF is identical in its application and very similar in many properties.

5.3 Combined Adhesive Approach

In the combined adhesive approach, it was investigated what effects the application of elastomeric adhesives in combination with much more rigid epoxy-based adhesives has on fiber-metal laminates. It was also of interest if a functionally graded approach could help increase the performance of elastomeric adhesives while maintaining the interesting benefits such as damping and increased deformation of the laminate.

Simple fiber metal laminate samples were prepared by bonding the CFRP part (2 mm) to a steel plate (2 mm) with a stack of two different adhesive tapes: First, an epoxy adhesive

(E-modul 1050 MPa) with internal mesh to provide a stable thickness. The steel was treated in accordance with the standard procedure with Gardoclean®. The second adhesive was a reactive polyurethane elastomer film (E-Modul 20 MPa). Because the PU-tape should not be cured above 160°C it was kept below, but the process prolonged by 5 minutes.

Table 13: Comparison of SAT 101 epoxy adhesive and DuploTec 690 SBF polyurethane adhesive

	3m, SAT 101	Lohmann, DuploTec 690 SBF
Modulus	1050 MPa	20 MPa
Standard curing	165°C. 15 min	Max. 160°C

The joint gap was kept at 200 µm. To avoid a spill of the epoxy, the plates were wrapped in a release tape and cured in a concealed mold. The gradient in accordance with the model derived from bionics was prepared by stacking the adhesive tapes with the epoxy facing the steel plate and the polyurethane facing the CFRP. To verify the effect of gradient's direction a plate was prepared with the epoxy on the CFRP and the polyurethane adhesive on the steel side. Samples using only the epoxy and polyurethane adhesive alone were prepared as references.



Figure 76: Cut sample to allow lap-shear testing

The samples were comparably large: 200 mm in long and 25.4 mm wide. This allowed cutting them (Figure 76) and testing them in both lap-shear and bending.

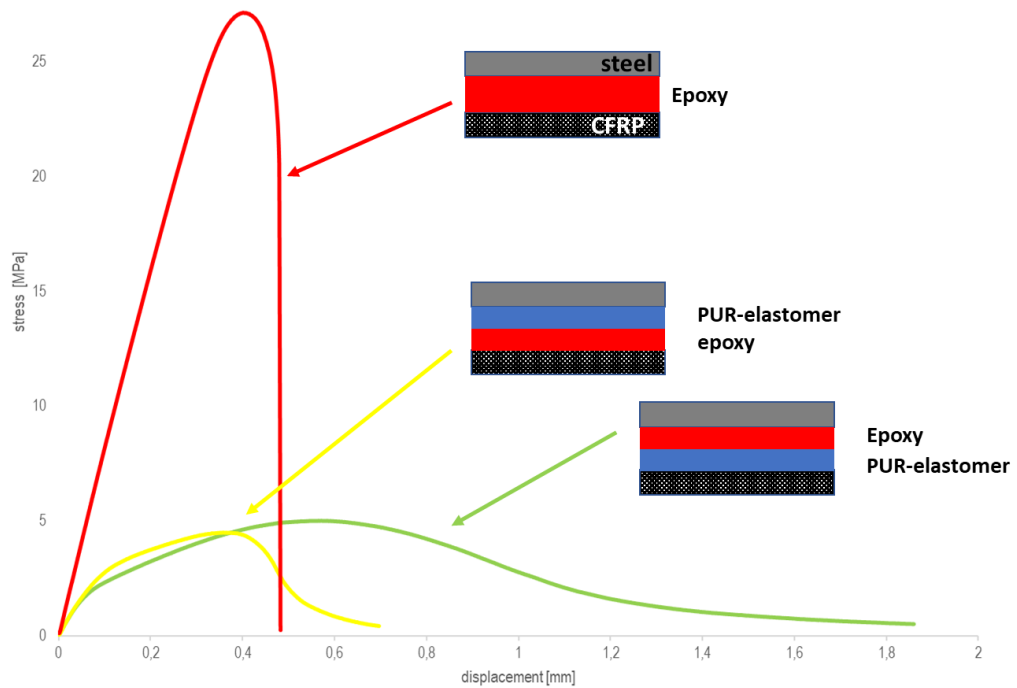


Figure 77: Results of the lap-shear tests of laminates with mixed adhesives and purely EP as reference.

As can be seen from the results in Figure 77, the lap-shear strength of the reference epoxy exceeds the other two samples by far. In a lap-shear test this is to be expected, since the structural epoxy is optimized for this conditions and the polyurethane's lap shear strength is much lower. Although the curing conditions were not within the standard boundaries of the SAT 101, the measured lap-shear strength is much higher than would have been anticipated from the material data sheet (14 MPa on steel). This might have been due to surface treatment.

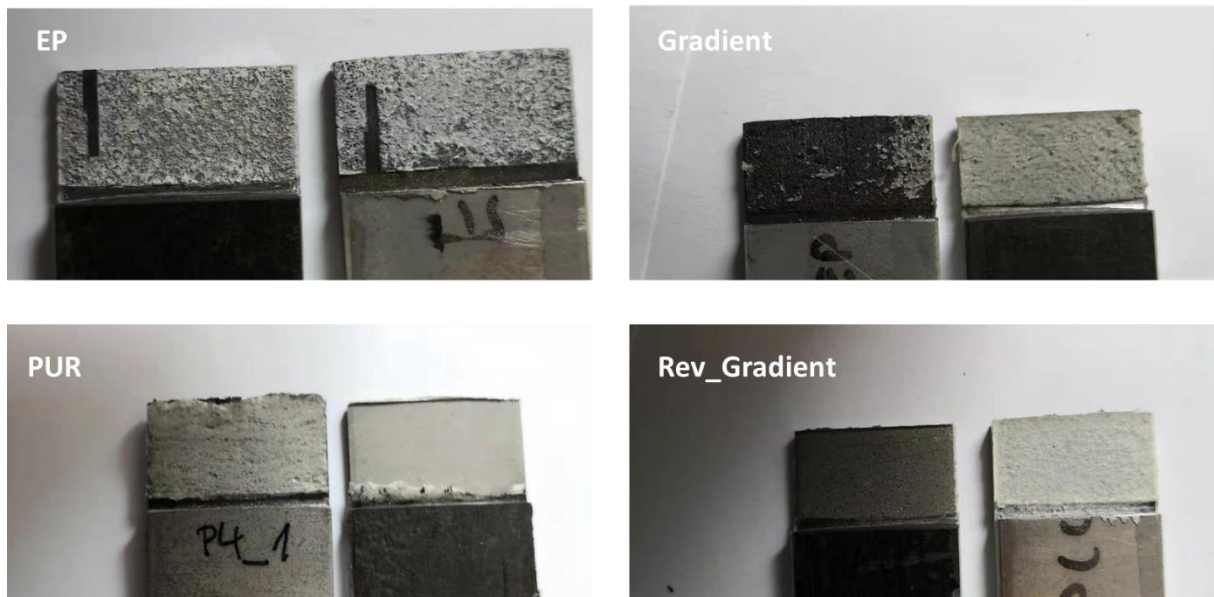


Figure 78: Photographs taken after the lap-shear test. The Gradient and Rev-Gradient samples have the PU-adhesive facing the steel (Rev_Gradient) and CFRP (Gradient). PUR and Rev_Gradient metal sides are blank (photo may be unclear because of reflection)

The sample failure mode in the lap shear tests was:

Table 14: Failure mode of lap-shear samples

PUR	adhesive, metal debonded
EP	cohesive
Rev-Gradient	adhesive, metal debonded
Gradient	mixed, CFRP debonded

The failure mode mirrors the expectations: adhesion of the pure PUR film is better on CFRP than on steel. The failure mode of the gradient samples shows that the apparent adhesion of the epoxy adhesive is slightly higher towards the PUR film, than the PUR film's apparent adhesion to the metal, since the failure mode is mixed in this case, with a tendency to adhesive debonding at the CFRP side.

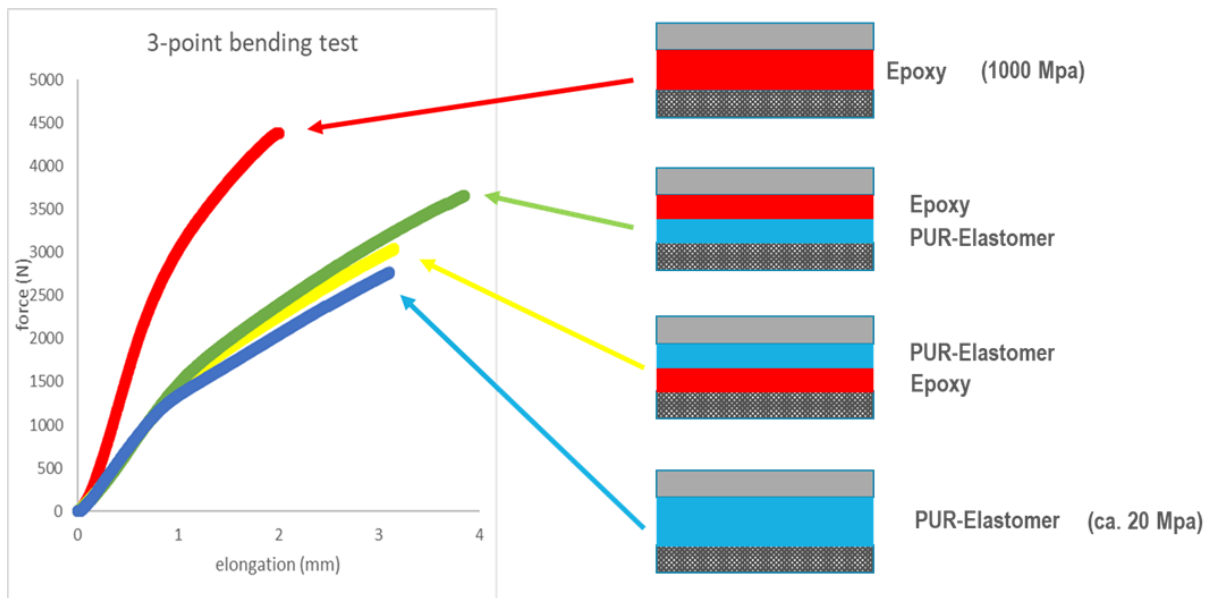


Figure 79: Results of a series of the 3-point bending tests of the gradient adhesive and 3 references. While the pure epoxy specimen shows a high total bending strength, the mixed gradient adhesive shows the highest yield elongation and a higher bending strength than the reversed direction reference and polyurethane-only specimen

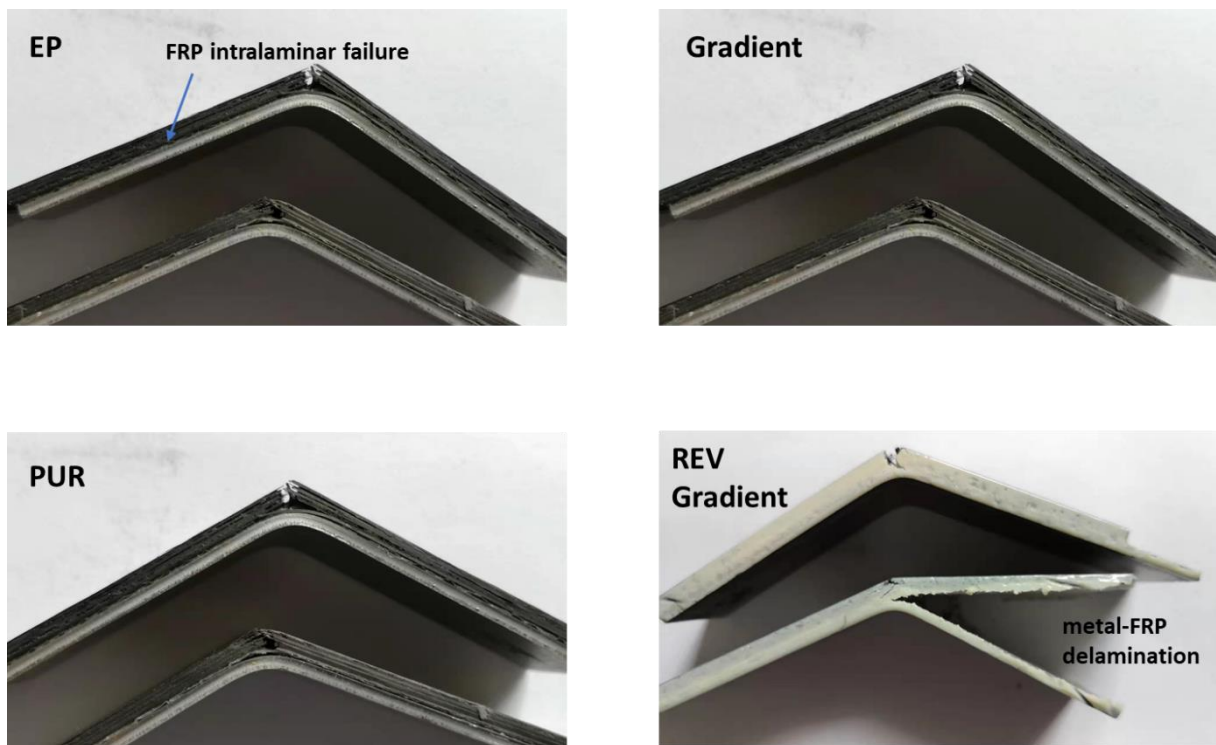


Figure 80: Photographs of the samples after 3-point bending.

All bending samples failed by breaking of the carbon fibers at the outmost layer. The only exception is one sample that was made with the PUR facing the metal and epoxy facing the FRP (reversed Gradient). The differences of force and displacement of these samples are only due to the different adhesive layers and in the case of the gradient and reversed gradient the order of stacking of the adhesives.

One EP-only sample showed signs of intralaminar delamination of the FRP.

As is pointed out in the theoretical part (about stress in single lap joints in section 3.6.1 and stress in 3-point bending testes in 4.6) the lap-shear joint is dominated by stress concentrations at the outer fringes where the overlap ends. The dominating stress in the test is of course shear stresses. Failure in the tests were all due to failure of the adhesives, not the substrate.

In the 3-point bending test both compression and tensile stresses are present. Failure of the laminate usually occurs either by delamination of the laminate layers or breakage of the carbon fibers.

In the bending test epoxy-only specimen shows the highest total bending strength, the mixed gradient adhesive shows the highest yield elongation (92% above the epoxy and 24% above the PUR reference) and a higher bending strength than the reversed direction reference and polyurethane-only specimen. The reversed direction gradient specimen is slightly above the polyurethane reference in both elongation and yield strength.

5.4 Thermoplastic Adhesives Approach

Thermoplastic adhesives are commonly referred to as hot melt adhesives and widely applied in the fields of textiles, shoes and book binding where only low adhesive strength is required. They are also widely applied in non-structural automotive application in the interior and exterior. Examples are usage in bumpers, lamps, car skirts and glass roofs.^[66]

Common thermoplastic adhesives in automotive are based on polyamides, polyurethanes, EVA (ethylene co-vinyl acetate copolymers) and polyolefins. Polyolefins are prevalent because of their high chemical resistance against acids, bases and alcohols as well as against moisture. The main advantage of thermoplastic adhesives is the short process time, which is seconds compared to 30- 45 minutes for most thermosetting epoxies. Other advantages are storability without cooling and shelf life as well as potential recyclability.^[66]

Today's thermoplastic adhesives have adhesive strength required for structural applications, as was discussed with representatives of adhesive and automotive supplier industries during this work. Nonetheless, they are still not widely accepted.

In this part of the work thermoplastic adhesives were tested as the bonding agent in fiber-metal laminates based on CFRP with a thermoplastic matrix.

The thermoplastic adhesives used in this work were obtained from the Nolax AG. They are based on polypropylene and high-density polyethylene. The films are modified to get a wide spectrum of elasticity. Although the vocabulary is not clean elasticity will be expressed in terms of hardness in this context to avoid bulky connotations.

Table 15: Adhesives used in the thermoplastic adhesives' studies, obtained from NOLAX AG

Film	Basis	Modification	T-Peel (N/mm)	Lap-shear strength (MPa)	E-Modulus (MPa)	Elongation at break (%)
Nox 17-2	PP	soft	3,5	5,1	20	1090
Nox 18-5	PP	normal	4,9	11,9	150	870
Cox 391	PP	hard	5,1	18,8	300	830
Nox 20-3	HDPE	soft	3,1	15,5	80	1260
Nox 20-4	HDPE	normal	4,6	16,4	180	1240
Nox 21-1	HDPE	hard	2,8	13,5	200	660

The adhesives are not tacky, their outward appearance is that of regular polyolefin films. The film thickness of individual films was 30 µm. This is the lowest possible thickness without deteriorating the film properties. It allows stacking of the films by 3 to 90 µm, which is desirable in FMLs.

5.4.1 Complex Fiber Metal Laminate with Thermoplastic Adhesive

The gradient was tested in a laminate that consisted of three layers of steel combined with two layers of organic sheets based on polyamide as the matrix and glass fiber as the fiber part. This gives 4 interfaces into which 3 adhesive films each were stacked. The laminate was then put into a hot press at 200°C for 5 minutes. Figure 81 shows the structure of the produced fiber-metal laminates.

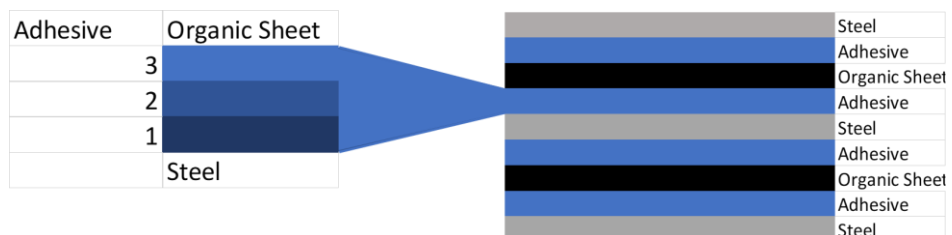


Figure 81: Structure of the Fiber-Metal-Laminate produced with a stacked adhesive layer. The adhesive segments are shown in blue, an example of the adhesive set up is shown on the left. In the reference laminates all adhesives were stacks of the same grade.

Table 16: Samples and the setup of the adhesive stacks in the laminates

Sample	Adhesive Code		
HDPE	1	2	3
Gradient	NOX 21-1	NOX 20-4	NOX-20-3
Reference 1	NOX 21-1	NOX 21-1	NOX-21-1
Reference 2	NOX 20-4	NOX 20-4	NOX-20-4
REV-Gradient	NOX 20-3	NOX 20-4	NOX 21-1
Reference 3	NOX-20-3	NOX 20-3	NOX 20-3
PP	1	2	3
Gradient	COX 391	NOX 18-5	NOX 17-2
Reference 1	COX 391	COX 391	COX 391
Reference 2	NOX 17-2	NOX 17-2	NOX 17-2
REV-Gradient	NOX 17-2	NOX 18-5	COX 391

The laminates were made in the dimension of 100mm x 150 mm. Samples were taken by water cutting to avoid any disturbances induced by thermic effects.

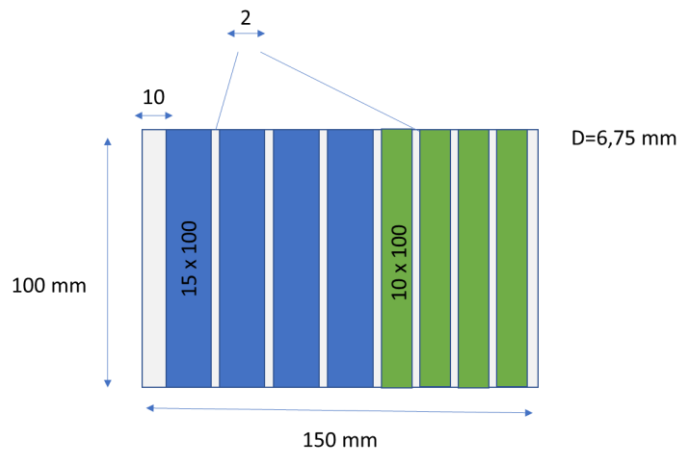


Figure 82: Dimensions of the laminate; the samples marked blue were tested in quasi-static 3-point bending, the samples marked green were tested in an impact-test (dynamic 3-point).

To test the influence of the adhesives on the laminates behavior two strain experiments were conducted: quasi-static bending and a dynamic impact test. Figure 82 shows the sample geometry.

The quasi static test gives more information about static loading of the sample than the dynamic test, which is closer to an actual crash situation. In both tests the failure of the laminate is analyzed. The bending test gives information about the applied force at breakage and the maximum displacement at breakage of the laminate. The dynamic impact test gives the peak energy, peak force and total energy during the impact.

In the following two sections the results of the bending and impact tests of the laminates are compared according to the adhesives used. In a discussion of the test results after the tests with the adhesive supplier it was concluded that with a higher process temperature used for the PP-based adhesive, its performance might have been increased. Therefore, in these

sections the HDPE-based and PP-based adhesives will be analyzed for themselves and not compared with each other. In the production of the angular component a higher process temperature was used.

5.4.2 Bending Test Results

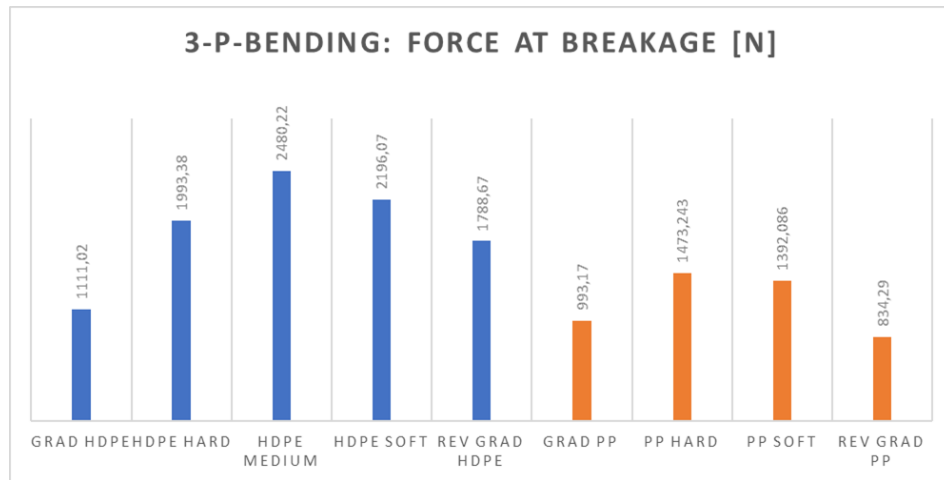


Figure 83: Force at the breakage of the laminate samples during the bending experiments. In blue on the left are laminates produced with adhesive based on HDPE, in orange on the right are samples produced with adhesive based on PP.

Among the HDPE-based adhesives the medium adhesive shows the highest force at breakage followed by the soft and reversed gradient adhesive. The gradient adhesive shows the lowest force. The PP-based adhesives show a somewhat different picture, the hard and soft modified adhesives show the highest force while the gradient adhesive shows a slightly higher force than the reversed gradient adhesive.

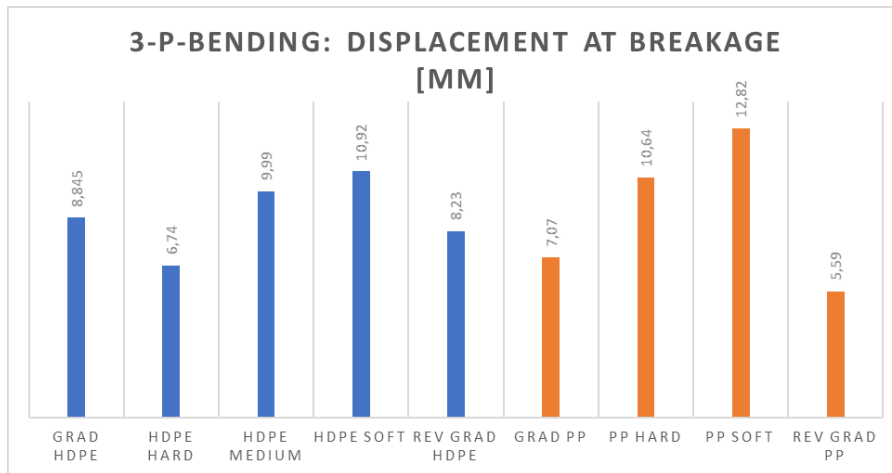


Figure 84: Displacement at breakage of the laminate samples during the bending experiments: on the left are the results of HDPE-based adhesives, on the right those of PP-based ones.

The results of the displacement at breakage show the best performance for the soft modified adhesives. The gradient adhesives perform slightly better for both HDPE and PP adhesives.

If the adhesives are regarded without the context of the laminate, the softer adhesives show a lower tensile strength and higher elongation. The lap-shear strength of the HDPE-adhesives is quite close to the PP-adhesives. The soft PP-based adhesives have a bigger difference to the hard-modified PP adhesive of more than three times higher lap-shear strength (Table 15). These characteristics do not translate to the laminate directly. This means a softer, more flexible adhesive does not necessarily imply that the laminate having a higher displacement in the bending experiment. A less flexible (harder) adhesive will not necessarily have a lower displacement. This is not surprising given the highly complicated nature of the laminate and its performance.

The failure of the FML-laminates in bending experiments is either due to delamination of the adhesive to either substrate or breakage of the fiber component. The metal substrate, within the boundaries of the quasi-static bending experiment, does never break but deforms proportionally to the displacement. **The interaction between the adhesive and the FRP part of the laminate is therefore the determining part in the laminates produced with the flexible adhesives' performance in bending experiments.**

5.4.3 Impact Test Results

In the following section the results of the impact testing are analyzed. The samples were tested on a Charpy impactor (impact energy 50J maximum force: 4kN, impact velocity 3,8m/s) in accordance with ISO 179-2.

As Figure 85 shows the failure behavior of the laminates is very diverse. In some cases, a high degree of interlaminar delamination occurred. Other laminates failed very differently by a local fracture.



Figure 85: Photo of a selection of samples after impact testing. The samples on the left show an optimal failure behavior, the samples on the right show a poor failure behavior. The samples on the left were produced using the soft HDPE adhesive, the samples on the right with a reversed gradient using PP-adhesives.

Figure 85 shows a photo of some of the samples after the impact test. The choice of adhesives is making a huge difference on the performance of the laminate. The samples showing the lowest performance delaminated on both sides. Samples with a high performance broke adjacent to the impact area or had signs of folding of the outer metal layer but no delamination at all.

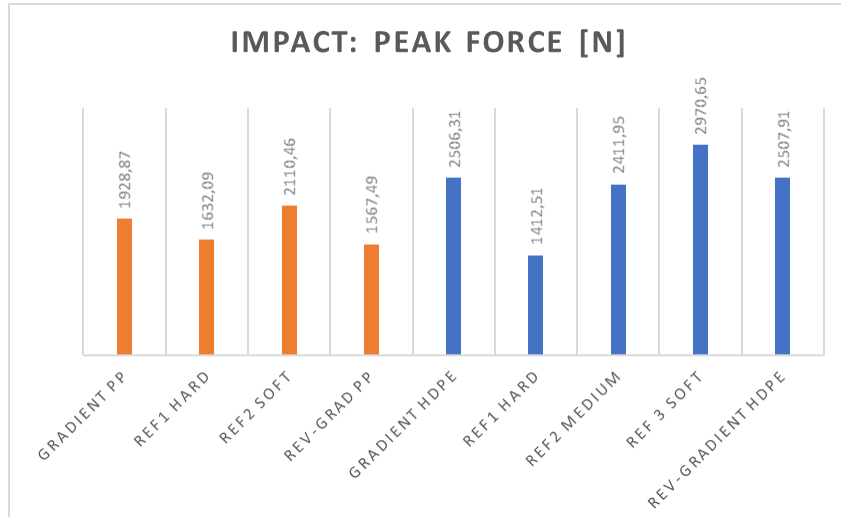


Figure 86: Measured peak forces in the impact test. PP-based adhesives in orange on the left, HDPE-based in blue on the right

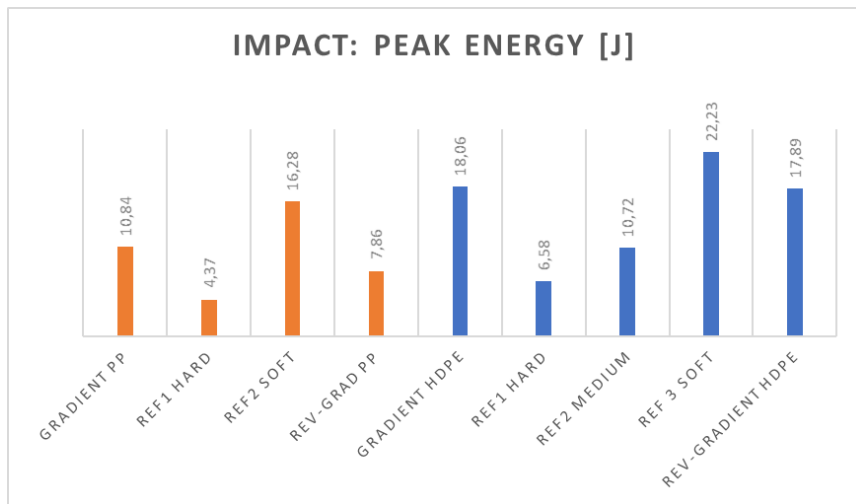


Figure 87: Measured peak energy

Figure 86 and Figure 87 depict the peak force and energy the laminates bear during the impact. The performance of the gradient is around 44% above the reversed gradient sample for the PP but only about 1 % for the HDPE series. An influence of the order of the adhesive stacks is

visible for the samples bonded by PP but negligible for the HDPE-bonded samples. Laminates bonded together by soft adhesives show higher energy peak energies.

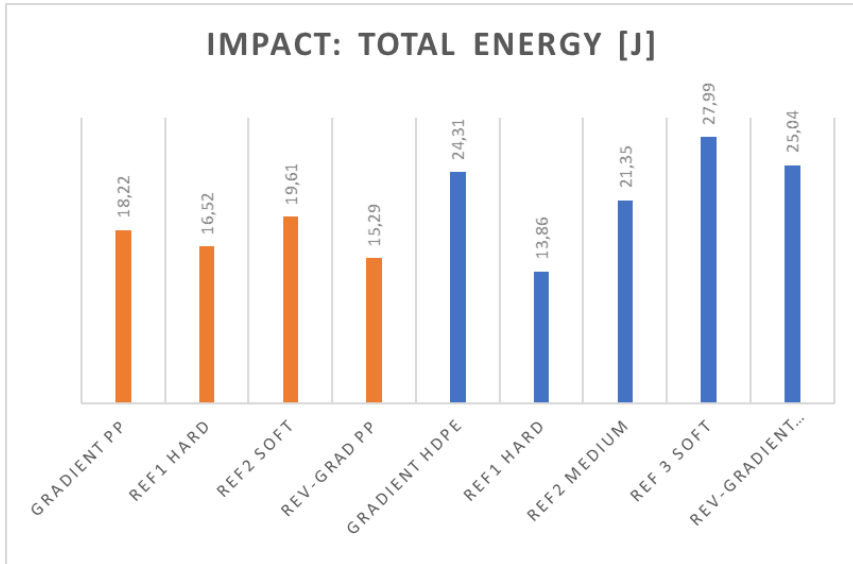


Figure 88: Total energy during the charpy impact tests of the laminates

In Figure 88 the total energy absorbed during the impact before failure is depicted. The soft samples' performance is best, both with PP- and HDPE based adhesives. An influence of the stack order is again low with the HDPE samples with the reversed gradient even performing slightly higher than the gradient (2% difference). In the PP-series the gradient is again visibly performing better with a 15% difference.

5.4.4 Fiber Metal Laminate Component with Thermoplastic Adhesive

To model the entire production cycle of a component made of a fiber metal laminate with thermoplastic fiber sheets and stacked gradient adhesive a less complex variant was used.

The laminate consisted of:

- DP K30/50 steel sheets with 0.55 mm thickness
- Tepex Dynalite 102-RGUD600 2mm thickness
- Adhesive layer 0,1 mm thickness or 3x 0,03 mm

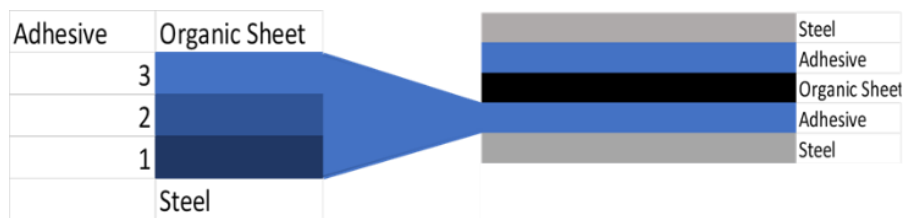


Figure 89: Structure of the fiber metal laminate produced for the reformation and strain experiment. The laminate was produced in the same way as in Figure 81, however less complex with a single fiber ply.

The laminate was produced as before by simple stacking of the material and fusing by pressing at 250°C for 13 seconds and 5kN. In a subsequent step the laminate was heated in an automatic hot press and reformed with an angle of 90°. To generally increase the adhesion to the metal plies of the laminate two samples were laser-treated to increase their surface area.

Table 17: Sample composition of the angular component

Sample Name	Metal	Adhesive 1	Adhesive 2	Adhesive 3	Fiber
1	Normal steel	Cox 391	18-02	17-02	GFRP
2	Normal steel	17-02	18-02	Cox 391	GFRP
3	Normal steel	21-1	20-4	20-3	GFRP
4	Laser treated steel	Cox 391	18-02	17-02	GFRP
REF 1	Normal steel	17-02	17-02	17-02	GFRP
REF 2	Normal steel	20-3	20-3	20-3	GFRP
REF 3	Normal steel	Cox 391			GFRP
REF 4	Laser treated steel	Cox 391			GFRP

In the following paragraph, the results of a pressing experiment are shown. The angular component was placed in the material testing machine and pressed perpendicular to the fiber direction of the CFRP ply (Figure 90). This was done to model a crash situation without the high complexity of an actual crash experiment. The velocity of the deformation is not comparable to an impact experiment, but information about the adhesion and failure of the laminate can be generated similar to quasi-static bending experiments.

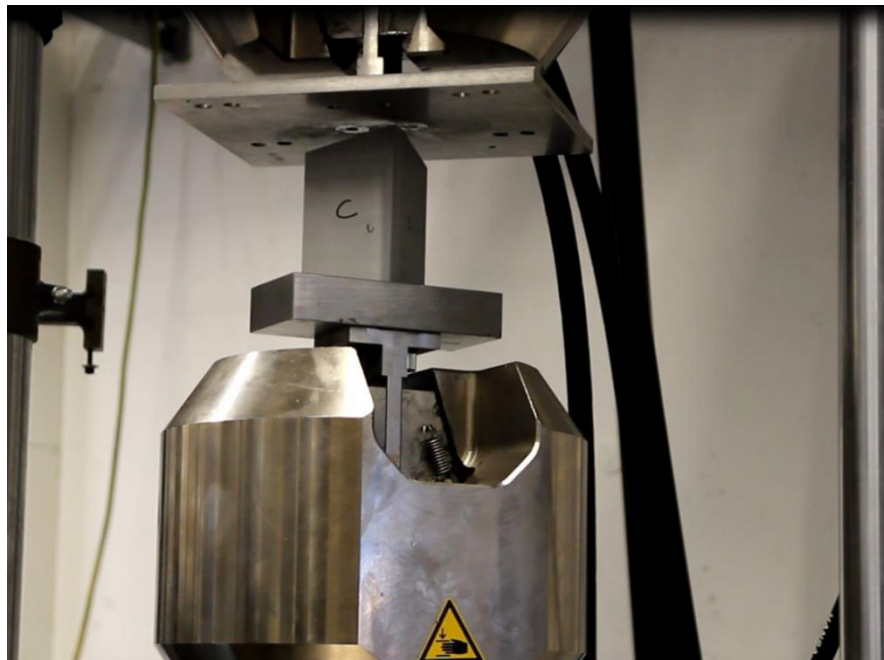


Figure 90: The setup of the pressing experiment. The angular component is placed in an indentation and then pressed against the counter plate.

With increased pressure different modes of failure will occur:

- delamination of the fiber- and steel parts of the laminate
- delamination of layers within the organic sheet
- breaking of fibers within the organic sheet
- bending and folding of the steel part

Compared to epoxy-matrix composite materials the organic sheets based on PP and PA are much less brittle and show different failure modes. Because the sheets contain glass fiber, they are tailored towards high impact strength. Carbon fibers are used to tailor a laminate towards high stiffness. As the modulus of an FRP part is a function of its matrix and fibers, a glass fiber reinforced polyamide has a lower overall modulus than a carbon fiber reinforced plastic.

Due to the high number of samples and reference samples this section contains several figures to filter out the information contained in this series. As in the impact and bending experiments in the section before, the gradient layered adhesive does not show the best performance compared to other systems. The order of the adhesives in the stack show a huge impact on the result, however.

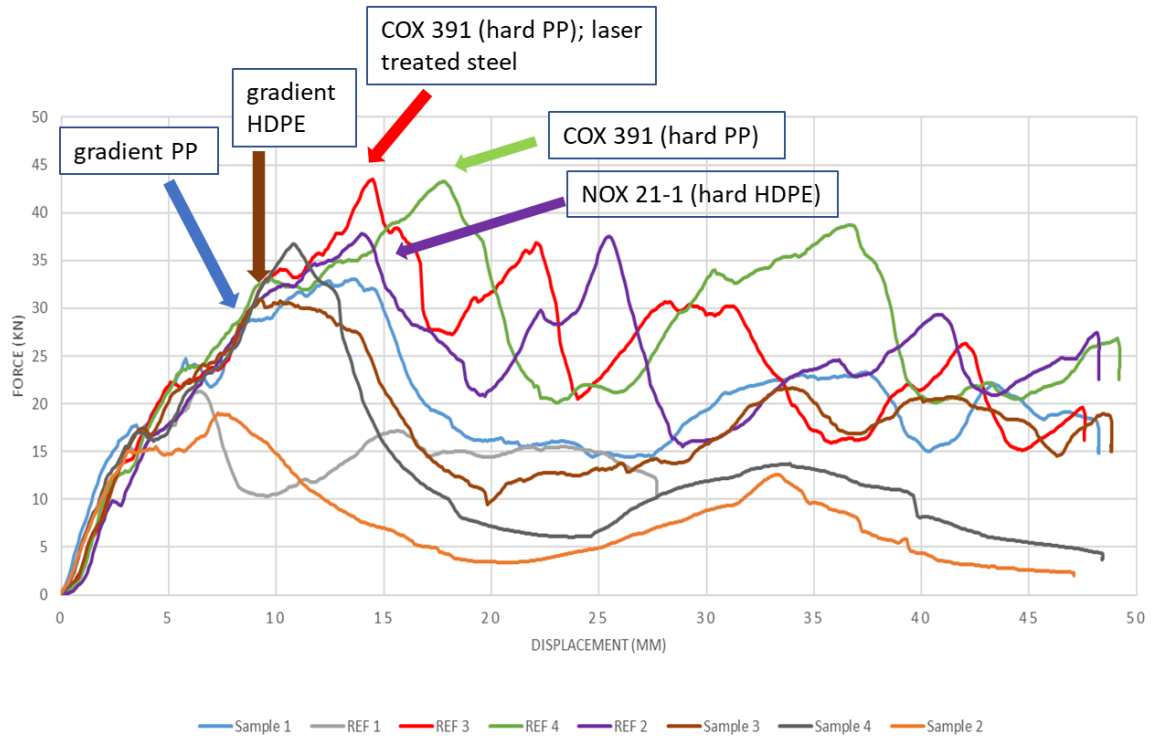


Figure 91: Complete overview of the results of the pressed angular component. A high peak force and large integral is a desirable outcome of the strain experiment. The high modulus PP adhesive COX391 (red graph) on laser treated steel followed by the same adhesive with normal steel (green) shows the best results. As in the bending/impact series with the double laminate the hard HDPE adhesive (purple) comes close but does not show the same peak force.

- The laminate with layers of the high modulus adhesive COX391 and laser treated steel shows the highest peak force, at a sharp peak at (43,41 kN | 14,38 mm) followed by the same adhesive without laser treated steel at (43,14 kN | 17,67 mm).
- The gradient layer adhesive based on polypropylene Sample 1 reaches (36,43 kN | 10,78 mm) and the same adhesive in a laminate with laser treated steel Sample 4 (33,1 kN | 13,48 mm).
- The reversed gradient adhesive reaches (18,79 kN | 7,39 mm)
- The monolithic hard HDPE reaches (37,37 kN | 14,28 mm)
- The gradient HDPE reaches (31,1 kN | 9,09 mm)

The gradient adhesive is obviously not superior under the tested circumstances. Probable reasons will be discussed at the end of this section and in the “Discussion and Conclusions” section. To find out more about the effect a graded layer adhesive has on fiber metal laminate systems, the graded samples will be compared against the reference samples in the following sub-section.

In Figure 92 the gradient layer adhesive based on PP (blue) is plotted against the PP adhesive with the highest modulus (green), the PP adhesive with the lowest modulus (grey) and the reversed gradient layer adhesive which has the modulus gradient set against the preferential direction (hard at the steel surface, soft at the FRP surface, orange).

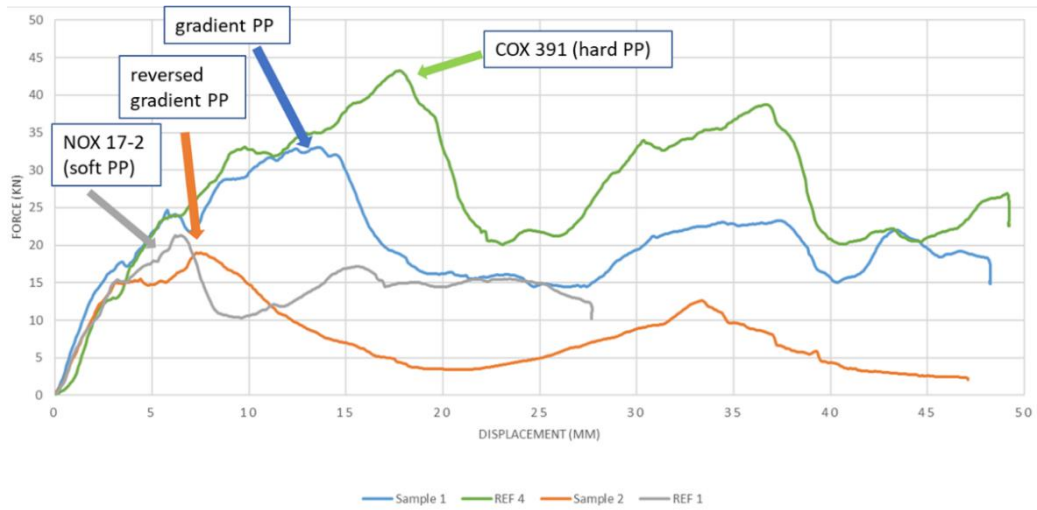


Figure 92: Comparison of the graded and reversely graded PP adhesive sample with the two references of maximum and minimum modulus adhesives contained within the graded samples

As can be seen the performance of the gradient PP is below the monolithic hard PP adhesive, but above the monolithic soft PP and reversed gradient adhesive.

In the gradient adhesive the highest modulus PP (COX391) faces the steel surface while the lowest modulus PP (NOX 17-02) faces the FRP surface. In the reversed gradient adhesive, the COX391 faces the FRP surface and the soft NOX 17-2 faces the steel surface.

As the reversed gradient layer adhesive's performance is below all other variants tested here it can be concluded that there is an inherent effect that is due to the direction of the gradient and not simply because the overall performance e.g. of COX391 is better than that of NOX 17-2.

This directional effect is superimposed by the overall better adhesive properties of COX391 compared to the other in means of peel strength and lap shear strength.

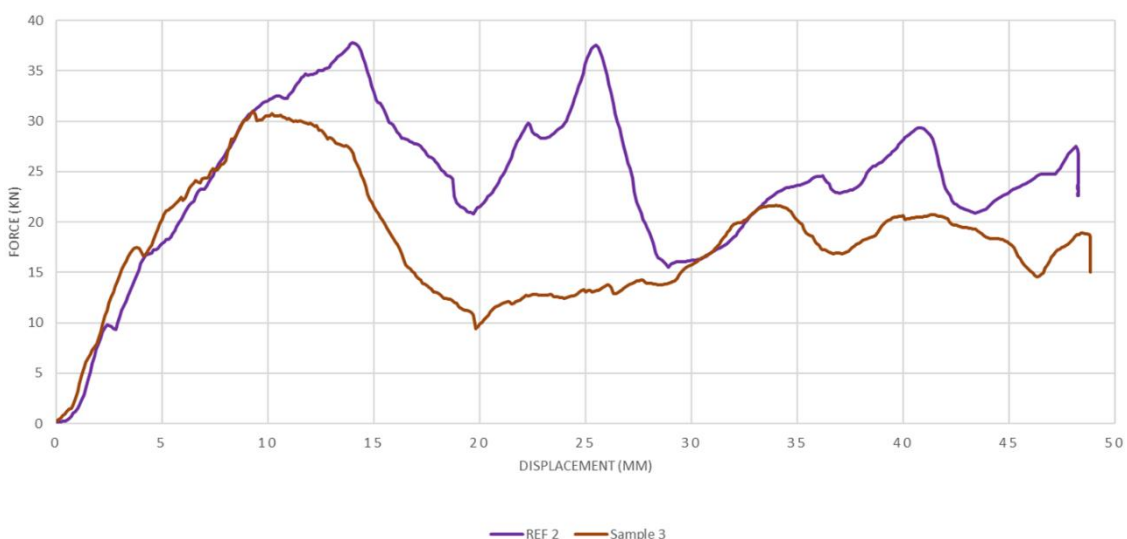


Figure 93: Graphs of gradient HDPE (brown) and reference hard HDPE (NOX 21-1) (purple)

The gradient layer adhesive based on HDPE compared to the reference monolithic hard HDPE adhesive shows generally the same trend that was observed with the PP-based adhesives. The shape of the gradient adhesive's graph (brown) has a similar shape with a blunt, broader peak. Again, the performance of the hard adhesive (purple) surpasses the performance of the gradient adhesive. Unfortunately, there is no reference sample of the monolithic soft HDPE sample present.

During the production of the laminates the adhesive stacks of the gradient adhesive are placed in a hot press and heated to 250°C. The thermoplastic adhesives are in essence hot melts in the form of films. During the time they are in the molten state their viscosity is very much reduced and therefore it must be assumed that they are subject to flow. The matrix material of the organic sheets is also in a molten state during the production and reformation of the laminates.

To find out more about the state of the adhesive layers and possible imperfections that a stacked approach might produce, samples of the angular component were taken after the reformation at different positions of the component. At the tip of the angle the fibers are subject to great forces that thin down the thickness of the organic sheet and press the matrix material in the direction opposite to the tip. The glass fibers, which are held together by the matrix are subject to flow also.

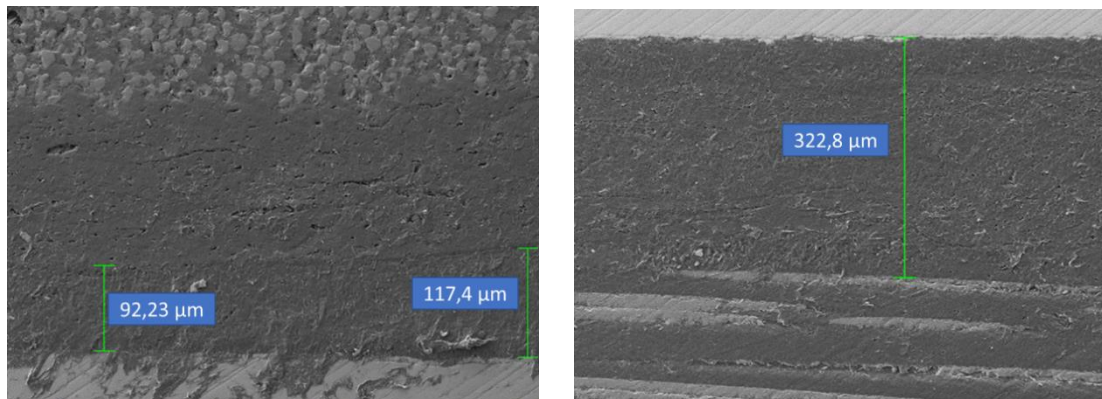


Figure 94: The SEM pictures show two sections of samples taken away from the angular component's tip. The layer between the steel and GFRP part is up to three times bigger than the original adhesive layer at this section. There are two phases visible in the organic, fiber-free phase of the laminate.

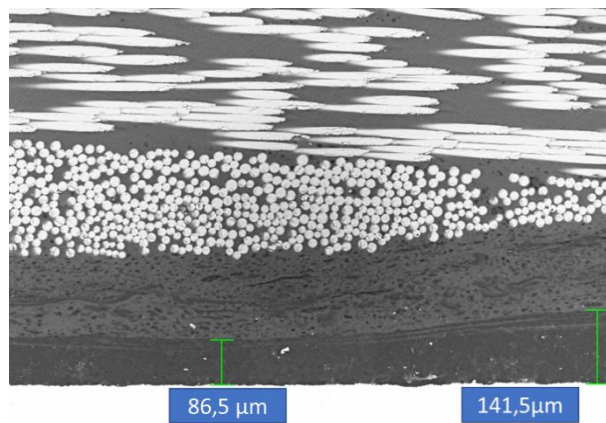


Figure 95: Section of a sample taken close to the tip of the angular component. The material was subject to pressure and subsequent flow. As can be seen the fibers are separated from their matrix material and the adhesive layer is compressed.

The REM analysis shows the effect of the reforming process on the fiber- and adhesive parts of the sample. Both parts are subject to pressure and flow. The adhesive is pressed from one part (Figure 95) leading to higher bond thicknesses in other parts of the sample.

The matrix's polyamide and adhesive's polypropylene do not mix. This was examined in an EDX mapping (Figure 96).

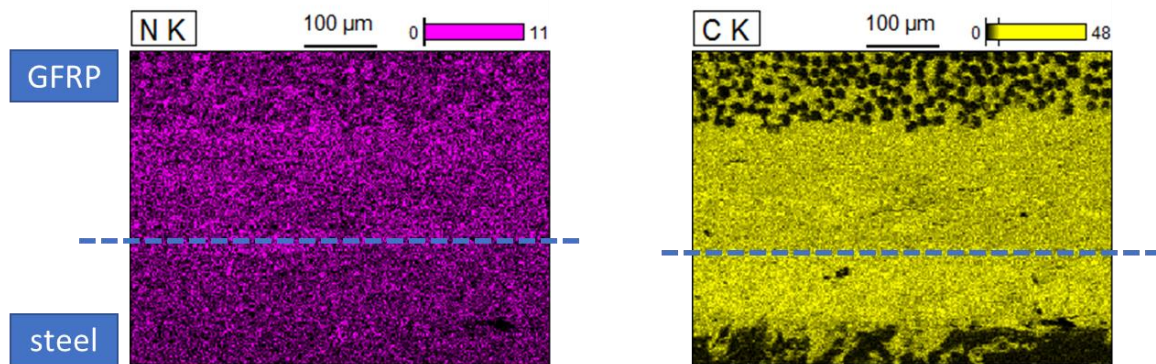


Figure 96: EDX mapping of the section depicted in Figure 94, left. The carbon content is slightly higher in the lower section, while the nitrogen content is higher in the top section. This indicates that the adhesive layer has retained its thickness (higher carbon content = PP, nitrogen → PA) while matrix material was separated from the fibers and displaced into this part of the interphase between steel, adhesive and GFRP.

It can be concluded that the bond line seems to remain homogenous with regards to the matrix material, which is subject to a high degree of flow. **The interface in the examined parts of the sample is PP (adhesive)|PA (matrix) rather than the fibers of the organic sheet encountering the adhesive.**

The adhesive stacking does not have any visible consequences on the bond line, as there are no flaws visible that might be caused by the procedure.

6 Summary

In this work the influence of different adhesives in fiber metal laminates were studied. The idea of an adhesive consisting of stacked layers with an inherent gradient of the elastic properties was studied. This concept can be found in nature and has been examined in other adhesive applications, with the same goal but very different application situations. The stress distribution and effect of a gradient layer adhesive in a FML was simulated prior to the experimental work.

Because adhesives are a wide field and currently a field of fast innovation three classes of adhesives were chosen and studied:

1. Modification of structural epoxy adhesive

The so to say classical structural epoxy adhesives that have been used extensively in the bonding of metal and CFRP material were modified using inorganic additives.

After testing several possible materials as modifiers, milled carbon fiber dust proved to be a very useful material. Its effect could be much enhanced by surface modification.

The built up of a gradient in adhesive was achieved and verified by SEM and EDX investigations. In bending experiments, the gradient set up proved advantageous for the fiber metal laminate. An adhesive layer with only modified epoxy however proved to be just as beneficial.

2. Elastomeric adhesives and combination with stiff adhesives

A reactive hotmelt adhesive based on latent reactive polyurethane, the use of which is an innovation in the field of lightweight construction, was tested in FMLs. A complete formulation of such an adhesive was successful. Its properties, toughness and tensile strength, were greatly improved by the addition of a functional filler made from montmorillonite clay and hyperbranched polyester polyol.

A commercial elastomeric polyurethane adhesive was combined with a stiff epoxy adhesive. The sequence of the adhesives in between the CFRP and metal sheets of the FML proved to be critical for the failure behavior of the FML. With the stiff epoxy facing the metal and the elastic PU facing the CFRP a much higher displacement in bending experiments was achieved.

Another innovation in adhesives, EPDM rubber-based adhesives made by Gummiwerk Kraiburg under the name KRAIBON, were tested. This kind of adhesive is characterized by an adhesive strength comparable to structural epoxies and an elastic behavior. The combination of different kinds of EPDM was successful, however no significant benefit could be measured. The combination with epoxies was not successful.

3. Thermoplastic Structural Adhesives

The third class of adhesives examined in this work are thermoplastic adhesives based on polyolefins PP and HDPE. They are characterized by their very fast and easy application.

A gradient layer was produced by stapling of adhesive films. SEM investigations showed the absence of probable flaws such as bubbles between layers. It was however impossible to verify that mixing of the adhesive's material did not happen to an extend where the gradient had disappeared.

Bending and reformation experiments showed an effect of the sequence of the adhesive films. The proposed gradient was beneficial in some experiments. It was however not the optimum for the application in any of the experiments.

7 Discussion and Conclusions

As was shown, the modification of structural epoxy adhesives and realization of distinct and continuous layers that survive heating under pressure is possible. Although the modified adhesive's performance was above the blank reference, the modified non-graded adhesive showed the same level of improvement.

The brittleness of epoxy-based reinforced plastics is a problem that is especially undesirable in crash relevant components. In materials development there is often a trade-off between high stiffness and less brittleness. By introducing an elastomeric adhesive into the fiber metal laminate, the brittleness was reduced. The failure behavior was changed dramatically, as the elastomeric adhesives seem to act as traps for the crack propagation. Because adhesives with a higher elasticity tend to be lower in their adhesive strength, their use seems to be restricted in structural applications. It was shown that polyurethane adhesives with high elasticity can be formulated that are significantly higher in strength and multiple times higher in toughness than the matrix material used in intrinsic laminate production. The tested EPDM-based adhesives even come close to structural epoxy adhesives.

It was also tested to combine different types of adhesives with a big difference in elasticity. The tested EPDM adhesive could not be combined with the tested epoxide adhesives. The combination of an elastomeric polyurethane adhesive with a structural epoxy gave a significant change in the performance. Maximum displacement and force at breakage were dependent on the order of the adhesives.

The history of continuous fiber reinforced plastics began with thermosetting matrix materials such as epoxies. Thermoplastic materials offer a great number of advantages such as faster cycle times, greater variety of cheap plastics, recyclability and shelf-life. Thermoplastic structural adhesives are a logical choice when producing fiber metal laminates with thermoplastic matrix. They offer advantages in handling and storage and enough strength for structural applications. A gradient of elasticity within the range of available PP and HDPE-based adhesives however did not prove useful. An influence of the stack order (direction of the gradient) was visible in the tests. The stacking technique was very easy in its application and did not cause any of the potential problems such a stacking might have caused. Problems might have been interfacial tensions, mixing problems and introduction of air bubbles between the stacked layers. The stacking technique could be useful to produce asymmetrical adhesive films with other properties than e-modulus.

Montmorillonite clay is an extremely cheap but powerful resource for the enhancement of plastics. A drawback is the increase of viscosity that comes with high filler concentrations. For the formulation of waterborne adhesives an increased viscosity is in most cases desirable. Often a thickener is used to raise the viscosity. The developed hyperbranched polymer/clay nanocomposite proved very useful and effective in the formulation of an adhesive. The effect of the clay on the hyperbranched polymer's dispersibility came as surprising as useful. It is postulated that the clay disrupts the hyperbranched polymer's H-bond similar to a chaotropic agent.

7.1 The functional gradient of modulus and functional adhesive in bonding FMLs

One major aspect of this work was the exploration of a functional gradients of modulus in the adhesive that bonds fiber metal laminates. The impetus of implementing the gradient was to control the mechanical causes (stress concentrations) that lead to the adhesive layer being in most cases the weakest link in the chain in the FML.

The weakest link can be:

- the adhesive (intrinsic)
- the CFRP matrix
- the interphases metal/adhesive
- the CFRP/adhesive
- the galvanized layer/metal
- the fiber/matrix

The metal substrate was never the weakest link in the conducted tests. Optimizing the adhesive leads to the weakest link changing within the laminar structure of the FML, for example, from the adhesive layer to the galvanized layer of a steel interphase.

From the tests conducted in this work, the first conclusion to be drawn is, that the effectiveness of an adhesive is always to be looked upon in its frame of reference. The performance of the adhesives is dependent on the loading, which ultimately depends on the function of the FML.

The mechanical effects that this work set out to explore are part of a complex interplay within the FML. This includes the surface characteristics of the substrate (substrate type, galvanization, sanding, cleaning and etching), the adhesive (electromagnetic interaction in the interphase, mechanical interlocking) and the laminar structure of the FML (crack propagation). Exploring the solely mechanical effect of modulus requires it to be isolated. Controlling it with a meaningful outcome requires the effect to be the dominant effect in the system.

In the examined systems, especially the tested thermoplastic systems, the gradient system was referenced against ungraded samples and samples with a reversed gradient (having a supposedly adversary effect). The functionally graded adhesives perform either on the same level as one of the reference systems (**section 5.2**) or underperform (**section 5.4.2**). In some cases, the order of the gradient had a large impact (e.g. in the part made using thermoplastic adhesive and CFRP system, **section 5.4.4**).

The exception is the behavior of the system including an elastomeric adhesive based on polyurethane (**section 5.3**). The modified adhesives attempt, and the thermoplastic attempt come closest isolating the purely mechanical effects. However, as **table 15** (section 5.4) shows for the thermoplastic adhesive, it is hardly possible to change the modulus of an adhesive while keeping parameters such as T-peel and lap-shear strength constant. These properties are not independent of the modulus.

The system containing the polyurethane-based elastomer is an exception from the other systems in that it combines completely different chemistries. The effects in this system are

most certainly a combination of mechanics and physiochemical reasons. A large part of the effect is probably due to the crack propagation. Another aspect is pure electromagnetic interaction of the adhesive's binder material with the substrate. During the experiments, the similar behavior of toughening in plastics came to mind.

7.2 Perspectives for further work

This work pioneered the applications of different and to some extent exotic adhesives in fiber metal laminates. Its results are therefore not the finish line but more of a home base for future work in the field.

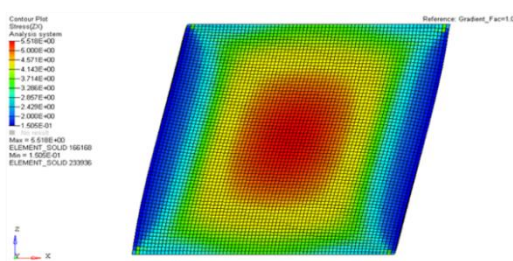
One aspect is the effect that clay has on the heat capacity and interaction with water in nanocomposites with hyperbranched polymers. In this work, the practical aspect of this dynamic was used. A theory was proposed but is to be verified.

As already pointed to, the process of stapling thermoplastic adhesives is a straightforward and easy way to introduce properties into a single film with a preferential distribution. The modification of other properties than elasticity could lead to worthwhile applications. This principle is already in use in some areas of adhesive development and could be further investigated in fiber metal laminates.

The use of elastomeric adhesives has some interesting effects, when it comes to vibrations, crack propagation and crash resistance. Both the development of stronger elastomeric adhesives, such as the ones demonstrated in this work (EPDM-based, nano-particle reinforced PU) and their targeted use in FMLs are interesting fields of research and development.

The idea of introducing a functionally graded adhesive into fiber metal laminates could be further assessed with a different premise: Disregarding the dissimilarity of the joint materials and focusing on the stress distribution in the joint that comes from the much higher dissimilarity of the adhesive from the joint partners.

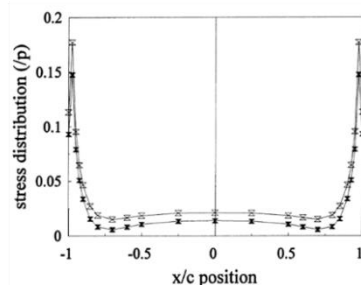
Single lap-shear optimization by FGM



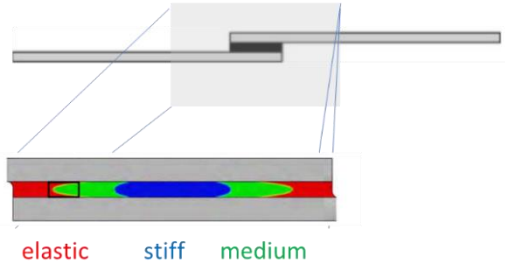
stress distribution in an FML, flexural loading



proposed „sandwich“ FGM adhesive in FML



stress distribution in the single-lap joint, shear load



FGM-adhesive developed by Chminelli et al. 2017

Figure 97: Proposed “sandwich” FGM in analogy to the FGM developed by Chemelli et al. and others

Following the approach of introducing a functional gradient in single lap joints, a similar “sandwich”-like FGM could be tested in fibre metal laminates as well. Figure 97 compares the stress situation in an FML and a single-lap joint in their most common load situation.

8 References

8.1 List of Figures

FIGURE 1: STRUCTURE OF A FIBER METAL LAMINATE (ADAPTATION FROM ^[1]).....	8
FIGURE 2: ONE OF MANY ADHESIVE LAYERS INSIDE A FIBER METAL LAMINATE AND THE GRADIENT LAYER APPROACH (ADAPTATION FROM ^[1]).....	9
FIGURE 3: COMPOSITES IN THE AIRBUS A380 ^[9]	13
FIGURE 4: " LANDSCAPE OF ADHESIVES" FROM BERND BURCHARDT, SIKA ADHESIVES. LSS IS THE LAP SHEAR STRENGTH, THE MOST COMMON VALUE TO CLASSIFY AN ADHESIVE'S STRENGTH. ^[16]	15
FIGURE 5: THE MOST COMMON BOND TYPES OF HYBRID MATERIALS ^[13]	16
FIGURE 6: EMERGENCE AND PROBLEMS OF TENSIONS BETWEEN THE ADHERENT AND ADHESIVE DUE TO DIFFERENT THERMAL EXPANSION	17
FIGURE 7: CONCEPT OF FUNCTIONALLY GRADED MATERIALS: GRADUAL OR STEPWISE PROPERTY DISTRIBUTION ^[18]	17
FIGURE 8: CONVENTIONAL THERMAL SHIELDING VS A FUNCTIONALLY GRADED MATERIAL (LEFT); THERMALLY INDUCED STRESS IN THE MATERIAL (RIGHT) (^[21])	18
FIGURE 9: SEM PICTURE [SOURCE: WIKIPEDIA COMMONS] OF A DIATOM. THIS PRIMITIVE KIND OF ALGAE DEVELOPED A STIFF SILICA-BASED SCAFFOLD. THIS TYPE OF ORGANISM IS CONTRIBUTING AROUND HALF THE ORGANIC MATERIAL IN THE OCEAN AND IS RESPONSIBLE FOR 20% OF OXYGEN PRODUCED ON THE PLANET EACH YEAR ^[24]	19
FIGURE 10: FUNCTIONAL GRADIENT IN A MUSSEL BYSSUS ^[6]	19
FIGURE 11: DEFORMATION OF A SINGLE-LAP-JOINT UNDER TENSILE LOADING ^[25]	20
FIGURE 12: LONGITUDINAL STRESS DISTRIBUTION ALONG THE CENTERLINE OF THE ADHESIVE LAYER OF A SINGLE LAP JOINT (CASE OF TWO COMPOSITE MATERIALS) ^[25]	20
FIGURE 13: ADJUSTMENT OF THE ADHESIVE MODULUS IN THE SINGLE-LAP JOINT BY CARBAS ET AL. ^[27]	21
FIGURE 14: APPLICATION APPARATUS FOR A FUNCTIONALLY GRADED ADHESIVE BY CHIMINELLI ET AL. (3M SCOTCH WELD DP490 TOUGH-ELASTIC EPOXY (BLUE), 3M SCOTCH WELD DP190 (RED), FLEXIBLE EPOXY ADHESIVE AND GREEN 1:1 MIXTURE OF THE TWO ADHESIVES) ^[31]	21
FIGURE 15: LOAD IMPROVEMENT BY A FUNCTIONALLY GRADED ADHESIVE IN A SINGLE-LAP JOINT ACCORDING TO CHIMINELLI ET AL. ^[31]	22
FIGURE 16: SUBSTRATES AND SUBSTRATE TESTING OF RUBBER AND METAL JOINTS AS DESCRIBED BY STABLER ET AL. ^[33]	23
FIGURE 17: A SAMPLE IS STRETCHED BY LONGITUDINAL FORCES F	24
FIGURE 18: THE GRAPHS SHOW THE RADIAL STRESS IN RELATION TO THE STIFFNESS OF ONE MATERIAL (B) IN A BUTT JOINT CONSISTING OF TWO MATERIALS WITH DIFFERENT STIFFNESS E. IN THE FIRST GRAPH THE POISSON RATIO V IS FIXED AT 0,4; IN THE SECOND GRAPH THE DIFFERENCE BETWEEN THE POISSON RATIOS VARIES AT A FIXED STIFFNESS RATIO OF 1 ^[6]	24
FIGURE 19: STRESS-STRAIN CURVES OF FIBER, MATRIX AND COMPOSITE (THE SI UNIT OF STRESS IS N/MM ² ; ADAPTATION FROM ^[37])	26
FIGURE 20: MTS UNIVERSAL TESTING MACHINE (MTS)	27
FIGURE 21: TEST SPECIMEN OF THE LAP SHEAR TEST ACCORDING TO ASTM D1002. DIMENSIONS GIVEN IN INCH AS IN THE STANDARD AND IN SI. [ADAPTATION FROM ^[38]]	28
FIGURE 22: SCHEMATIC OF THE PERKINS ELMER DMA 8000 ^[40] LVDT STANDS FOR "LINEAR VARIABLE DIFFERENTIAL TRANSFORMER", A SENSOR THAT MEASURES THE MOVEMENT OF THE DRIVESHAFT.	28
FIGURE 23: ARRANGEMENT OF A 3-POINT FLEXURAL TEST [COURTESY OF DEVI PRASAD CHALICHEEMALAPALLI JAYASANKAR, LIA UNIVERSITY OF PADERBORN]	29
FIGURE 24: MICROSCOPIC FAILURE THAT LEADS TO THE FAILURE OF FMLS IN 3-POINT BENDING TESTS ^[42]	30
FIGURE 25: CEAST PENDULUM IMPACT TESTER FOR CHARPY TESTS	30
FIGURE 26: THE FIGURE SHOWS THE SAME SAMPLE (A POLYURETHANE BASED ADHESIVE WITH MINERAL FILLERS) REGION MAPPED BY THE SE2-DETECTOR AND THE IN-LENS DETECTOR. THE UPPER SECTION OF THE FIGURE SHOWS THE PLACEMENTS OF THE LENSES INSIDE THE SEM AND THE REGIONS THE DIFFERENT TYPES OF DETECTED ELECTRONS ORIGINATE FROM. ^[47]	33
FIGURE 27: HANDHELD XRF AND STAND-ALONE XRD-DEVICE [DONGGUAN HONGTUO (LEFT) AND WIKIPEDIA COMMONS (RIGHT)]	34
FIGURE 28: MODULUS IN A FIBER MEAL LAMINATE IN THE INTERPHASE OF THE ADHERENTS AND INTERLAYER	36
FIGURE 29: 1/4-MODEL OF A 4-POINT BENDING OF A FIBER METAL LAMINATE WITH TWO LAYERS (ONE FRP, ONE STEEL AS IN FIGURE 28). THE GAP OF MODULUS IN THE INTERLAYER LEADS TO A STRESS- AND STRAIN DISTRIBUTION THAT ACTS AS A NOTCHED BAR IMPACT.....	36

FIGURE 30: FEA-ANALYSIS OF A FIBER METAL LAMINATE'S INTERPHASE BETWEEN THE STEEL (TOP) AND FRP (BOTTOM) PARTS.....	37
FIGURE 31: STRESS DISTRIBUTION IN THE FLM'S JOINT WITH A GRADIENT INTERLAYER. THE GRADIENT FACTOR IS 1.6 AND TRENDS LINEARLY BETWEEN THE JOINTS. AS IN THE PRECEDING FIGURES THE STEEL IS IN THE BOTTOM AND THE FRP IN THE TOP.	37
FIGURE 32: HYPERBRANCHED POLYESTER POLYOL, 64 PRIMARY OH GROUPS ^[53]	39
FIGURE 33: SUI ET AL: GRAFTING OF HYPERBRANCHED GLYCEROLS ONTO CARBON FIBER SURFACES ^[54]	40
FIGURE 34: SEM PICTURES AND EDX OF SIGRAFIL 200-UN MILLED CARBON FIBER. THE DIFFERENT COUNT RATES OF OXYGEN AND CARBON AS WELL AS RESIDUAL CHLORINE TOGETHER WITH SLIGHTLY CHANGED MORPHOLOGY INDICATE A CHEMICAL GRAFTING OF THE POLYMER	40
FIGURE 35: MORPHOLOGY OF THE MILLED CARBON FIBER IN DIFFERENT STAGES OF THE TREATMENT. AFTER THE OXIDIZATION STEP THE NUMBER OF FIBER DEBRIS PARTICLES ON THE SURFACE HAS DIMINISHED. THE CONTOURS OF THE FIBER AFTER THE GRAFTING PROCEDURE ARE LESS SHARP. THE PROMINENT FURROWS SEEM TO HAVE BEEN PARTIALLY FILLED.	41
FIGURE 36: COMPARISON OF THE RESULTS OF TENSILE EXPERIMENTS OF MODIFIED AND UNMODIFIED SIGRAFIL MILLED CARBON FIBER. 5 SAMPLES EACH WERE TESTED. THE FILLER AMOUNT FOR THE COMPARISON WAS 5%.....	42
FIGURE 37: COMPARISON OF THE FORCE AT BREAKING OF THE MODIFIED ADHESIVE SPECIMENS.....	43
FIGURE 38: COMPARISON OF THE DISPLACEMENT (PROPORTIONAL TO THE ELONGATION) OF THE MODIFIED ADHESIVE SPECIMENS ...	43
FIGURE 39: GRAPHS OF THE TENSILE TESTING OF SIGRAFIL MILLED CARBON FIBER- MODIFIED BETAMATE 1630	44
FIGURE 40: SLOPE IN THE LINEAR SECTION AS A FUNCTION OF THE BRASS-CHIP CONCENTRATION	44
FIGURE 41: SLOPE IN THE LINEAR SECTION AS FUNCTION OF THE CONCENTRATION OF TITANIUM DIOXIDE	45
FIGURE 42: SLOPE OF THE LINEAR SECTION AS A FUNCTION OF THE CONCENTRATION OF MILLED CARBON FIBER	45
FIGURE 43: 15 x 15 MM STEEL SHEETS COVERED WITH ADHESIVE OF DIFFERENT MODIFIER RATIO	46
FIGURE 44: SKETCH OF THE PRODUCTION OF 2-LAYER BOND LINES WITH LIQUID ADHESIVES	46
FIGURE 45: HYBRID PLATES AFTER WATER CUTTING. THE BIGGER SPECIMENS ARE FOR STATIC 3-POINT BENDING, THE THINNER SPECIMENS FOR DYNAMIC BENDING (IMPACT) TESTING.....	46
FIGURE 46: REM IMAGES AND SKETCH OF THE BOND LINE. RED ARROWS MARK THE ADDED MILLED FIBERS IN THE ADHESIVE. THE PICTURE AT THE TOP RIGHT SHOWS MATERIAL THAT WAS DISPLACED DURING THE CURING PROCESS IN THE PRESS. AS CAN BE SEEN THE LAYERS REMAIN INTACT EVEN AFTER FLOWING OUT OF THE BOND LINE.	47
FIGURE 47: EDX-MAPPING IMAGES OF THE BOND WITH A 10% FILLER RATIO ON THE LEFT AND A GRADED BOND (10% AT THE STEEL INTERFACE, 0% AT THE CFRP INTERFACE) ON THE RIGHT. A DEEPER RED SIGNIFIES A HIGHER CARBON CONCENTRATION. THE ARROWS MARK SOME OF THE MILLED CARBON FIBER FRAGMENTS WITHIN THE ADHESIVE LAYER.....	47
FIGURE 48: COMPARISON OF 3-POINT BENDING RESULTS OF THE GRADED AND UNGRADED ADHESIVE SAMPLES	48
FIGURE 49: COMPARISON OF THE RESULTS OF THE BENDING TEST OF THE UNMODIFIED- AND GRADIENT ADHESIVE WITH THE REFERENCE FMLs (BENDING STRENGTH)	48
FIGURE 50: COMPARISON OF THE RESULTS OF THE BENDING TEST OF THE UNMODIFIED- AND GRADIENT ADHESIVE WITH THE REFERENCE FMLs (ELONGATION AT BREAK)	49
FIGURE 51: LINE-UP OF THE RESULTS OF THE BENDING TEST RESULTS.....	49
FIGURE 52: COMPARISON OF STRUCTURAL EPOXIES TO RUBBER BASES ADHESIVES, ACCORDING TO KRAIBURG DATA SHEETS	50
FIGURE 53: LAP SHEAR TEST WITH EPDM-BASED ADHESIVE KRAIBON, IN THE CASE OF HAA9275/45 (0,4 MM) ON PREPREG (SIGRAPREG) AND STEEL	50
FIGURE 54: CONFOCAL MICROSCOPE PICTURE OF A LAMINATE BONDED BY A STACK OF TWO EPDM-GRADES. THE DIFFERENCE OF THE ELASTIC MODULI CAN BE DESCRIBED BY A GRADIENT FACTOR OF 1.9.....	51
FIGURE 55: GRAPHIC REPRESENTATIONS OF THE 3-POINT BENDING TESTS OF KRAIBON-BONDED LAMINATES.....	52
FIGURE 56: CHEMICAL EQUILIBRIUM OF ISOCYANATES AND URETDIONE. AT HIGH TEMPERATURES THE EQUILIBRIUM IS ON THE SIDE OF THE MORE STABLE ISOCYANATES. THE REACTION SPEED CAN BE INCREASED BY CATALYSIS ^[55]	53
FIGURE 57: THE PICTURE SHOWS DIFFERENT ATTEMPTS AT BLADING A FILM ONTO SILICONIZED PAPER. THE FILM IN THE UPPER LEFT SHOWS LITTLE DEWETTING, WHILE THE FILMS ON THE UPPER AND LOWER RIGHT SHOW ALMOST NO WETTING OF THE SURFACE.	54
FIGURE 58: THE HYDRAULIC HOT PRESS USED TO PREPARE THE SAMPLES. THE PRESS HAS A MAXIMUM PRESSURE OF 31 MPa AND MAXIMUM TEMPERATURE OF 600°C.....	55
FIGURE 59: FACTORS INFLUENCING THE PERFORMANCE OF THE ADHESIVE INVESTIGATED DURING THE FORMULATION PROCESS	55
FIGURE 60: FIRST ATTEMPTS OF JOINING STEEL CUTS AFTER HAND-TESTING	56
FIGURE 61: TWO ADHESIVE TAPES, ONE WITHOUT FILLERS, THE BLACK FILM CONTAINS MILLED CARBON FIBER	56
FIGURE 62: THE PICTURE SHOWS LAP-SHEAR SAMPLES OF ADHESIVES MODIFIED BY SIGRAFIL® MILLED CARBON FIBER. THE THREE SAMPLES ARE FROM THE SAME SERIES. THE SAMPLES ARE STAPLED TO ENABLE DIRECT COMPARISON OF THE LAP AREAS.....	56

FIGURE 63: RESULTS OF THE LAP-SHEAR TEST OF MILLED CARBON FIBER FILLED ADHESIVE IN COMPARISON TO A REFERENCE ADHESIVE WITHOUT FILLING. THE REFERENCE WITHOUT MILLED CARBON FIBER IS SHOWN IN GREEN.....	57
FIGURE 64: COMPLETE STRUCTURE OF THE HYPERBRANCHED POLYMER USED IN THE FIRST TESTS. IT IS A HYPERBRANCHED POLYESTER POLYOL OF THE 4 TH PSEUDO-GENERATION	57
FIGURE 65: SEM-MICROGRAPH OF A CUT THROUGH A PARTICLE OF THE HYPERBRANCHED (POLYESTER PSEUDO GEN. 4) /CLAY MIXTURE. THE CLAY IS MOSTLY EXFOLIATED. THE LARGER WHITE OBJECTS INDICATE STACKS OF SILICA CLAY THAT IS ONLY PARTLY INTERCALATED OR PRESENT AS INTACT STACKS.....	58
FIGURE 66: A SECTION OF THE SEM-MICROGRAPH OF FIGURE 65 AT A HIGHER MAGNIFICATION	59
FIGURE 67: SURVEY OF THE LAYER THICKNESS OF THE INTERCALATED CLAY IN THE HYPERBRANCHED/CLAY MIXTURE. THE THICKNESS INDICATES EXFOLIATION.....	59
FIGURE 68: DSC CURVES FOR PRISTINE AND VARIOUSLY MODIFIED PSEUDO GENERATION 4 (HB40) SAMPLES, FROM BOTTOM UP DECREASED NUMBER OF OH: PRISTINE HB40; HBPT14, HBPT18; HBPT119; HBPT140 (ADAPTATION FROM ^[62])	60
FIGURE 69: DSC CURVES OF PURE HYPERBRANCHED POLYESTER PSEUDO GENERATION 4 AND THE HYPERBRANCHED/CLAY MIXTURE. THE PEAK AT 70°C IS DIMINISHED.....	61
FIGURE 70: CLASSIFICATION OF IONS AS KOSMOTROPES (FROM GREEK ΚΟΣΜΟΣ = (WORLD)ORDER) AND CHAOTROPES (FROM GREEK ΧΑΟΣ =VOID, EMPTYNESS, DISORDER) AS PUBLISHED BY COLLINS ET AL IN 1997 ^[63]	62
FIGURE 71: LAP SHEAR STRENGTH OF ADHESIVE FILMS WITH VARIED HBP/MMT-PORTIONS	64
FIGURE 72: A PHOTOGRAPH OF THE SIMPLIFIED FORMULATION DOCTOR BLADED ONTO A SILICONIZED PAPER	65
FIGURE 73: RESULTS OF THE DMA FREQUENCY SWEEP OF 5 DIFFERENT FILMS BASED ON POLYURETHANE DISPERSIONS. FOR COMPARATIVE REASONS A FILM OF THE EPDM-BASED ADHESIVE KRAIBON WAS INCLUDED IN THE TESTS.....	65
FIGURE 74: PLOT OF STORAGE MODULUS AGAINST THE ADDITIVE (COMPOSITE) CONTENT	66
FIGURE 75: LAP-SHEAR TEST OF PU-ADHESIVES AND INTRINSICALLY BONDED PREPREG (SIGRAFIL)	67
FIGURE 76: CUT SAMPLE TO ALLOW LAP-SHEAR TESTING.....	68
FIGURE 77: RESULTS OF THE LAP-SHEAR TESTS OF LAMINATES WITH MIXED ADHESIVES AND PURELY EP AS REFERENCE.....	69
FIGURE 78: PHOTOGRAPHS TAKEN AFTER THE LAP-SHEAR TEST. THE GRADIENT AND REV-GRADIENT SAMPLES HAVE THE PU-ADHESIVE FACING THE STEEL (REV_GRADIENT) AND FRP (GRADIENT). PUR AND REV_GRADIENT METAL SIDES ARE BLANK (PHOTO MAY BE UNCLEAR BECAUSE OF REFLECTION)	70
FIGURE 79: RESULTS OF A SERIES OF THE 3-POINT BENDING TESTS OF THE GRADIENT ADHESIVE AND 3 REFERENCES. WHILE THE PURE EPOXY SPECIMEN SHOWS A HIGH TOTAL BENDING STRENGTH, THE MIXED GRADIENT ADHESIVE SHOWS THE HIGHEST YIELD ELONGATION AND A HIGHER BENDING STRENGTH THAN THE REVERSED DIRECTION REFERENCE AND POLYURETHANE-ONLY SPECIMEN	71
FIGURE 80: PHOTOGRAPHS OF THE SAMPLES AFTER 3-POINT BENDING.....	71
FIGURE 81: STRUCTURE OF THE FIBER-METAL-LAMINATE PRODUCED WITH A STACKED ADHESIVE LAYER. THE ADHESIVE SEGMENTS ARE SHOWN IN BLUE, AN EXAMPLE OF THE ADHESIVE SET UP IS SHOWN ON THE LEFT. IN THE REFERENCE LAMINATES ALL ADHESIVES WERE STACKS OF THE SAME GRADE.....	73
FIGURE 82: DIMENSIONS OF THE LAMINATE; THE SAMPLES MARKED BLUE WERE TESTED IN QUASI-STATIC 3-POINT BENDING, THE SAMPLES MARKED GREEN WERE TESTED IN AN IMPACT-TEST (DYNAMIC 3-POINT)	74
FIGURE 83: FORCE AT THE BREAKAGE OF THE LAMINATE SAMPLES DURING THE BENDING EXPERIMENTS. IN BLUE ON THE LEFT ARE LAMINATES PRODUCED WITH ADHESIVE BASED ON HDPE, IN ORANGE ON THE RIGHT ARE SAMPLES PRODUCED WITH ADHESIVE BASED ON PP	75
FIGURE 84: DISPLACEMENT AT BREAKAGE OF THE LAMINATE SAMPLES DURING THE BENDING EXPERIMENTS: ON THE LEFT ARE THE RESULTS OF HDPE-BASED ADHESIVES, ON THE RIGHT THOSE OF PP-BASED ONES.....	75
FIGURE 85: PHOTO OF A SELECTION OF SAMPLES AFTER IMPACT TESTING. THE SAMPLES ON THE LEFT SHOW AN OPTIMAL FAILURE BEHAVIOR, THE SAMPLES ON THE RIGHT SHOW A POOR FAILURE BEHAVIOR. THE SAMPLES ON THE LEFT WERE PRODUCED USING THE SOFT HDPE ADHESIVE, THE SAMPLES ON THE RIGHT WITH A REVERSED GRADIENT USING PP-ADHESIVES	77
FIGURE 86: MEASURED PEAK FORCES IN THE IMPACT TEST. PP-BASED ADHESIVES IN ORANGE ON THE LEFT, HDPE-BASED IN BLUE ON THE RIGHT	77
FIGURE 87: MEASURED PEAK ENERGY	77
FIGURE 88: TOTAL ENERGY DURING THE CHARPY IMPACT TESTS OF THE LAMINATES.....	78
FIGURE 89: STRUCTURE OF THE FIBER METAL LAMINATE PRODUCED FOR THE REFORMATION AND STRAIN EXPERIMENT. THE LAMINATE WAS PRODUCED IN THE SAME WAY AS IN FIGURE 81, HOWEVER LESS COMPLEX WITH A SINGLE FIBER PLY.	78
FIGURE 90: THE SETUP OF THE PRESSING EXPERIMENT. THE ANGULAR COMPONENT IS PLACED IN AN INDENTATION AND THEN PRESSED AGAINST THE COUNTER PLATE.....	80

FIGURE 91: COMPLETE OVERVIEW OF THE RESULTS OF THE PRESSED ANGULAR COMPONENT. A HIGH PEAK FORCE AND LARGE INTEGRAL IS A DESIRABLE OUTCOME OF THE STRAIN EXPERIMENT. THE HIGH MODULUS PP ADHESIVE COX391 (RED GRAPH) ON LASER TREATED STEEL FOLLOWED BY THE SAME ADHESIVE WITH NORMAL STEEL (GREEN) SHOWS THE BEST RESULTS. AS IN THE BENDING/IMPACT SERIES WITH THE DOUBLE LAMINATE THE HARD HDPE ADHESIVE (PURPLE) COMES CLOSE BUT DOES NOT SHOW THE SAME PEAK FORCE.....	81
FIGURE 92: COMPARISON OF THE GRADED AND REVERSELY GRADED PP ADHESIVE SAMPLE WITH THE TWO REFERENCES OF MAXIMUM AND MINIMUM MODULUS ADHESIVES CONTAINED WITHIN THE GRADED SAMPLES.....	82
FIGURE 93: GRAPHS OF GRADIENT HDPE (BROWN) AND REFERENCE HARD HDPE (NOX 21-1) (PURPLE)	82
FIGURE 94: THE SEM PICTURES SHOW TWO SECTIONS OF SAMPLES TAKEN AWAY FROM THE ANGULAR COMPONENT'S TIP. THE LAYER BETWEEN THE STEEL AND GFRP PART IS UP TO THREE TIMES BIGGER THAN THE ORIGINAL ADHESIVE LAYER AT THIS SECTION. THERE ARE TWO PHASES VISIBLE IN THE ORGANIC, FIBER-FREE PHASE OF THE LAMINATE.	83
FIGURE 95: SECTION OF A SAMPLE TAKEN CLOSE TO THE TIP OF THE ANGULAR COMPONENT. THE MATERIAL WAS SUBJECT TO PRESSURE AND SUBSEQUENT FLOW. AS CAN BE SEEN THE FIBERS ARE SEPARATED FROM THEIR MATRIX MATERIAL AND THE ADHESIVE LAYER IS COMPRESSED.	84
FIGURE 96: EDX MAPPING OF THE SECTION DEPICTED IN FIGURE 94, LEFT. THE CARBON CONTENT IS SLIGHTLY HIGHER IN THE LOWER SECTION, WHILE THE NITROGEN CONTENT IS HIGHER IN THE TOP SECTION. THIS INDICATES THAT THE ADHESIVE LAYER HAS RETAINED ITS THICKNESS (HIGHER CARBON CONTENT = PP, NITROGEN -> PA) WHILE MATRIX MATERIAL WAS SEPARATED FROM THE FIBERS AND DISPLACED INTO THIS PART OF THE INTERPHASE BETWEEN STEEL, ADHESIVE AND GFRP.....	84
FIGURE 97: PROPOSED "SANDWICH" FGM IN ANALOGY TO THE FGM DEVELOPED BY CHEMELLI ET AL. AND OTHERS	90

8.2 List of Tables

TABLE 1: ADVANTAGES AND DISADVANTAGES OF FMLS[5].....	12
TABLE 2: TABLE 2: BETAMATE 1630 PROPERTIES LIST ACCORDING TO THE TECHNICAL DATA SHEET[50].....	38
TABLE 3: MATERIAL DATA OF SIGRAFIL C M80-3.0/200-UN[51]	39
TABLE 4: TEST SPECIMENS OF MODIFIED BETAMATE 1630.....	41
TABLE 5: PROPERTIES OF KRAIBON HVV9632/59.....	51
TABLE 6: PROPERTIES OF KRAIBON HAA9275/45.....	51
TABLE 7: RESULTS OF THE 3-POINT BENDING (FLEXURAL) TEST OF KRAIBON-BONDED LAMINATES	52
TABLE 8: RAW MATERIALS TESTED IN THE DEVELOPMENT OF THE WATER-BASED ADHESIVE TAPE	54
TABLE 9: CALCULATED CHARGE DENSITIES OF ANIONS AND REGRESSED CHARGE DENSITY OF MONTMORILLONITE PARTICLES	62
TABLE 10: STRUCTURES AND SOLUBILITY OF HYPERBRANCHED POLYMERS TESTED AS CLAY-POLYMER COMPOSITES [61,66][66,67] .	63
TABLE 11: OPTIMIZED ADHESIVE FORMULATION.....	63
TABLE 12: SIMPLIFIED ADHESIVE FORMULATION.....	64
TABLE 13: COMPARISON OF SAT 101 EPOXY ADHESIVE AND DUPLOTEC 690 SBF POLYURETHANE ADHESIVE	68
TABLE 14: FAILURE MODE OF LAP-SHEAR SAMPLES	70
TABLE 15: ADHESIVES USED IN THE THERMOPLASTIC ADHESIVES' STUDIES, OBTAINED FROM NOLAX AG	73
TABLE 16: SAMPLES AND THE SETUP OF THE ADHESIVE STACKS IN THE LAMINATES.....	74
TABLE 17: SAMPLE COMPOSITION OF THE ANGULAR COMPONENT	79

8.3 Literature References

- [1] R. Rodi, R.' Alderliesten, R. Benedictus, *Engineering Fracture Mechanics* **2010**, 77, 1012.
- [2] M. D. Fitton, J. G. Broughton, *International Journal of Adhesion and Adhesives* **2005**, 25, 329.
- [3] J. F. Durodola, *International Journal of Adhesion and Adhesives* **2017**, 76, 83.
- [4] S. Kumar, R. D. Adams, *International Journal of Adhesion and Adhesives* **2017**, 76, 1.
- [5] T. Sinmazçelik, E. Avcu, M. Ö. Bora, O. Çoban, *Materials & Design* **2011**, 32, 3671.

[6] J. H. Waite, H. C. Lichtenegger, G. D. Stucky, P. Hansma, *Biochemistry* **2004**, *43*, 7653.

[7] D. Stefaniak, R. Prussak, *AML* **2019**, *10*, 91.

[8] [8a] *Flight International*, 2003; [8b] U. P. Breuer, *Commercial Aircraft Composite Technology*, Springer International Publishing, Cham **2016**.

[9] Dr Roland Thévenin, *Airbus Composite Structures* **2007**.

[10] *Composites World*.

[11] Sara Black, "Fiber-metal laminates in the spotlight", in *Composites World*.

[12] A. Vlot, *Fibre Metal Laminates: An Introduction*, Springer Netherlands, Dordrecht **2001**.

[13] *Joining of polymer-metal hybrid structures: Principles and applications*, J. F. d. Santos, S. T. Amancio Filho, Eds., John Wiley & Sons Inc, Hoboken, NJ **2018**.

[14] *Encyclopedia of materials: Science and technology*, K. H. J. Buschow, Ed., Elsevier, Amsterdam **2001**.

[15] *Woodhead Publishing Series in Welding and Other Joining Technologies*, D. A. Dillard, Ed., Woodhead Pub. Ltd, Boca Raton, Fla, Oxford **2010**.

[16] B. Burchardt, "Advances in polyurethane structural adhesives", in *Advances in Structural Adhesive Bonding*, Elsevier **2010**, p. 35 ff.

[17] J. G. Quini, G. Marinucci, *Mat. Res.* **2012**, *15*, 434.

[18] Z. Liu, M. A. Meyers, Z. Zhang, R. O. Ritchie, *Progress in Materials Science* **2017**, *88*, 467.

[19] *Progress in adhesion and adhesives*, K. L. Mittal, Ed., Wiley, Hoboken, New Jersey **2015**.

[20] M. Naebe, K. Shirvanimoghaddam, *Applied Materials Today* **2016**, *5*, 223.

[21] A. Gupta, M. Talha, *Progress in Aerospace Sciences* **2015**, *79*, 1.

[22] M. Kashtalyan, M. Menshykova, I. A. Guz, *Journal of Adhesion Science and Technology* **2009**, *23*, 1591.

[23] S. Suresh, *Science (New York, N.Y.)* **2001**, *292*, 2447.

[24] P. Tréguer, D. M. Nelson, A. J. van Bennekom, D. J. Demaster, A. Leynaert, B. Quéguiner, *Science (New York, N.Y.)* **1995**, *268*, 375.

[25] G. Li, P. Lee-Sullivan, R. W. Thring, *Composite Structures* **1999**, *46*, 395.

[26] O. Volkersen, *Luftfahrtforschung* **1938**, *15*:41–7.

[27] R.J.C. Carbas, L.F.M. da Silva, L.F.S. Andrés, *International Journal of Adhesion and Adhesives* **2017**, *76*, 30.

[28] A. Calik, *Engineering Review*, 2016, 29.

[29] V. K. Ganesh, S. Ramakrishna, H. J. Leck, *Advanced Composites Letters* **2019**, *7*.

[30] L. F.M. da Silva, P. J.C. das Neves, R. D. Adams, J. K. Spelt, *International Journal of Adhesion and Adhesives* **2009**, *29*, 319.

[31] A. Chiminelli, R. Breto, S. Izquierdo, L. Bergamasco, E. Duvivier, M. Lizaranzu, *International Journal of Adhesion and Adhesives* **2017**, *76*, 3.

[32] M. Kemal Apalak, R. Gunes, *Materials & Design* **2007**, *28*, 1597.

[33] Christopher B. Stabler, Faye R. Toulan, and John J. La Scala, *Functionally Graded Adhesive* **2009**.

[34] W. Demtröder, *Springer-Lehrbuch*, 7th edition, Springer Spektrum, Berlin, Heidelberg **2015**.

[35] *Tensile testing*, 2nd edition, J. R. Davis, Ed., ASM International, Materials Park, Ohio **2010**.

[36] *Springer handbooks*, H. Czichos, T. Saito, L. Smith, Eds., Springer, Berlin **2006**.

[37]D. B. Miracle, *ASM handbook, / prepared under the direction of the ASM International Handbook Committee ; Vol. 21*, 2nd edition, ASM International, Materials Park, Ohio **2002**.

[38]S. Khoei, Z. Kachoei, *RSC Adv.* **2015**, 5, 21023.

[39]D14 Committee, *Test Method for Apparent Shear Strength of Single-Lap-Joint Adhesively Bonded Metal Specimens by Tension Loading (Metal-to-Metal)*, ASTM International, West Conshohocken, PA **2010**.

[40]Perkin Elmer Inc., *Introduction to Dynamic Mechanical Analysis: A Beginner's Guide* (2008), https://www.perkinelmer.com/CMSResources/Images/44-74546GDE_IntroductionToDMA.pdf (accessed 6.2.19).

[41]DIN Deutsches Institut für Normung e. V., DIN German Institute for Standardization, *Metallische Werkstoffe- Biegeversuch* **2016-07-00**.

[42]M. Ostapiuk, J. Bieniaś, B. Surowska, *Science and Engineering of Composite Materials* **2018**, 25, 1095.

[43]E. Hornbogen, H. Warlimont, *Springer-Lehrbuch*, Springer Berlin Heidelberg, Berlin, Heidelberg, s.l. **1991**.

[44]Forschungszentrum Jülich, *Das Know-How hinter den höchstauf lösenden Elektronenmikroskopen* (Letzte Änderung: 2017), <https://www.fz-juelich.de/portal/DE/Forschung/Schluesseltechnologien/Elektronenmikroskopie/know-how-mikroskope.html?nn=930658> (accessed 2.7.19).

[45]UTB, vol. 4864, S. Kühl, S. Kühle, B. Ilsinger, S. Lenz, M. Thaler, Eds., Verlag Eugen Ulmer, Stuttgart **2018**.

[46]J. I. Goldstein, D. E. Newbury, P. Echlin, D. C. Joy, A. D. Romig, C. E. Lyman, C. Fiori, E. Lifshin, *Scanning Electron Microscopy and X-Ray Microanalysis: A Text for Biologists, Materials Scientists, and Geologists*, 2nd edition, Springer US, Boston, MA **1992**.

[47]T. Klein, E. Buhr, C. Georg Frase, "TSEM", in *Advances in Imaging and Electron Physics*, Tobias Klein, Egbert Buhr, Carl-Georg Frase, Ed., Elsevier **2012**, p. 297 ff.

[48][48a] F. Eggert, *Standardfreie Elektronenstrahl-Mikroanalyse: Mit dem EDX im Rasterelektronenmikroskop ; ein Handbuch für die Praxis*, Books on Demand, Norderstedt **2005**; [48b] *Moderne Methoden der Werkstoffprüfung*, H. Biermann, L. Krüger, Eds., Wiley-VCH Verlag GmbH & Co. KGaA, Weinheim **2015**.

[49]C. Wu, P. Feng, Y. Bai, Y. Lu, *Polymers* **2014**, 6, 76.

[50]B. I. Voit, A. Lederer, *Chemical reviews* **2009**, 109, 5924.

[51]Q. Fu, L. Cheng, Y. Zhang, W. Shi, *Polymer* **2008**, 49, 4981.

[52]K. Sui, Q. Zhang, Y. Liu, L. Tan, L. Liu, *e-Polymers* **2014**, 14.

[53]*Lehrbuch der Lacke und Beschichtungen, / H. Kittel ; Bd. 2*, 2nd edition, W. Krauss, S. Schröter, H. Kittel, Eds., Hirzel, Stuttgart **1998**.

[54]H. Du, Y. Zhao, Q. Li, J. Wang, M. Kang, X. Wang, H. Xiang, *J. Appl. Polym. Sci.* **2008**, 110, 1396.

[55](2014), H.B. Fuller Company, inv.: Felix D. MAI, Brian Carlson; *Polyurethane adhesive film* **2015**.

[56]M. Rodlert, C. J. G. Plummer, Y. Leterrier, J.-A. E. Månon, H. J. M. Grünbauer, *Journal of Rheology* **2004**, 48, 1049.

[57]M. Rodlert, C. J.G. Plummer, L. Garamszegi, Y. Leterrier, H. J.M. Grünbauer, J.-A. E. Månon, *Polymer* **2004**, 45, 949.

[58]M. M. Rahman, H.-J. Yoo, C. J. Mi, H.-D. Kim, *Macromol. Symp.* **2007**, 249-250, 251.

[59]M. Seiler, *Fluid Phase Equilibria* **2006**, 241, 155.

[60]D. Thomasson, F. Boisson, E. Girard-Reydet, F. Méchin, *Reactive and Functional Polymers* **2006**, 66, 1462.

[61]K. D. Collins, *Biophysical Journal* **1997**, 72, 65.

[62]R. D. Shannon, *Acta Cryst A* **1976**, 32, 751.

[63]Y. Guo, X. Yu, *AIMS Materials Science* **2017**, 4, 582.

[64]P. Bhaganna, R. J. M. Volkers, A. N. W. Bell, K. Kluge, D. J. Timson, J. W. McGrath, H. J. Ruijsenaars, J. E. Hallsworth, *Microbial biotechnology* **2010**, 3, 701.

[65]J. H. Huh, M. M. Rahman, H.-D. Kim, *Journal of Adhesion Science and Technology* **2009**, 23, 739.

[66]G. Belingardi, V. Brunella, B. Martorana, R. Ciardiello, "Thermoplastic Adhesive for Automotive Applications", in *Adhesives - Applications and Properties*, A. Rudawska, Ed., InTech **2016**.

9 Appendix

9.1 List of commonly used abbreviations in this work

CFRP	Carbon fiber reinforced plastic
EDX	energy-dispersive X-ray spectroscopy
FEA	finite element analysis
FGA	functionally graded adhesive
FGM	functionally graded material
FML	fiber metal laminate
FRP	fiber reinforced plastic
GFRP	glass fiber reinforced plastic
HBP	hyperbranched polymer
MMT	Montmorillonite
SEM	Scanning electron microscopy

9.2 Publications and Patents

Top-down-Entwicklung von Faser-Metall-Laminaten Alan A. Camberg, Katja Engelkemeier, Jan Dietrich, Thomas Heggemann, Lightweight Design, Ausgabe 2/2018

DE 10 2017 123 788 A1 2019.04.18 Hybridmaterial aus Metall und Faserverbundkunststoff

9.3 Technical Data sheets of used commercially available adhesives

9.3.1 DuploTEC® 690 SBF

DuploTEC® 690 SBF – Topaz Technology

- Vorläufiges Datenblatt -

Art. No. 11 16 96

Materialbeschreibung

DuploTEC® 690 SBF (Superior Bonding Film) ist ein reaktiver Klebefilm auf Polyurethan-Basis. Er ist geeignet für schnelle Klebeprozesse mit niedriger Härtungstemperatur. Der hitzeaktivierbare Film verbindet die Vorteile einer einfachen Handhabung mit den Leistungen struktureller Klebeverbindungen. DuploTEC® 690 SBF kann zur Verklebung unterschiedlichster Materialien und Bauteile verwendet werden.

	Material	Farbe	Dicke in µm
Abdeckung	Silikonpapier	gelb	80
Klebstoff	Wärmehärtender PU-Film mit Inlay	transluzent	100

Eigenschaften & Vorteile

- ✓ Vor-applizierbar auf den meisten Materialien
- ✓ Hohe Festigkeit nach Vernetzung
- ✓ Starke Klebkraft auf einer Vielzahl von Substraten
- ✓ Schnelle und saubere Applikation (pick & place; manuell, halbautomatisch oder vollautomatisch)
- ✓ Bei Raumtemperatur (ca 25°C) nicht klebrig
- ✓ Handfestigkeit erlaubt schnelle Weiterverarbeitung im Prozess
- ✓ Die konstante und gleichmäßige Filmdicke ermöglicht optimale Klebefugen
- ✓ Exzellente Stanz- & Schneideigenschaften
- ✓ DuploTEC® 690 SBF kann sowohl als Rolle, Spule oder Präzisionsstanzteil in Produktionsprozesse integriert werden
- ✓ DuploTEC® 690 SBF ist benzol-, phenol-, toluol- und formaldehydfrei
- ✓ DuploTEC® 690 SBF ist frei von APEO's und Styrol gemäß dem aktuellen GADSL Richtwert

Verarbeitungshinweise

Oberflächenvorbereitung:

- Die Oberfläche muss sauber, trocken und frei von Staub, Fett, Öl und groben Verschmutzungen sein.
- Die Reinigung sollte mit einem sauberen Tuch und geeigneten Lösungsmitteln erfolgen.
- Die Oberflächenenergie sollte mindestens 38 mN/m betragen.

Wir empfehlen die Temperaturbeständigkeit der Materialien vorher zu überprüfen. Gängige Methoden zur Optimierung der Oberflächenenergie können angewendet werden.

Vorapplikation (optional):

- Anfangshaftung erfolgt durch Wärmeeintrag ab ca. 55°C (Optimaler Bereich ca. 60-70°C)
- Empfohlener Druck: 15 - 75 N/cm²
- Empfohlene Zeit: 3 - 10 sek

Kleben und Aushärten:

- Empfohlene Härtungstemperatur: 100 - 150°C
- Empfohlener Druck bei Härtung: 15 - 75 N/cm²
- Zur Vermeidung übermäßigen Ausblutens des Klebstoffs, empfehlen wir eine Klebstofftemperatur von 160°C beim Aushärten nicht zu überschreiten.

Nachhärtung (optional):

- Wir empfehlen die Fügepartner nach dem Klebeprozess unter Druck auf < 50°C abzukühlen.

Die Wärmeübertragung (Zeit) hängt von der Dicke des Substrates und dessen Wärmeleitfähigkeit ab. Das Kleben kann in einer Vielzahl von Maschinen stattfinden, wie zum Beispiel in Laminiergeräten, Wärmepressen Verschmelzungsanlagen, Pressformen und vergleichbaren Geräten.

Lohmann GmbH & Co. KG
Irlicher Str. 55
D-56567 Neuwied
Phone: + 49 (0) 26 31 34-0
Fax: + 49 (0) 26 31 34-6661
www.lohmann-tapes.com

 **Lohmann**
The Bonding Engineers.

DuploTEC® 690 SBF – Topaz Technology

- Vorläufiges Datenblatt -

Art. No. 11 16 96



Technische Daten	Methode	Wert	
Glasübergangstemperatur (nach Aushärtung)	DSC	- 30°C	
Erweichungstemperatur		ca. 55°C	
Härtungstemperatur		min. 100°C	
Dynamische Scherfestigkeit (23 ± 2°C)	Gemäß DIN EN 1465	N/312,5 mm ²	MPa
Polycarbonat (3 mm)		2900	9.3
CFK (3 mm)		5000	16
Aluminium (2 mm)		1600	5
Temperaturbeständigkeit, langfristig	Interne Prüfmethode	< 140°C	
Temperaturbeständigkeit, kurzzeitig	Interne Prüfmethode	< 170°C	

Aufbewahrung / Lagerzeit

- Lagerung und Transport des Films hat bei unter +30°C (für max. einen Tag ≤ +35°C) und normaler Luftfeuchtigkeit (50-70 %) zu erfolgen
- Die Lagerfähigkeit beträgt 1 Jahr nach Auslieferung
- Nach Vorapplikation auf ein Substrat mit ≤ 60°C ist die Lagerfähigkeit drei Monate nach Vorapplikation

Sicherheitshinweise

- Bitte beachten Sie die allgemeinen Sicherheitshinweise bevor Sie DuploTEC® 690 SBF das erste Mal verwenden
- DuploTEC® 690 SBF erfüllt die Anforderungen der Direktive 2011/65/EU - RoHS und dieses Produkt enthält keine SVHC Substanzen nach Artikel 57 der Verordnung (EC) Nr. 1907/2006 – REACH

Anmerkungen

Die in diesem Datenblatt beschriebenen physikalischen Eigenschaften sind typische Messwerte oder Durchschnittsmesswerte. Alle anwendungsbezogenen Beurteilungen, Informationen und Empfehlungen beruhen auf unserem besten Wissen und praktischen Erfahrungen. Viele Einflussfaktoren liegen außerhalb unserer Kontrolle allein im Bereich des Käufers und können den Gebrauch und die Wirkungen unserer Bänder in der konkreten Anwendung beeinflussen. Sofern nicht ausdrücklich schriftlich vereinbart, übernehmen wir keine Haftung für die Geeignetheit oder Gebrauchsfähigkeit unserer Bänder für bestimmte Einsatzzwecke und Anwendungen, die in der speziellen Verwendung der Bänder durch den Käufer liegen. Soweit gesetzliche Regelungen nicht entgegenstehen, ist unsere Haftung für unmittelbare oder mittelbare, materielle oder immaterielle Schäden des Käufers, die durch die Verwendung unserer Bänder entstehen, ausgeschlossen. Die Verantwortung für die Geeignetheit für den vom Käufer beabsichtigten Einsatzzweck liegt allein in dessen Verantwortungsbereich. Bei speziellen Fragen wenden Sie sich bitte an unsere Anwendungstechnik.

Stand: Juli 2016

Bei Anfragen bezüglich Produktsicherheit (Bestätigungen, Konformitäten mit Richtlinien, REACH, etc.) verwenden Sie bitte folgende E-Mail-Adresse: product.safety@lohmann-tapes.com

Lohmann GmbH & Co. KG
Irlicher Str. 55
D-56567 Neuwied
Phone: + 49 (0) 26 31 34-0
Fax: + 49 (0) 26 31 34-6661
www.lohmann-tapes.com

 **Lohmann**
The Bonding Engineers.

9.3.2 3M™ Structural Adhesive Tape



Oct. 2014

3M™ Structural Adhesive Tape

SAT 1010

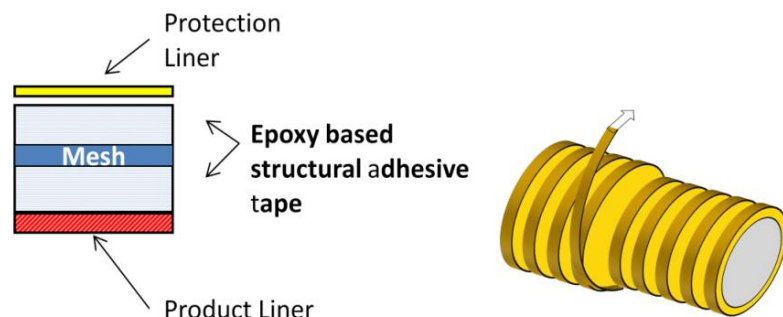
Description

3M™ Structural adhesive tape (SAT) is a one layer-epoxy based adhesive tape for the Automotive industry (BIW) formulated for metal bonding applications. The tape delivered structural bonding strengths for various application but specially for hem bonding on metal closures. Besides the bonding performance the tape had gap filling properties due to expansion function. Tape should be apply in BIW and run through the automotive paint pre-treatment& E-Coat process. In E-coat oven the tape expand and cure under the below describe conditions.

Tape has good compatibility to stamp oils and features broad adhesive gap and bake tolerances.
The tape will be delivered on level wound rolls , geometries see below .

Note : Using a BIW oven can leads to performance defects of SAT1010. The Tape don't need a pre-cure process e.g. Induction or BIW oven. Hem bonding tape application should be conduct in close communication with the responsible 3m TechService engineer.

Construction



Product Features	Performance Advantages	Customer Benefits
Epoxy Chemistry	High bond strength with cohesive failure mode on metal substrates Compatible with press and stamp oil's Excellent long-term durability (to heat, humidity, salt water)	Robust, structural bonding performance Provides good bond strength under various process conditions



Process	Wash out resistance	Broad handling and dispensing windows
	Gap closing properties via expansion	Sealing and corrosion protection
	Contain glass-beads/mesh (M-version) for bond line control	Safe application
Final Heat Cure	In E-coat oven w broad over-bake tolerance	no extra curing process

Shelf Life six months from dispatch of 3M warehouse when stored at room temperature.

99+% Solids Reduced emissions/vapours/odour Low regulatory concern

Performance Properties (Typical Values)

Tape geometries (uncured tape)

Thickness tape	0.2- 0.4mm (depend on application)
Width of tape	10-30mm (depend on application)
color	White
Length	Level wound roll up to 800 m
Liner:	Release Liner (red) plus Top-Liner: PE

Curing

Curing conditions min .15 min at 165 °C max. 40 min at 195 °C



3M Deutschland GmbH
Automotive Laboratory
 Carl-Schurz-Strasse-1
 D-41453 Neuss
 Tel. (+49)-2131-14-3580
 Fax: (+49)-2131-14-12-3580

SAT1010_E_01/bk
 Date: 10/ 2014
 Revision: 01

9.3.3 BETAMATE™ 1620 MB



Technical Datasheet

BETAMATE™ 1620 MB

Crashresistant Structural Adhesive

Description / Application:

BETAMATE™ 1620 MB is a one component, epoxy based adhesive especially developed for the body shop. The adhesive is used in the car to increase the operation durability, the crash performance and the body stiffness.

Properties:

- Excellent adhesion to automotive steels, including coated steels and pretreated aluminium with good tolerance to oil and drylubes.
- Helps to increase the stiffness and the crash stability of the entire car body.
- High durability of the adhesive and the adhesive bond.
- Due to its sealing capability the metal and weld points are protected against corrosion.
- Compatible with other mechanical and thermal joining techniques.
- Compatible with the electrocoat process.
- Precurable and pregelable.
- Until four weeks open time in the uncured bond

Application:

The product is cold pumpable, swirlable, streamable and applicable as a bead. It can be applied with the following parameters:

application speed	Until 500 mm/s
temperatures:	recommended:
follower plate	unheated
follower plate - doser	Unheated possible, Maximum temperature at doser 55°C
nozzle	55 - 65°C

For an optimum tack of the adhesive, the parts to bond should be stored at 15°C or higher. In case of an application break longer than 30 minutes the heating of the application equipment should be switched off.

All Dow Automotive products are primarily developed in co-operation with the automobile manufacturers, according to their needs and their specifications; they are approved for the specific applications as defined by the customer.

The use of the product other than approved application have to be released in written form by the Technical Service of Dow Automotive.

Technical Data:

Basis	epoxy resin
Color	red
Density 23°C (DIN 52451)	1.22 g/ml
Solid Content	> 99%
Viscosity/Yield Point (45°C, Bohlin, Casson)	30 Pas / 130 Pa
Curing Condition	> 140°C / 30 minutes
Standard Curing	180°C / 30 minutes
Tensile Strength (DIN EN ISO 527-1)	31 MPa
Elongation at Break (DIN EN ISO 527-1)	approx. 12%
E-Modulus (DIN EN ISO 527-1)	1500 MPa
Lap Shear Strength (DIN EN 1465) (CRS 1403, 1.5mm) (Bonding dimension: 25mm x 10mm Adhesive layer thickness: 0.2mm)	31 MPa
T-Peel Strength (DIN EN ISO 11339) (DX56 D Z100 MB, 0.8mm) (Bonding dimension: 25mm x 100mm Adhesive layer thickness: 0.2mm)	7N/mm
T-Peel Strength (DIN EN ISO 11339) (H340 LAD + Z 0.8mm) (Bonding dimension: 25mm x 100mm Adhesive layer thickness: 0.2mm)	10 N/mm
Impact Peel Strength (ISO 11343) (CRS 1403, 1.0mm, 23°C, 2m/s) (Bonding dimension: 20mm x 30mm Adhesive layer thickness: 0.2mm)	40 N/mm
Bonding Surface Preparation	The material has been designed to tolerate up to 5 g/m ² of surface oil.
Application Tool	Cartridges: hand-operated or pneumatic heated gun with mechanical piston. Drums, pails: heated pumping system.
Cleaning	Uncured material can be removed with BETACLEAN 3510. Attention: The contact with bonded areas should be avoided.
Containers	Drums, pails: 20 kg, 45 kg and 200 kg (re-usable pails with PE-liner). Cartridges: 0,36 kg
Shelf life	Storable at temperatures below 30°C for four month.

The given data are standard values.